Cultivation and molecular ecological studies of microbes relevant to marine sedimentary carbon and sulfur cycling

Doctoral thesis by Masataka Aoki

Department of Energy and Environment Science
Nagaoka University of Technology

March 2016

-Table of contents-

Chapter I

1. Introduction

Marine sediments cover ~70% of the Earth's surface, and ~0.6% of Earth's total living biomass live in subseafloor sediments (Kallmeyer *et al*., 2012). Most marine sedimentary microbes are phylogenetically distinct from previously isolated microbes, and thus, the details regarding the microbial ecology of marine sediments and key biogeochemical processes remain largely unknown. The following introduction gives an overview of the fundamental knowledge relevant to the course of this doctoral thesis.

1.1 Key microbiological processes in marine sediments

1.1.1 Organic matter degradation using various electron acceptors

Photosynthetic organisms capture energy from sunlight, and drive subsequent energy and organic matter transformations at the sea surface (DeLong, 2004; D'Hondt *et al*., 2004). In continental margin subseafloor environments, most of the sedimentary microbial populations are heterotrophic and use the organic matter produced by photosynthesis (Biddle *et al*., 2006). Oxygen, sulfate, and nitrate, diffuse into the sediments from the seawater and are consumed sequentially in a predictable series of metabolic reactions (*i.e.*, reduction of oxygen, followed by nitrate, manganese, iron, sulfate, and finally carbon dioxide) (**Fig. 1-1**) (DeLong, 2004; D'Hondt *et al*., 2004). D'Hondt *et al*. (2004) observed that oxygen, nitrate, and sulfate were also supplied as microbial energy sources from the deep basaltic basement of the sediment. Notice that oxygen and aerobic communities may occur

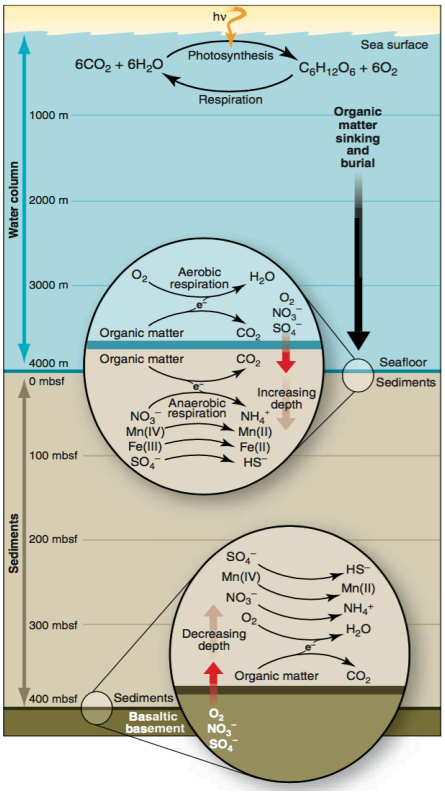

Figure 1-1. Microbial respiration at the ocean's surface and in the sediments of the subseafloor. Adapted from DeLong (2004).

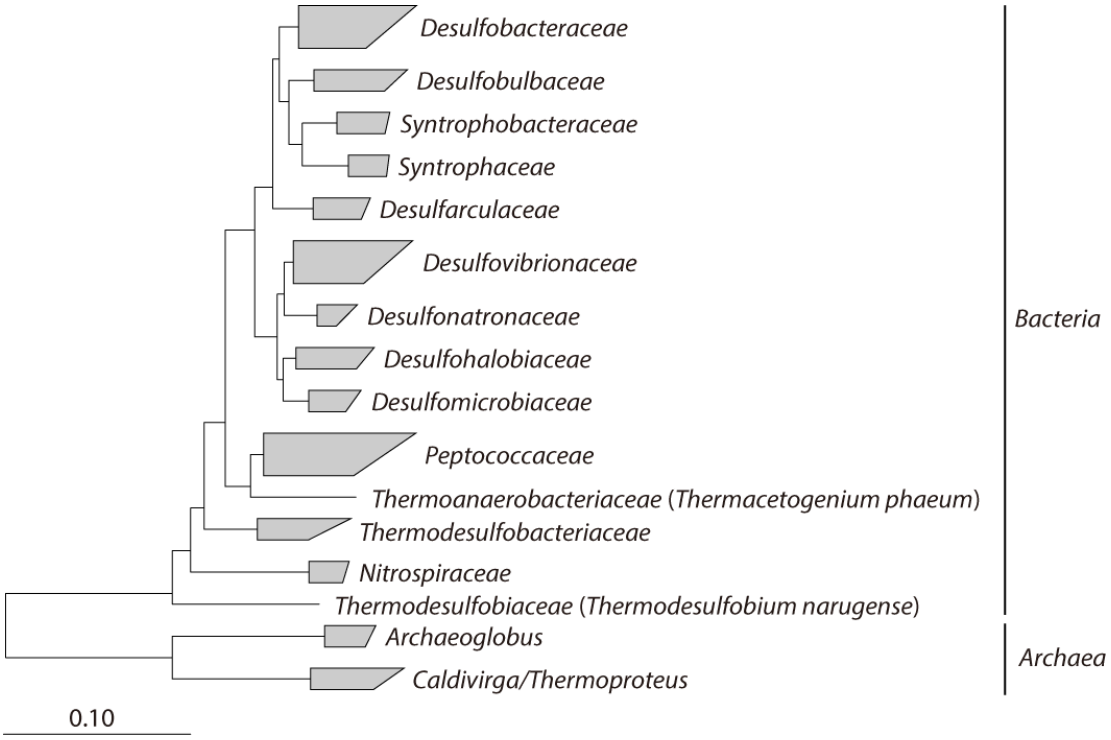

Figure 1-2. Neighbor-joining phylogenetic tree based on the 16S rRNA gene sequences of previously cultivated sulfate-reducing microbes. The scale bar represents the estimated number of nucleotide changes per sequence position.

throughout the entire sediment sequence in areas with low sedimentary respiration (D'Hondt *et al*., 2015).

1.1.2 Sulfate reduction

The microbial process of sulfate reduction is possibly one of the oldest metabolic pathways on Earth (Castresana and Moreira, 1999; Shen *et al*., 2001), which reflects the importance of sulfate reduction for biogeochemical cycling both previously and at present. Based on the 16S rRNA phylogeny, the known sulfate-reducing bacteria can be classified into phylogenetically diverse prokaryotic lineages (**Fig. 1-2**) (Rabus *et al*., 2015). Most of the cultivated sulfate-reducing bacteria belong to the class *Deltaproteobacteria* (including the families *Desulfobacteraceae*, *Desulfobulbaceae*, *Syntrophobacteraceae*, *Syntrophaceae*, *Desulfarculaceae*, *Desulfovibrionaceae*, *Desulfonatronaceae*, *Desulfohalobiaceae*, and *Desulfomicrobiaceae*) and spore-forming gram-positive bacteria within the phylum *Firmicutes* (including families *Peptococcaceae*, *Thermoanaerobacteraceae,* and *Thermodesulfobiaceae*) (Rabus *et al*., 2015). Some archaeal isolates affiliated with the genus *Archaeoglobus* in the phylum *Euryarchaeota*, and the genera *Thermocladium* and *Caldivirga* in the phylum *Crenarchaeota* are known to be capable of sulfate reduction (Rabus *et al*., 2015).

The ability to use a broad range of organic substrates, such as, short- and long-chain fatty acids, aromatic compounds, aromatic hydrocarbons, and C_1 compounds have been shown in phylogenetically diverse

sulfate-reducing microbes (Rabus *et al*., 2015). In marine sediments, sulfate-reducing microbes are important for the biodegradation of organic matter possibly due to the high concentration of sulfate (~28 mM) in the seawater that contributes to the sulfate content in the anoxic sedimentary environment. Bowles *et al*. (2014) reported that 11.3 Tmols of sulfate are reduced yearly, accounting for the oxidation of 12 to 29% of the organic carbon flux to the seafloor. The net sulfate reduction reaction follows a two carbon–to–one sulfur stoichiometric ratio (eq. 1) (D'Hondt *et al*., 2002; Bowles *et al*., 2014).

$$C_6H_{12}O_6 + 3SO_4^{2-} \rightarrow 3S^{2-} + 6CO_2 + 6H_2O \qquad (1)$$

The detection of potential sulfate reduction activity in deep subseafloor sediments in which sulfate is rarely present (Knab *et al*., 2009; Holmkvist *et al*., 2011; Treude *et al*., 2014) suggests that sulfate reduction also has a significant role in deep subseafloor ecosystems. The presence of high-affinity sulfate reduction in marine sediments suggested that some marine sedimentary sulfate-reducing microbial communities have the potential to utilize effectively low concentrations of sulfate (Tarpgaard *et al*., 2011). In contrast, only a few sulfate-reducing isolates have been obtained from deep subseafloor sediment. *Desulfovibrio profundus* strains were isolated from deep subseafloor sediment (80 and 500 m below the seafloor [mbsf]) of the Japan Sea (Bale *et al*., 1997). More recently, strains related to the sulfate-reducing genera *Desulfovibrio* and *Desulfotignum* were obtained from deep sediments of the Juan de Fuca Ridge, Northeast Pacific (Site U1301 of the International Ocean Discovery Program; 240–262 mbsf) (Fichtel *et al*., 2012). These isolates could grow chemolithotrophically with hydrogen as the electron donor. Hydrogen could be generated by organic matter fermentation, tectonic activity (Hirose *et al*., 2011), serpentinization of ultramafic rocks (McCollom and Bach, 2009), and radiolysis of interstitial water (D'Hondt *et al*., 2009) in deep subseafloor sediments. Thus, hydrogen might be an important electron donor for sulfate reducers proliferates in the deep subseafloor ecosystems, where the availability of organic substrates derived from the photosynthetic reaction is severely limited (Fichtel *et al*., 2012).

Due to the phylogenetic complexity of sulfate reducers, the concomitant detection of all recognized sulfate-reducing microbes from environmental samples by using a single 16S rRNA gene-targeted probe or PCR primer pair is difficult (Meyer and Kuever, 2007c). A useful approach for the detection of putative sulfate reducers in the environment is the use of functional marker genes that encode key enzymes in the sulfate reduction. Useful functional marker genes for sulfate reduction are the *dsrAB* gene encodes the dissimilatory sulfite reductase alpha and beta subunits, and the *aprBA* gene encodes the adenosine-5'-phosphosulfate reductase alpha and beta subunits (Meyer and Kuever, 2007c and 2007d; Müller *et al*., 2015).

1.1.3 Sulfur compound disproportionation

Bak and Cypinoka discovered the microbial mediated inorganic sulfur compound disproportionation in 1987 (Bak and Cypinoka; 1987). In the report by Bak and Cypinoka (1987), the disproportionation of thiosulfate (eq. 2)

and sulfite (eq. 3) was found in *Desulfovibrio desulfodismutans* in the class *Deltaproteobacteria*.

$$S_2O_3^{2-} + H_2O \rightarrow SO_4^{2-} + HS^- + H^+ \quad (2)$$

$$4SO_3^{2-} + H^+ \rightarrow 3SO_4^{2-} + HS^- \quad (3)$$

After the discovery of thiosulfate and sulfite disproportionation, the occurrence of elemental sulfur disproportionation (eq. 4) was confirmed in anaerobic marine enrichment cultures (Thamdrup *et al*., 1993):

$$4S^0 + 4H_2O \rightarrow SO_4^{2-} + 3HS^- + 5H^+ \quad (4)$$

In contrast to the disproportionation of thiosulfate and sulfite, sulfur disproportionation requires the effective removal of the produced sulfide to be thermodynamically favorable (Finster, 2008). Mn (IV) (eq. 5), Fe (III) (eq. 6), and Cr (VI) (eq. 7), are known as the sulfide scavengers and anaerobically produce S^0 (Thamdrup *et al*., 1993; Lovley and Philips, 1994; Finster *et al.*, 1998; Obraztsova *et al*., 2002; Lan *et al*., 2005).

$$HS^- + MnO_2 + 3H^+ \rightarrow S^0 + Mn^{2+} + 2H_2O \quad (5)$$

$$3HS^- + 2Fe(OH)_3 + 3H^+ \rightarrow S^0 + 2FeS + 6H_2O \quad (6)$$

$$3HS^- + 2CrO_4^{2-} + 7H^+ \rightarrow 3S^0 + 2Cr(OH)_3 + 2H_2O \quad (7)$$

Recently, disulfide disproportionation (eq. 8) mediated by an uncultured *Desulfosarcina*/*Desulfococcus* (DSS) clade bacteria within the family *Desulfobacteraceae* was reported (Milucka *et al*., 2012):

$$4HS_2^- + 14H_2O \rightarrow SO_4^{2-} + 7HS^- + 5H^+ \quad (8)$$

To date, many microbes capable of disproportionation of inorganic sulfur compounds have been isolated (Bak and Cypionka, 1987; Bak and Pfennig, 1987; Krämer and Cypionka, 1989; Mohn and Tiedje, 1990; Lovley and Philips, 1994; Janssen *et al.* 1996; Krekeler *et al*., 1997; Baena *et al*. 1998; Finster *et al*., 1998; Hernandez-Eugenio *et al*., 2000; Jackson and McInerney, 2000; Obraztsova *et al*., 2002; Peduzzi *et al*., 2003; Warthmann *et al*., 2005; Finster, 2008; Sorokin *et al*., 2008; Slobodkin *et al*., 2012; Poser *et al*., 2013; Slobodkin *et al*., 2013) (**Table 1-1**). Most of the sulfur compound disproportionators are typically associated with sulfate reducer-related deltaproteobacterial lineages. Interestingly, some strains perform sulfur compound disproportionation without microbial growth (**Table 1-1**). It should be noted that the facultative anaerobic bacterium *Pantoea agglomerans* strain SP1 distantly related to previously isolated sulfate reducers can thrive on the disproportionation of elemental sulfur (Obraztsova *et al*., 2002).

Table 1-1. Organisms that disproportionate thiosulfate, sulfite, and/or elemental sulfur. Modified after Finster (2008).

Organism	SO_3^{2-}	$S_2O_3^{2-}$	S^0	Reference
Desulfobacter curvatus DSM 3379	–	D	nd	Krämer and Cypionka (1989)
Desulfobacter hydrogenophilus DSM 3380	–	D	nd	Krämer and Cypionka (1989)
Desulfococcus multivorans DSM 2059	–	D	nd	Krämer and Cypionka (1989)
Desulfobulbus propionicus DSM 2032	–	D	G	Krämer and Cypionka (1989); Lovley and Phillips (1994)
Desulfofustis glycolicus PerGlyS	nd	nd	G	Finster (2008)
Desulfocapsa thiozymogenes Bra2	G	G	G	Janssen *et al*. (1996)
Desulfocapsa sulfoexigens SB164P1	G	G	G	Finster *et al*. (1998)
Desulfocapsa sp. Cad626	G	G	G	Peduzzi *et al*. (2003)
Desulfovibrio desulfuricans CNS	G	D	nd	Krämer and Cypionka (1989)
Desulfovibrio sulfodismutans ThAc01	G	G	nd	Bak and Cypionka (1987); Bak and Pfenning (1987)
Desulfovibrio mexicanus Lup1	–	D	nd	Hernandez-Eugenio *et al*. (2000)
Desulfovibrio aminophilus ALA-3	D	D	nd	Baena *et al*. (1998)
Desulfovibrio brasiliensis LVform1	nd	G	nd	Warthmann *et al*. (2005)
Desulfovibrio oxyclinae P1B	G	G	nd	Krekeler *et al*. (1997)
Desulfurivibrio alkaliphilus AHT2	nd	nd	G	Poser *et al*. (2013)
Desulfurivibrio sp. AMeS2	nd	nd	G	Poser *et al*. (2013)
Desulfonatronospira thiodismutans ASO3-1	G	G	nd	Sorokin *et al*. (2008)
Desulfonatronospira thiodismutans AHT 8	G	G	nd	Sorokin *et al*. (2008)
Desulfonatronospira delicata AHT 6	G	G	nd	Sorokin *et al*. (2008)
Desulfomonile tiedje DCB-1	nd	G	nd	Mohn and Tiedje (1990)
Dissulfuribacter thermophilus S69	G	G	G	Slobodkin *et al*. (2013)
Pantoea agglomerans SP1	nd	nd	G	Obraztsova *et al*. (2002)
Desulfotomaculum nigrificansa DSM 574	–	D	–	Krämer and Cypionka (1989)
Desulfotomaculum thermobenzoicum ATCC 49756	nd	G	nd	Jacksen and McInerney (2000)
Dethiobacter alkaliphilus AHT 1	nd	nd	G	Poser *et al*. (2013)
Thermosulfurimonas dismutans	G	G	G	Slobodkin *et al*. (2012)

G: growth.
D: disproportionated without growth.
–: not disproportionated.
nd: not determined.

Holmkvist *et al*. (2011) noted that the sulfate reduction in the sulfate-deleted deep subseafloor sediment might be driven by sulfate derived from re-oxidation of reduced sulfur species with oxidized iron species (so-called cryptic sulfur cycle; **Fig. 1-3**). Assuming that the interpretation by Holmkvist *et al*. (2011) is correct, thiosulfate disproportionation may have important function in the cryptic sulfur cycle and bioavailable thiosulfate may repeatedly be produced by the reaction of hydrogen sulfide with Fe (III) species (eq. 9 and 10):

$$2H_2S + 8FeOOH + 14H^+ \rightarrow S_2O_3^{2-} + 8Fe^{2+} + 13H_2O \quad (9)$$

$$2H_2S + 8Fe^{3+} + 4H_2O \rightarrow S_2O_3^{2-} + 8Fe^{2+} + 10H^+ \quad (10)$$

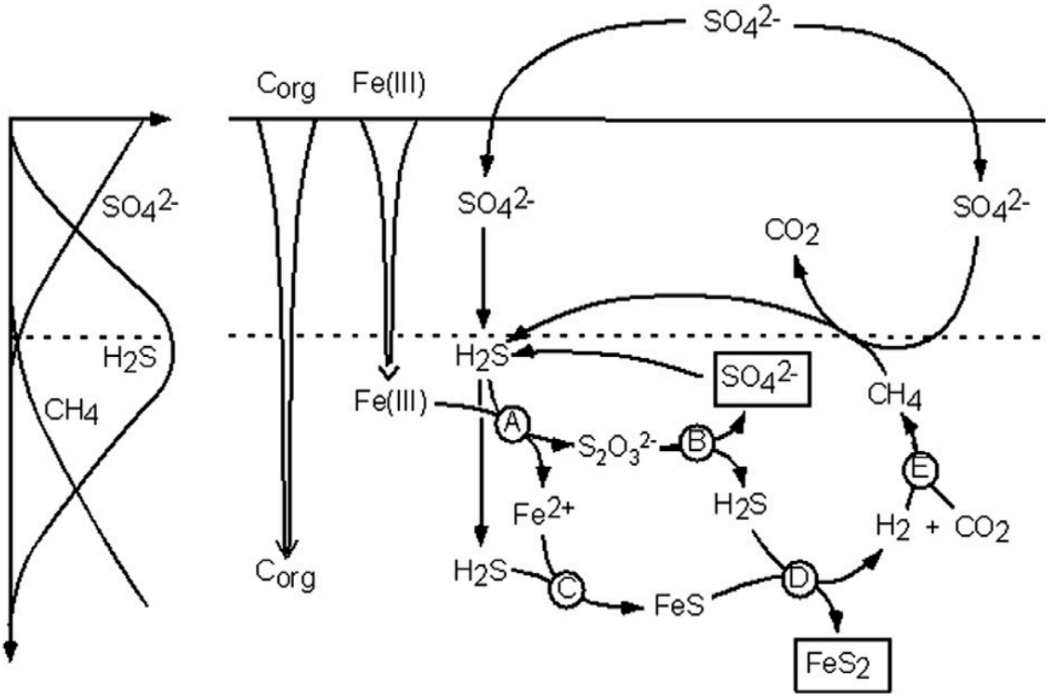

Figure 1-3. Conceptual diagram of the cryptic sulfur cycle driven by iron in the methane zone of marine sediment. Adapted from Holmkvist *et al*. (2011).

1.1.4 Sulfur (compound) oxidation

Microbial sulfur (compound) oxidation is a key biological process in the oxidative sulfur cycling on the Earth. Various types of reduced inorganic sulfur compounds (sulfide, polysulfides, sulfur, sulfite, thiosulfate, and polythionates) can serve as electron donors for sulfur oxidation. Sulfur oxidation can occur under either aerobic or anaerobic condition. In most cases, the end product of sulfur oxidation is sulfate. Oxygen is a general electron acceptor for sulfur oxidizers, and the significant aerobic sulfur oxidation reactions can be summarized as follows (eq. 11−14) (Tang *et al*., 2009):

$$H_2S + 0.5O_2 \rightarrow S^0 + H_2O \quad (11)$$

$$H_2S + 2O_2 \rightarrow SO_4^{2-} + 2H^+ \quad (12)$$

$$S^0 + 1.5O_2 + H_2O \rightarrow SO_4^{2-} + 2H^+ \quad (13)$$

$$S_2O_3^{2-} + 2O_2 + H_2O \rightarrow 2SO_4^{2-} + 2H^+ \quad (14)$$

Phylogenetically diverse sulfur-oxidizing microbes are known to be able to grow anaerobically. The use of nitrate as the terminal electron acceptor is one of the best-studied sulfur oxidation metabolisms (eq. 15−20) (Tang *et al*., 2009):

$$S^{2-} + 1.6NO_3^- + 1.6H^+ \rightarrow SO_4^{2-} + 0.8N_2 + 0.8H_2O \quad (15)$$

$$S^{2-} + 0.4NO_3^- + 2.4H^+ \rightarrow S^0 + 0.2N_2 + 1.2H_2O \quad (16)$$

$$S^{2-} + 4NO_3^- \rightarrow SO_4^{2-} + 4NO_2^- \quad (17)$$

$$S^{2-} + NO_3^- + 2H^+ \rightarrow S^0 + NO_2^- + H_2O \quad (18)$$

$$S^0 + 1.2NO_3^- + 0.4H_2O \rightarrow SO_4^{2-} + 0.6N_2 + 0.8H^+ \quad (19)$$

$$S_2O_3^{2-} + 1.6NO_3^- + 0.2H_2O \rightarrow 2SO_4^{2-} + 0.8N_2 + 0.4H^+ \quad (20)$$

Anaerobic sulfur oxidation also occurs in photic zones where sunlight is available (eq. 21) (Tang *et al*., 2009). Phototrophic sulfur oxidation would not be an essential function in sulfur cycling in bathypelagic and abyssopelagic zones due to the limitation of available sunlight.

$$2H_2S + CO_2 \rightarrow 2S + CH_2O\,(\text{carbohydrate}) + H_2O \quad (21)$$

As with sulfate-reducing microbes, sulfur-oxidizing microbes are distributed in phylogenetically diverse lineages (Muyzer *et al*., 2013). Therefore, the use of functional marker genes that encode key enzymes in the sulfur oxidation is a useful approach for the detection of putative sulfur-oxidizing components in the environment. The enzymatic pathways for dissimilatory sulfur oxidation have been found to be widely variable due to the abilities of sulfur-oxidizing prokaryotes to utilize the various sulfur compounds. Consequently, several functional marker gene assays have been developed: *aprBA* coding for the adenosine-5′-phosphosulfate reductase (Meyer and Kuever, 2007b and 2007c), *soxB* coding the SoxB component of the periplasmic thiosulfate-oxidizing Sox enzyme complex (Meyer *et al*., 2007a), and *dsrAB* coding for the reverse dissimilatory sulfite reductase (Loy *et al*., 2009).

Although little is known about the phylogenetic diversity and distribution of marine sedimentary sulfur-oxidizing bacteria, sulfur-oxidizing bacteria-affiliated with the classes *Gammaproteobacteria* and *Epsilonproteobacteria* may have a vital function in marine sedimentary sulfur cycling (Lenk *et al*., 2011; Pjevac *et al*., 2014; Ruff *et al*., 2015). Recently, it was reported that filamentous *Deltaproteobacteria* of the *Desulfobulbaceae* family (so-called cable bacteria) could perform sulfide oxidation in anoxic sediment layers by long-distance electron transport from sulfide to oxygen using electrical currents (Pfeffer *et al*., 2012).

1.1.5 Methanogenesis

Complex organic matters are converted to methane by the cooperation of anaerobes in anoxic environments (**Fig. 1-4**) (Liu and Whitman, 2008). Methanogenesis is observed as the terminal step in the biodegradation of organic matters. All of the previously cultivated methanogens are phylogenetically classified into the following seven orders within the phylum *Euryarchaeota*: *Methanopyrales*, *Methanococcales*, *Methanobacteriales*, *Methanomicrobiales*, *Methanosarcinales*, *Methanocellales,* and *Methanomassiliicoccales* (Liu and Whitman, 2008; Iino *et al*., 2013) (**Fig. 1-5**). Although methanogenic archaea are phylogenetically diverse, their substrates

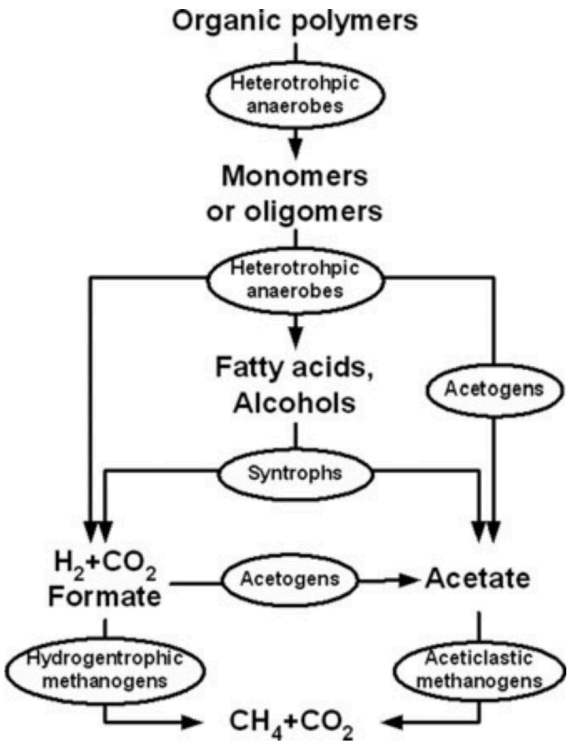

Figure 1-4. Anaerobic food chain for the conversion of organic matter to methane. Adapted from Liu and Whitman (2008).

are classified into three major types: CO_2 (eq. 22−25), acetate (eq. 26), and methylated compounds (eq. 27−33) (Liu and Whitman, 2008):

$$4H_2 + CO_2 \rightarrow CH_4 + 2H_2O \quad (22)$$

$$4HCOOH \rightarrow CH_4 + 3CO_2 + 2H_2O \quad (23)$$

$$CO_2 + 4\ (\text{isopropanol}) \rightarrow CH_4 + 4\ (\text{acetone}) + 2H_2O \quad (24)$$

$$4CO + 2H_2O \rightarrow CH_4 + 3CO_2 \quad (25)$$

$$CH_3COOH \rightarrow CH_4 + CO_2 \quad (26)$$

$$4CH_3OH \rightarrow 3CH_4 + CO_2 + 2H_2O \quad (27)$$

$$CH_3OH + H_2 \rightarrow CH_4 + H_2O \quad (28)$$

$$2(CH_3)_2\text{-}S + 2H_2O \rightarrow 3CH_4 + CO_2 + 2H_2S \quad (29)$$

$$4CH_3\text{-}NH_2 + 2H_2O \rightarrow 3CH_4 + CO_2 + 4NH_3 \quad (30)$$

$$2(CH_3)_2\text{-}NH + 2H_2O \rightarrow 3CH_4 + CO_2 + 2NH_3 \quad (31)$$

$$4(CH_3)_3\text{-}N + 6H_2O \rightarrow 9CH_4 + 3CO_2 + 4NH_3 \quad (32)$$

$$4CH_3NH_3Cl + 2H_2O \rightarrow 3CH_4 + CO_2 + 4NH_4Cl \quad (33)$$

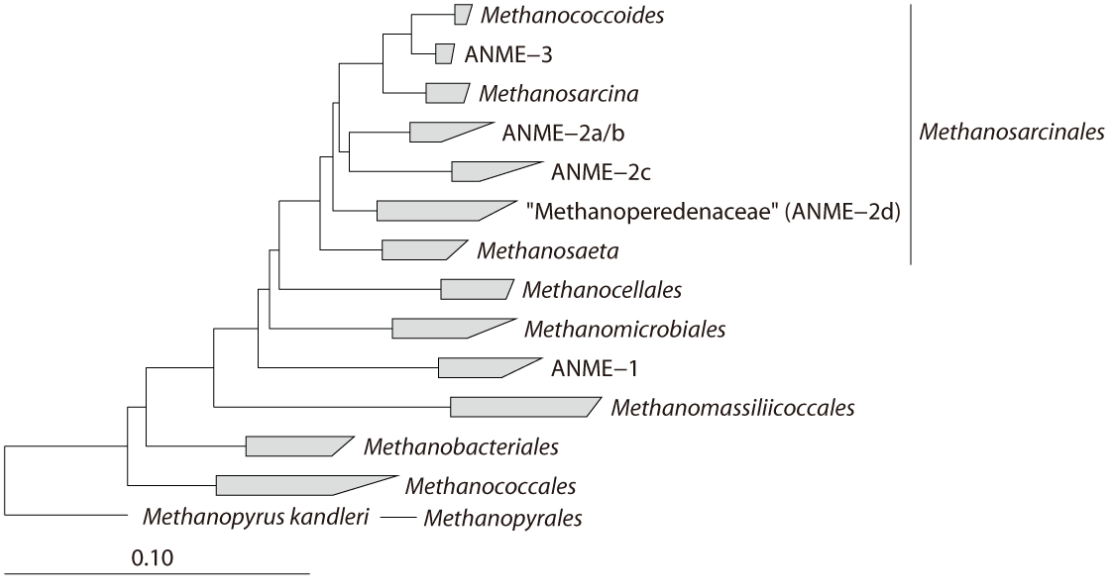

Figure 1-5. Neighbor-joining phylogenetic tree showing the phylogenetic positions of methanogens and anaerobic methanotrophs (ANMEs) within the phylum *Euryarchaeota*. The scale bar represents the estimated number of nucleotide changes per sequence position.

The recent estimate of the global rate of microbial methane formation in marine sediments is in the range of 4−25 Tg-carbon year^{-1} (Wallman *et al*., 2012). $\delta^{13}C$–CH_4 analysis suggested that CO_2 reduction with H_2 is the dominant methanogenic pathway in marine sediments (Whiticar, 1999). It remains largely unknown if syntrophic acetate oxidation coupled to hydrogenotrophic methanogenesis in deep subseafloor sediments exists, although acetogenesis is considered as an important metabolic pathway in some deep subseafloor environments (Parkes *et al*., 2005; Lever *et al*., 2010). Due to the higher affinity of sulfate reducers for hydrogen and acetate, methanogenesis may become a dominant process only in deeper sediment layers in which the sulfate has been exhausted (Liu and Whitman, 2008). Methylated compounds for methanogenesis would be generated from osmolytes of bacteria, algae, phytoplankton, and plants in marine sediments (Liu and Whitman, 2008). Marine sedimentary sulfate reducers do not utilize methylotrophic compounds effectively, and thus, theses compounds have been suggested as non-competitive substrates between sulfate reduction and methanogenesis (Oremland and Polcin, 1982).

The microbially mediated methanogenesis is catalyzed by several enzymatic reactions. The last enzymatic step catalyzed by the methyl-coenzyme M reductase (MCR) is common to all methanogenic pathways. MCR with coenzyme F_{430} converts methyl-coenzyme M (CH_3-S-CoM) and coenzyme B (H-S-CoB) into CH_4 and the heterodisulfide of coenzymes M and B (CoM-S-S-CoB) (eq. 34) (Thauer, 1998):

$$CH_3\text{-S-CoM} + \text{H-S-CoB} \rightarrow CH_4 + \text{CoM-S-S-CoB} \qquad (34)$$

Comparative phylogenetic studies have shown that the trees of the *mcrA* gene, which encodes the alpha subunit of MCR, and 16S rRNA, have strikingly similar topologies (Luton *et al*., 2002). Thus, the use of the *mcrA* gene as the target marker gene is widely accepted as a detection method for methanogens in the environment (Narihiro and Sekiguchi, 2011).

1.1.6 Anaerobic oxidation of methane

The evidence of the microbially mediated anaerobic oxidation of methane (AOM) was firstly obtained by geochemical observations showing that methane rises from deeper sediment horizons disappears before contact with oxygen (Martens and Berner, 1974; Barnes and Goldberg, 1976; Reeburgh, 1976) (**Fig. 1-6**). Subsequently, radioactive tracer incubations using $^{14}CH_4$ and $^{35}SO_4$ showed that methane oxidation coincided with sulfate reduction (Iversen and Jørgensen, 1985). This field observation suggested that the AOM is coupled to sulfate reduction (eq. 35):

$$CH_4 + SO_4^{2-} \rightarrow HCO_3^- + HS^- + H_2O \quad (35)$$

In 2000, the microbes involved in AOM were visualized by fluorescence *in situ* hybridization (FISH) targeting 16S rRNA (Boetius *et al*., 2000). The FISH observation suggested that the consortia of archaeal anaerobic methanotrophs (ANMEs) and sulfate-reducing bacteria (SRB) mediate AOM. FISH-secondary ion mass spectrometry (SIMS) analysis showed that ANME cells were highly depleted in ^{13}C as expected when methane is utilized as the carbon source (Orphan *et al*., 2001). Today, AOM is recognized as the major methane sink of the Earth and is an important microbial process in the planet's carbon cycle and control of greenhouse gas emission from marine sediments (Reeburgh, 2007). Recently, AOM coupled to manganese (eq. 36), iron (eq. 37), and nitrate reduction (eq. 38) by ANME archaea have been reported (Beal *et al*., 2009; Haroon *et al*., 2013):

$$CH_4 + 4MnO_2 + 7H^+ \rightarrow HCO_3^- + 4Mn^{2+} + 5H_2O \quad (36)$$

$$CH_4 + 8Fe(OH)_3 + 15H^+ \rightarrow HCO_3^- + 8Fe^{2+} + 21H_2O \quad (37)$$

$$CH_4 + 4NO_3^- \rightarrow CO_2 + 4NO_3^- + 2H_2O \quad (38)$$

ANMEs are phylogenetically close to known methanogenic archaeal lineages and are classified into three phylogenetic lineages called ANME-1, -2, and -3 (Knittel and Boetius, 2009 and 2010). Based on the 16S rRNA phylogeny, ANME-1 is distantly related to the orders *Methanosarcinales* and *Methanomicrobiales* (Hinrichs *et al*., 1999), while ANME-2 (Orphan *et al*., 2001) and ANME-3 (Niemann *et al*., 2006) belong to the *Methanosarcinales* (**Fig. 1-5**). Within the ANME-2 clade, four subgroups, ANME-2a to -2d, can be distinguished (Orphan *et al*., 2001; Knittel *et al*., 2005; Haroon *et al*., 2013). Haroon *et al*. (2013) revealed that the ANME-2d lineage is capable of AOM coupled nitrate reduction, and proposed the family 'Methanoperedenaceae' for the

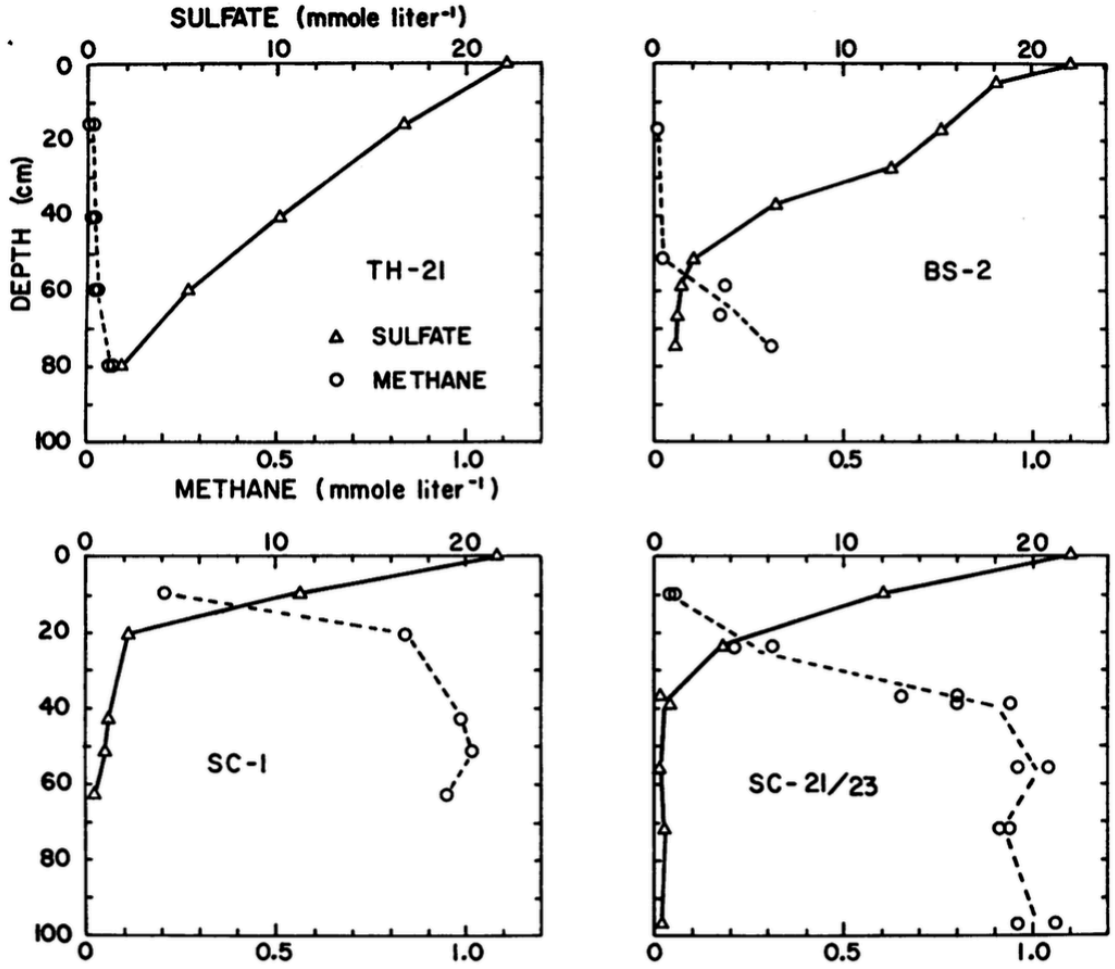

Figure 1-6. Concentrations of sulfate and methane in the interstitial waters of Long Island Sound sediments. Adapted from Martens and Berner (1974).

ANME-2d lineage.

AOM has been hypothesized to be operated via a reversal of the methanogenesis reaction called 'reverse methanogenesis' (Hoehler *et al*., 1994). This hypothesis has been supported by metagenomic, metatranscriptomic, and metaproteomic analyses (Hallam *et al*., 2004; Meyerdierks *et al*., 2010; Stokke *et al*., 2012; Wang *et al*., 2013). Purified MCR (a key enzyme of methanogenesis) from a methanogen, *Methanothermobacter marburgensis*, converts methane into methyl-coenzyme M under equilibrium conditions with an apparent maximum rate and Michaelis constant value consistent with the observed *in vivo* kinetics of the AOM (Scheller *et al*. 2010). This result also supports the hypothesis of 'reverse methanogenesis'. In contrast, a complete reverse methanogenesis pathway has been identified in only ANME-2a and ANME-2d genomes (Haroon *et al*., 2013; Wang *et al*., 2013).

Microscopic observation by FISH demonstrated that ANME-1 cells typically have a rectangular morphology and most often occur as single cells or in chains (**Fig. 1-7a**), whereas ANME-2 and -3 archaea are mostly coccoid-type shapes (**Fig. 1-7b**, **1-7c**, and **1-7d**) (Knittel and Boetius, 2009 and 2010). To date, the SEEP-SRB1 (**Fig. 1-8**),

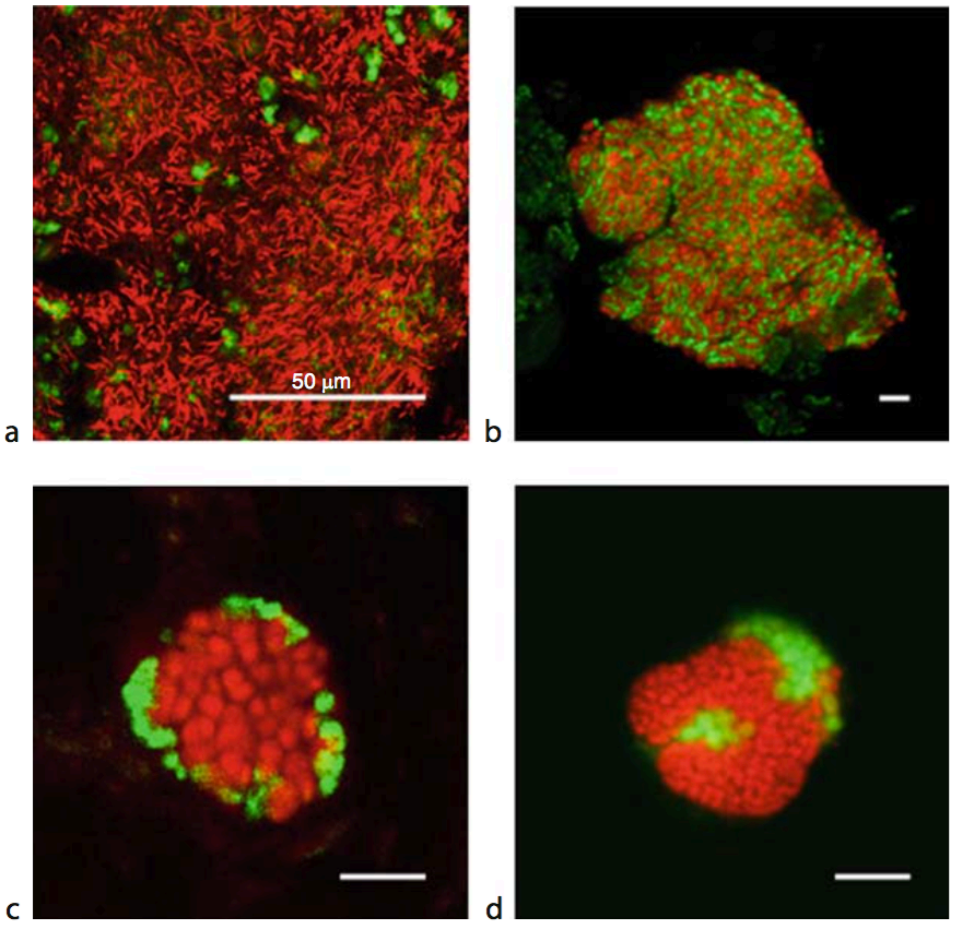

Figure 1-7. ANME consortia visualized by FISH. (a) Mat-type consortia of ANME-1 (red) and DSS (green); (b) mixed-type consortium of ANME-2a (red) and DSS (green); (c) shell-type consortium of ANME-2c (red) and DSS (green); (d) ANME-3 (red)/*Desulfobulbus* consortium (green). The scale bar in (b), (c), and (d) is 5 μm. Adapted from Knittel and Boetius (2010).

SEEP-SRB2 (also known as Eel-2 group; **Fig. 1-8**), HotSeep-1, seepDBB, and genus *Desulfobulbus* relatives (shown as "ANME-3-patrtner bacteria" in **Fig. 1-8**) within the class *Deltaproteobacteria* have been identified as the potential SRB partners (Niemann *et al*., 2006; Schreiber *et al*., 2010; Holler *et al*., 2011; Kleindienst *et al*., 2012; Green-Saxena *et al*., 2014). Schreiber *et al*. (2010) divided SEEP-SRB1 into six sub-groups (SEEP-SRB1a to SEEP-SRB1f) and identified SEEP-SRB1a as the dominant bacterial partner of ANME-2. In addition to the potential deltaproteobacterial SRB partners, the presence of alpha- and beta-proteobacterial microbes in association with ANME-2 has been reported (**Fig. 1-8**) (Pernthaler *et al*., 2008). ANME-2 aggregates without any potential bacterial partners were also found in the natural ecosystems (Orphan *et al*., 2002; Treude *et al*., 2005).

The intermediate(s) of AOM is thought to be scavenged as the electron donor for the SRB partner (Hoehler *et al*., 1994; Valentine and Reeburgh, 2000; Nauhaus *et al*., 2002). In contrast, *in vitro* studies using the potential

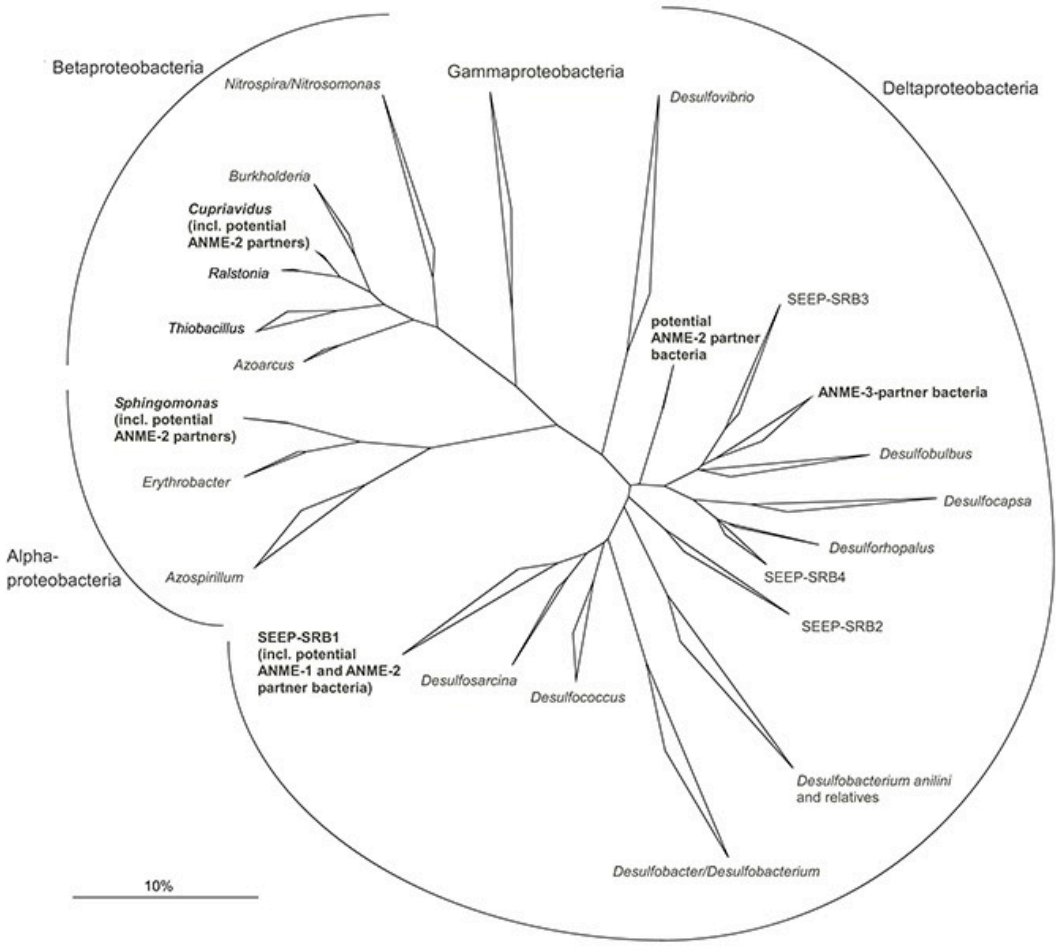

Figure 1-8. Phylogenetic tree showing the affiliations of 16S rRNA gene sequences of ANME partner bacteria to selected reference sequences. Bar, 10% estimated sequence divergence. Adapted from Knittel and Boetius (2009).

intermediate(s) (*e.g.*, H_2, formate, acetate, and methanol) suggested that these compounds are unlikely to be the intermediate of AOM (Nauhaus *et al*., 2002; Knittel and Boetius, 2009; Wegener *et al*., 2015). Milucka *et al*. (2012) demonstrated that ANME-2 archaea perform AOM coupled to sulfate reduction alone. Based on the mechanism proposed by Milucka *et al*. (2012), zero-valent sulfur—in the form of disulfide—is formed during AOM coupled to sulfate reduction by ANME-2 archaea (eq. 39), and subsequently, the produced disulfide is disproportionated by the DSS associated with the ANME-2 (eq. 8).

$$7CH_4 + 8SO_4^{2-} + 5H^+ \rightarrow 4HS_2^- + 7HCO_3^- + 11H_2O \qquad (39)$$

In contrast, all genes and proteins for dissimilatory sulfate reduction that have been retrieved from AOM systems are thought to be of bacterial origin (Basen *et al*., 2011; Milcka *et al*., 2012). Thus, the enzymatic mechanism of

sulfate reduction by ANME-2 archaea is still unclear. Recently, Wegener *et al*. (2015) reported that direct electron transfer using bacterial nanowires is likely to be a principal mechanism in thermophilic AOM microbial consortia. Single cell activity as measured by FISH-nanoSIMS also provides evidence of direct electron transfer in the AOM consortia (McGlynn *et al*., 2015).

1.2 Numerically and ecologically important marine sedimentary uncultivated archaea

Phylogenetic analysis of PCR-amplified 16S rRNA gene sequences revealed the presence of phylogenetically diverse uncultured microbial life in marine sediments. Members of Deep-Sea Archaeal Group (DSAG), Miscellaneous Crenarchaeotic Group (MCG), and Marine Benthic Group-D (MBG-D) within the domain *Archaea* have been hypothesized to be numerically and ecologically important in marine sediments because they often dominate archaeal 16S rRNA gene clone libraries (Fry *et al*., 2008; Lloyd *et al*., 2013).

DSAG (also known as Marine Benthic Group-B and 'Lokiarchaeota'; Vetriani *et al*., 1996; Spang *et al*., 2015) is an uncultivated archaeal lineage defined by Inagaki *et al*. (2003). Phylogenetic analysis revealed that the existence of three distinct monophyletic lineages (Alpha, Beta, and Gamma) within the DSAG (Jørgensen *et al*., 2013). DSAG sequences have repeatedly been detected in marine sediments, but some of DSAG sequences were retrieved from freshwater and terrestrial environments (Jørgensen *et al*., 2013). Archaeal lipids/cells-targeted stable carbon isotope analysis suggested that DSAG might assimilate sedimentary organic matter as a carbon source while performing AOM (Biddle *et al*., 2006). In contrast, geophysical and geochemical parameters, and DSAG-affiliated 16S rRNA gene distribution patterns suggested that members of DSAG are heterotrophic and involved in the iron and/or manganese cycle (Jorgensen *et al*., 2012; Jørgensen *et al*., 2013). FISH visualized DSAG archaeal cells from Black Sea microbial mats were small coccoid cells (0.2 to 0.4 μm) and occurred mostly in large clusters (Knittel *et al*., 2005). The genomic characteristics of DSAG showed that DSAG archaea encode eukaryotic signature proteins that are suggestive of sophisticated membrane remodeling capabilities (Spang *et al*., 2015).

MCG (also known as 'Bathyarchaeota'; Meng *et al*., 2014) is an uncultivated archaeal lineage proposed by Inagaki *et al*. (2003). Kubo *et al*. (2012) first divided MCG into 17 phylogenetically distinct sub-groups, and then, Lazar *et al*. (2015) proposed additional MCG sub-groups of MCG-18, MCG-19, and MCG-20. Most of the MCG cells reported by Kubo *et al*. (2013) were small coccoid with a cell size of 0.4–0.5 μm, and aggregates of 2–5 cells of MCG were also found. Biddle *et al*. (2006) hypothesized that MCG archaea perform 'dissimilatory' anaerobic methane oxidation. This hypothesis is partly supported by the recent discovery of the existence of homologs of the genes necessary for methane metabolism in the genomes of MCG (Evans *et al*., 2015). In contrast, the distribution patterns of 16S rRNA genes of MCG have not supported the AOM by MCG (Kubo *et al*., 2012). Stable isotope probing experiments with ^{13}C-labeled acetate showed that some members of MCG utilize acetate (Webster *et al*., 2010; Na *et al*., 2015). Lloyd *et al*. (2013) reported that a genome of MCG encoded extracellular

protein-degrading enzymes such as gingipain and clostripain. Metagenomic and functional gene expression analyses reported by Meng *et al*. (2014) suggested that some MCG members might have a role in the degradation of aromatic compounds.

MBG-D (also known as Marine Group III and Deep Sea Hydrothermal Vent Group I; DeLong, 1998; Takai and Horikoshi, 1999) is an uncultured archaeal group proposed by Vetriani *et al*. (1999). Comparative 16S rRNA-based phylogenetic study showed that the MBG-D is a well-supported clade affiliated with *Thermoplasatales* (Durbin and Teske, 2011). As with MCG, the MBG-D archaeal genome encodes extracellular protein-degrading enzymes and might have the potential to degrade detrital protein in marine sediments (Lloyd *et al*., 2013).

1.3 Cold seeps

Cold seeps are the areas where the upward advection of methane and other accompanying gases from the subsurface to the seafloor occurs (Boetius and Wenzhöfer, 2013) (**Fig. 1-9**). In contrast to hydrothermal vent fluids, seepage fluids at cold seeps are not induced by hydrothermal activity. Seepage fluids at cold seeps are generally enriched in methane or hydrogen sulfide. Thus, chemosynthetic microbes, which use methane or hydrogen sulfide as their energy source, proliferate as primary producers. In addition, the chemosynthetic microbial communities are regarded as an important food source for the cold seep-associated fauna. Active cold seeps are located in subduction zones and in passive margins. Cold-seep sites were first discovered in the marine sediments in the Gulf of Mexico in 1983 (Paull *et al*., 1984). Now, thousands of cold-seep systems have been detected at continental margins worldwide (Boetius and Wenzhöfer, 2013). A major type of cold-seep systems is the submarine mud volcano (Niemann and Boetius, 2010). The global inventory of methane hydrates in marine sediments is ≥455 Gt-carbon (Wallmann *et al*., 2012) and cold seeps are often associated with gas (methane) hydrate deposits. In contrast, a very small amount of 0.03 Gt-methane is released annually from cold seeps as the result of microbial activity (Boetius and Wenzhöfer, 2013) (**Fig. 1-9**). At most cold seeps, it is assumed that aerobic methanotrophy plays an insignificant role at cold seeps due to the very thin oxygenated layers observed at cold seeps (Knittel and Boetius, 2009; Ruff *et al*., 2013). ANME archaea predominate the anoxic sediment and mainly occur in association with putative SRB partners. Sulfur-oxidizing bacterial lineages of the order *Thiotrichales* in the class *Gammaproteobacteria* is often found as the dominant microbial components at methane seeps (Ruff *et al*. 2015). Recent estimates suggested that between 20% and 80% of the methane is consumed by methanotrophic microorganisms at cold seeps and the proportion of methane consumed varies with fluid flow rate (Boetius and Wenzhöfer, 2013).

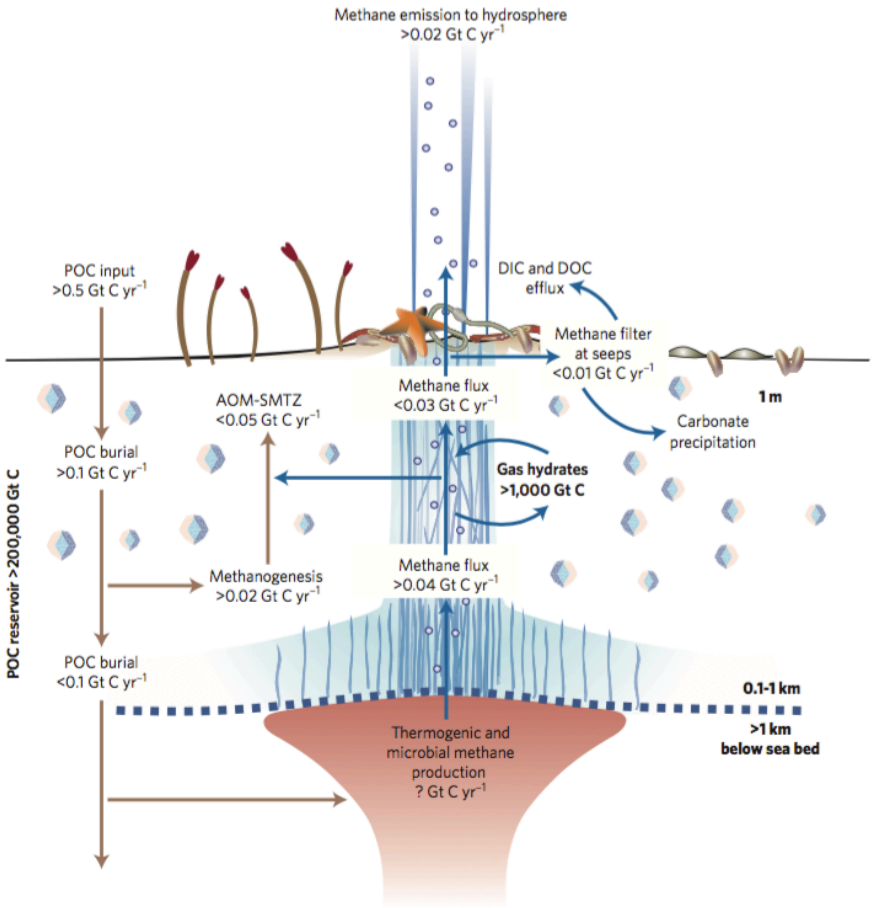

Figure 1-9. Cold-seep methane and carbon fluxes at continental slopes. DOC, dissolved organic carbon; DIC, dissolved inorganic carbon; POC, particulate organic carbon; AOM-SMTZ, anaerobic oxidation of methane in the sulfate–methane transition zone. Adapted from Boetius and Wenzhöfer (2013).

1.4 The objective of this thesis

The objective of this thesis was to promote a better understanding of the ecology of microbes relevant to marine sedimentary carbon and sulfur cycling, especially that of the phylogenetic diversity and distributions of the microbes. Culture-dependent and -independent experiments were performed using the sediment samples retrieved from marine sediments on the northwestern Pacific margin off Japan, to achieve the objective. The precise objective of each chapter is summarized as follows:

Cultivation of AOM microbial community using a continuous-flow bioreactor (Chapter II).

The microbially mediated anaerobic oxidation of methane (AOM) is an important microbial process of the Earth's biogeochemical cycling. In contrast, due to the difficulties associated with the cultivation of AOM-associated microbes, the details of marine sedimentary AOM systems and physiological properties of AOM-associated microbes remain poorly understood. Chapter II described the enrichment result of AOM

microbial community using a continuous-flow bioreactor, so-called down-flow hanging sponge (DHS) bioreactor. The main objective of this chapter was to evaluate the applicability of the DHS bioreactor to cultivate an AOM microbial community and obtain new insights into the AOM systems in the methane seep-sediment of the Nankai Trough.

Possible effect of redox potential on methane-seep sediment microbial community structure development (Chapter III).

Methane seeps show moderate levels of microbial richness compared with other marine sedimentary ecosystems and possess microbes that play an important role in carbon and sulfur cycling. In addition, the local variation of methane-seep microbial community structure within the same sediment core has been reported. In contrast, knowledge of the factor(s) controlling the methane-seep microbial community structure development remains limited. The objective of Chapter III was to reveal possible effect of quinone compound-mediated anaerobic redox potential difference on AOM-associated microbial community structure development in the methane-seep sediment of the Nankai Trough. The methane-seep sediment-associated AOM community obtained in Chapter II was subsequently cultivated using a bio-electrochemical reactor and a model quinone compound of anthraquinone-2, 6-disulfonate (AQDS) to achieve the objective.

Phylogenetic diversity survey of *aprA* genes in subseafloor sediments (Chapter IV).

Sulfur-metabolizing microbes have significant roles in biogeochemical processes in marine sediments. However, the phylogenetic diversity and distribution of functional marker genes relevant to the subseafloor sulfur cycling remains largely unknown. The goal of Chapter IV was to identify putative sulfur-metabolizing microbial components in the subseafloor sediment on the northwestern Pacific off Japan and obtain new insights into the microbial sulfur cycling using adenosine-5′-phosphosulfate reductase alpha subunit (*aprA*) gene, which encodes a key enzyme in microbial sulfate reduction and sulfur oxidation, as a functional marker gene.

1.5 References

Baena S, Fardeau M-L, Labat M, Ollivier B, Garcia J-L, Patel BKC (1998) *Desulfovibrio aminophilus* sp. nov., a novel amino acid degrading and sulfate reducing bacterium from an anaerobic dairy wastewater lagoon. *Syst Appl Microbiol* 21:498–504.

Bak F, Cypionka H (1987) A novel type of energy metabolism involving fermentation of inorganic sulphur compounds. *Nature* 326:891–892.

Bak F, Pfennig N (1987) Chemolithotrophic growth of *Desulfovibrio sulfodismutans* sp. nov. by disproportionation of inorganic sulfur compounds. *Arch Microbiol* 147:184–189.

Bale SJ, Goodman K, Rochelle PA, Marchesi JR, Fry JC, *et al*. (1997) *Desulfovibrio profundus* sp. nov., a novel barophilic sulfate-reducing bacterium from deep sediment layers in the Japan Sea. *Int J Syst Bacteriol* 47:515–521.

Barnes RO, Goldberg ED (1976) Methane production and consumption in anoxic marine sediments. Geology 4:297–300.

Basen M, Krüger M, Milucka J, Kuever J, Kahnt J, *et al*. (2011) Bacterial enzymes for dissimilatory sulfate reduction in a marine microbial mat (Black Sea) mediating anaerobic oxidation of methane. *Environ Microbiol* 13:1370–1379.

Beal EJ, House CH, Orphan VJ (2009) Manganese- and iron-dependent marine methane oxidation. *Science* 325:184–187.

Biddle JF, Lipp JS, Lever MA, Lloyd KG, Sørensen KB, *et al*. (2006) Heterotrophic Archaea dominate

sedimentary subsurface ecosystems off Peru. *Proc Natl Acad Sci U S A* 103:3846–3851.
Boetius A, Ravenschlag K, Schubert CJ, Rickert D, Widdel F, *et al*. (2000) A marine microbial consortium apparently mediating anaerobic oxidation of methane. *Nature* 407:623–626.
Boetius A, Wenzhöfer F (2013) Seafloor oxygen consumption fuelled by methane from cold seeps. *Nat Geosci* 6:725–734.
Bowles MW, Mogollón JM, Kasten S, Zabel M, Hinrichs, K-U (2014) Global rates of marine sulfate reduction and implications for sub-sea-floor metabolic activities. *Science* 344:889–891.
Castresana J, Moreira D (1999) Respiratory chains in the last common ancestor of living organisms. *J Mol Evol* 49:453–460.
DeLong EF (1998) Everything in moderation: archaea as "non-extremophiles". *Curr Opin Genet Devel* 8:649−654.
DeLong EF (2004) Microbial life breathes deep. *Science* 306:2198–2200.
Durbin AM, Teske A (2011) Microbial diversity and stratification of South Pacific abyssal marine sediments. *Environ Microbiol* 13:3219–3234.
D'Hondt S, Rutherford S, Spivack AJ (2002) Metabolic activity of subsurface life in deep-sea sediments. *Science* 295:2067–2070.
D'Hondt S, Jørgensen BB, Miller DJ, Batzke A, Blake R, *et al*. (2004) Distributions of microbial activities in deep subseafloor sediments. *Science* 306:2216–2221.
D'Hondt S, Spivack AJ, Pockalny R, Ferdelman TG, Fischer JP, *et al*. (2009) Subseafloor sedimentary life in the South Pacific Gyre. *Proc Natl Acad Sci U S A* 106:11651–11656.
D'Hondt S, Inagaki F, Zarikian CA, Abrams LJ, Dubois N, *et al*. (2015) Presence of oxygen and aerobic communities from sea floor to basement in deep-sea sediments. *Nat Geosci* 8:299–304.
Evans PN, Parks DH, Chadwick GL, Robbins SJ, Orphan VJ, *et al.* (2015) Methane metabolism in the archaeal phylum Bathyarchaeota revealed by genome-centric metagenomics. *Science* 350:434–438.
Fichtel K, Mathes F, Könneke M, Cypionka H, Engelen B (2012) Isolation of sulfate-reducing bacteria from sediments above the deep-subseafloor aquifer. *Front Microbiol* 3:65.
Finster K, Liesack W, Thamdrup B (1998) Elemental sulfur and thiosulfate disproportionation by *Desulfocapsa sulfoexigens* sp. nov., a new anaerobic bacterium isolated from marine surface sediment. *Appl Environ Microbiol* 64:119–125.
Finster K (2008) Microbiological disproportionation of inorganic sulfur compounds. *J Sulfur Chem* 29:281–292.
Fry JC, Parkes RJ, Cragg BA, Weightman AJ, Webster G (2008) Prokaryotic biodiversity and activity in the deep subseafloor biosphere. *FEMS Microbiol Ecol* 66:181–196.
Green-Saxena A, Dekas AE, Dalleska NF, Orphan VJ (2014) Nitrate-based niche differentiation by distinct sulfate-reducing bacteria involved in the anaerobic oxidation of methane. *ISME J* 8:150–163.
Hallam SJ, Putnam N, Preston CM, Detter JC, Rokhsar D, *et al*. (2004) Reverse methanogenesis: testing the hypothesis with environmental genomics. *Science* 305:1457–1462.
Haroon MF, Hu S, Shi Y, Imelfort M, Keller J, *et al*. (2013) Anaerobic oxidation of methane coupled to nitrate reduction in a novel archaeal lineage. *Nature* 500:567–570.
Hernandez-Eugenio G, Fardeau ML, Patel B (2000) *Desulfovibrio mexicanus* sp. nov., a sulfate-reducing bacterium isolated from an upflow anaerobic sludge blanket (UASB) reactor treating cheese wastewaters. *Anaerobe* 6:305–312.
Hinrichs K-U, Hayes JM, Sylva SP, Brewer PG, DeLong EF (1999) Methane-consuming archaebacteria in marine sediments. *Nature* 398:802–805.
Hirose T, Kawagucci S, Suzuki K (2011) Mechanoradical H_2 generation during simulated faulting: Implications for an earthquake‐driven subsurface biosphere. *Geophys Res Lett* 38:L17303.
Hoehler TM, Alperin MJ, Albert DB, Martens CS (1994) Field and laboratory studies of methane oxidation in an anoxic marine sediment: Evidence for a methanogen-sulfate reducer consortium. *Glob Biogeochem Cycles* 8:451–463.
Holler T, Widdel F, Knittel K, Amann R, Kellermann MY, *et al*. (2011) Thermophilic anaerobic oxidation of methane by marine microbial consortia. *ISME J* 5:1946–1956.
Holmkvist L, Ferdelman TG, Jørgensen, BB (2011) A cryptic sulfur cycle driven by iron in the methane zone of marine sediment (Aarhus Bay, Denmark). *Geochim Cosmochim Acta* 75:3581–3599.
Iino T, Tamaki H, Tamazawa S, Ueno Y, Ohkuma M, *et al*. (2013) *Candidatus* Methanogranum caenicola: a novel methanogen from the anaerobic digested sludge, and proposal of *Methanomassiliicoccaceae* fam. nov. and *Methanomassiliicoccales* ord. nov., for a methanogenic lineage of the class *Thermoplasmata*. *Microbes Environ* 28:244–250.
Inagaki F, Suzuki M, Takai K, Oida H, Sakamoto T, *et al*. (2003) Microbial communities associated with geological horizons in coastal subseafloor sediments from the sea of Okhotsk. *Appl Environmental Microbiol*,

69:7224–7235.
Iversen N, Jørgensen BB (1985) Anaerobic methane oxidation rates at the sulfate-methane transition in marine sediments from Kattegat and Skagerrak (Denmark). *Limnol Oceanogr* 30:944−955.
Jackson BE, McInerney MJ (2000) Thiosulfate disproportionation by *Desulfotomaculum thermobenzoicum*. *Appl Environ Microbiol* 66:3650–3653.
Janssen PH, Schuhmann A, Bak F, Liesack W (1996) Disproportionation of inorganic sulfur compounds by the sulfate-reducing bacterium *Desulfocapsa thiozymogenes* gen. nov., sp. nov. *Arch Microbiol* 166:184–192.
Jorgensen SL, Hannisdal B, Lanzén A, Baumberger T, Flesland K, *et al*. (2012) Correlating microbial community profiles with geochemical data in highly stratified sediments from the Arctic Mid-Ocean Ridge. *Proc Natl Acad Sci U S A* 109:E2846–55.
Jørgensen SL, Thorseth IH, Pedersen RB, Baumberger T, Schleper C (2013) Quantitative and phylogenetic study of the Deep Sea Archaeal Group in sediments of the Arctic mid-ocean spreading ridge. *Front Microbiol* 4:299.
Kallmeyer J, Pockalny R, Adhikari RR, Smith DC, D'Hondt S (2012) Global distribution of microbial abundance and biomass in subseafloor sediment. *Proc Natl Acad Sci U S A* 109:16213–16216.
Kleindienst S, Ramette A, Amann R, Knittel K (2012) Distribution and *in situ* abundance of sulfate-reducing bacteria in diverse marine hydrocarbon seep sediments. *Environ Microbiol* 14:2689–2710.
Knab NJ, Cragg BA, Hornibrook ERC, Holmkvist L, Pancost RD, *et al*. (2009) Regulation of anaerobic methane oxidation in sediments of the Black Sea. *Biogeosciences* 6:1505–1518.
Knittel K, Lösekann T, Boetius A, Kort R, Amann R (2005) Diversity and distribution of methanotrophic archaea at cold seeps. *Appl Environ Microbiol* 71:467–479.
Knittel K, Boetius A (2009) Anaerobic oxidation of methane: progress with an unknown process. Annu Rev Microbiol 63:311–334.
Knittel K, Boetius A (2010) Anaerobic Methane Oxidizers. *In* Timmis KN (Ed.), Handbook of Hydrocarbon and Lipid Microbiology, Springer Berlin Heidelberg, pp. 2023–2032.
Krekeler D, Sigalevich P, Teske A, Cypionka H, Cohen Y (1997) A sulfate-reducing bacterium from the oxic layer of a microbial mat from Solar Lake (Sinai), *Desulfovibrio oxyclinae* sp. nov. *Arch Microbiol* 167:369–375.
Krämer M, Cypionka H (1989) Sulfate formation via ATP sulfurylase in thiosulfate- and sulfite-disproportionating bacteria. *Arch Microbiol* 151:232–237.
Kubo K, Lloyd KG, Biddle JF, Amann R, Teske A, Knittel K (2012) Archaea of the Miscellaneous Crenarchaeotal Group are abundant, diverse and widespread in marine sediments. *ISME J* 6:1949–1965.
Lan Y, Deng B, Kim C, Thornton EC, Xu H (2005) Catalysis of elemental sulfur nanoparticles on chromium (VI) reduction by sulfide under anaerobic conditions. *Environ Sci Technol* 39:2087–2094.
Lazar CS, Biddle JF, Meador TB, Blair N, Hinrichs K-U, Teske AP (2015) Environmental controls on intragroup diversity of the uncultured benthic archaea of the miscellaneous Crenarchaeotal group lineage naturally enriched in anoxic sediments of the White Oak River estuary (North Carolina, USA). *Environ Microbiol* 17:2228–2238.
Lenk S, Arnds J, Zerjatke K, Musat N, Amann R, Mußmann M. (2011) Novel groups of *Gammaproteobacteria* catalyse sulfur oxidation and carbon fixation in a coastal, intertidal sediment. *Environ Microbiol* 13:758–774.
Lever MA, Heuer VB, Morono Y, Masui N, Schmidt F, *et al*. (2010) Acetogenesis in deep subseafloor sediments of the Juan de Fuca Ridge Flank: a synthesis of geochemical, thermodynamic, and gene-based evidence. *Geomicrobiol J* 27:183–211.
Liu Y, Whitman WB (2008) Metabolic, phylogenetic, and ecological diversity of the methanogenic archaea. Ann N Y Acad Sci 1125:171–189.
Lloyd KG, Schreiber L, Petersen DG, Kjeldsen KU, Lever MA, *et al*. (2013) Predominant archaea in marine sediments degrade detrital proteins. *Nature* 496:215–218.
Lovley DR, Phillips EJ (1994) Novel processes for anaerobic sulfate production from elemental sulfur by sulfate-reducing bacteria. *Appl Environ Microbiol* 60:2394–2399.
Loy A, Duller S, Baranyi C, Mußmann M, Ott J, *et al*. (2009) Reverse dissimilatory sulfite reductase as phylogenetic marker for a subgroup of sulfur-oxidizing prokaryotes. *Environ Microbiol* 11:289–299.
Luton PE, Wayne JM, Sharp RJ, Riley PW (2002) The *mcrA* gene as an alternative to 16S rRNA in the phylogenetic analysis of methanogen populations in landfill. *Microbiology* 148:3521–3530.
Martens CS, Berner RA (1974) Methane production in the interstitial waters of sulfate-depleted marine sediments. *Science* 185:1167–1169.
McCollom TM, Bach W (2009) Thermodynamic constraints on hydrogen generation during serpentinization of ultramafic rocks. *Geochim Cosmochim Acta* 73:856–875.
McGlynn SE, Chadwick GL, Kempes CP, Orphan VJ (2015) Single cell activity reveals direct electron transfer in methanotrophic consortia. *Nature* 526:531–535.
Meng J, Xu J, Qin D, He Y, Xiao X, Wang F (2014) Genetic and functional properties of uncultivated MCG archaea assessed by metagenome and gene expression analyses. *ISME J* 8:650–659.

Meyer B, Imhoff JF, Kuever J (2007a) Molecular analysis of the distribution and phylogeny of the *soxB* gene among sulfur-oxidizing bacteria - evolution of the Sox sulfur oxidation enzyme system. *Environ Microbiol* 9:2957–2977.

Meyer B, Kuever J (2007b) Molecular analysis of the distribution and phylogeny of dissimilatory adenosine-5'-phosphosulfate reductase-encoding genes (*aprBA*) among sulfur-oxidizing prokaryotes. *Microbiology* 153:3478–3498.

Meyer B, Kuever J (2007c) Molecular analysis of the diversity of sulfate-reducing and sulfur-oxidizing prokaryotes in the environment, using *aprA* as functional marker gene. *Appl Environ Microbiol* 73:7664–7679.

Meyer B, Kuever J (2007d) Phylogeny of the alpha and beta subunits of the dissimilatory adenosine-5'-phosphosulfate (APS) reductase from sulfate-reducing prokaryotes –origin and evolution of the dissimilatory sulfate-reduction pathway. *Microbiology* 153:2026–2044.

Meyerdierks A, Kube M, Kostadinov I, Teeling H, Glöckner FO, Reinhardt R, Amann R (2010) Metagenome and mRNA expression analyses of anaerobic methanotrophic archaea of the ANME-1 group. *Environ Microbiol* 12:422–439.

Milucka J, Ferdelman TG, Polerecky L, Franzke D, Wegener G, *et al*. (2012) Zero-valent sulphur is a key intermediate in marine methane oxidation. *Nature* 491:541–546.

Mohn WW, Tiedje JM (1990) Catabolic thiosulfate disproportionation and carbon dioxide reduction in strain DCB-1, a reductively dechlorinating anaerobe. *J Bacteriol* 172:2065–2070.

Muyzer G, Kuenen JG, Robertson, LA (2013) Colorless Sulfur Bacteria. *In* Rosenberg E, DeLong EF, Lory S, Stackebrandt E, Thompson F (eds.), The Prokaryotes (4th edition), Springer-Verlag Berlin Heidelberg, pp. 555–588.

Müller AL, Kjeldsen KU, Rattei T, Pester M, Loy A (2015) Phylogenetic and environmental diversity of DsrAB-type dissimilatory (bi)sulfite reductases. *ISME J* 9:1152–1165.

Na H, Lever MA, Kjeldsen KU, Schulz F, Jørgensen BB (2015) Uncultured Desulfobacteraceae and Crenarchaeotal group C3 incorporate ^{13}C-acetate in coastal marine sediment. *Environ Microbiol Rep* 7:614–22

Narihiro T, Sekiguchi Y (2011) Oligonucleotide primers, probes and molecular methods for the environmental monitoring of methanogenic archaea. *Microb Biotechnol* 4:585–602.

Nauhaus K, Boetius A, Kruger M, Widdel F (2002) *In vitro* demonstration of anaerobic oxidation of methane coupled to sulphate reduction in sediment from a marine gas hydrate area. *Environ Microbiol* 4:296–305.

Niemann H, Lösekann T, de Beer D, Elvert M, Nadalig T, *et al*. (2006) Novel microbial communities of the Haakon Mosby mud volcano and their role as a methane sink. *Nature* 443:854–858.

Niemann H, Boetius A (2010) Mud volcanoes. *In* Timmis KN (ed.), Handbook of Hydrocarbon and Lipid Microbiology, Springer Berlin Heidelberg, pp. 205–214.

Obraztsova AY, Francis CA, Tebo BM (2002) Sulfur disproportionation by the facultative anaerobe *Pantoea agglomerans* SP1 as a mechanism for chromium (VI) reduction. *Geomicrobiol J* 19:121–132.

Oremland RS, Polcin S (1982) Methanogenesis and sulfate reduction: competitive and noncompetitive substrates in estuarine sediments. *Appl Environ Microbiol* 44:1270–1276.

Orphan VJ, House CH, Hinrichs K-U, McKeegan KD, DeLong EF (2001) Methane-consuming archaea revealed by directly coupled isotopic and phylogenetic analysis. *Science* 293:484–487.

Orphan VJ, House CH, Hinrichs K-U, McKeegan KD, DeLong EF (2002) Multiple archaeal groups mediate methane oxidation in anoxic cold seep sediments. *Proc Natl Acad Sci U S A* 99:7663–7668.

Parkes RJ, Webster G, Cragg BA, Weightman AJ, Newberry CJ, *et al*. (2005) Deep sub-seafloor prokaryotes stimulated at interfaces over geological time. *Nature* 436:390–394.

Paull CK, Hecker B, Commeau R, Freeman-Lynde RP, Neumann C, *et al*. (1984) Biological communities at the Florida escarpment resemble hydrothermal vent taxa. *Science* 226:965–967.

Peduzzi S, Tonolla M, Hahn D (2003) Isolation and characterization of aggregate-forming sulfate-reducing and purple sulfur bacteria from the chemocline of meromictic Lake Cadagno, Switzerland. *FEMS Microbiol Ecol* 45: 29–37.

Pernthaler A, Dekas AE, Brown CT, Goffredi SK, Embaye T, Orphan VJ (2008) Diverse syntrophic partnerships from deep-sea methane vents revealed by direct cell capture and metagenomics. *Proc Natl Acad Sci U S A* 105:7052–7057.

Pfeffer C, Larsen S, Song J, Dong M, Besenbacher F, *et al*. (2012) Filamentous bacteria transport electrons over centimetre distances. *Nature* 491:218–221.

Pjevac P, Kamyshny A Jr, Dyksma S, Mußmann M. (2014) Microbial consumption of zero-valence sulfur in marine benthic habitats. *Environ Microbiol* 16:3416–3430.

Poser A, Lohmayer R, Vogt C, Knoeller K, Planer-Friedrich B, *et al*. (2013) Disproportionation of elemental sulfur by haloalkaliphilic bacteria from soda lakes. *Extremophiles* 17:1003–1012.

Rabus R, Venceslau SS, Wöhlbrand L, Voordouw G, Wall JD, Pereira IAC (2015) A post-genomic view of the

ecophysiology, catabolism and biotechnological relevance of sulphate-reducing prokaryotes. *Adv Microb Physiol* 66:55–321.

Reeburgh WS (1976) Methane consumption in Cariaco Trench waters and sediments. *Earth Planet Sc Lett* 28:337–344.

Reeburgh WS (2007) Oceanic methane biogeochemistry. *Chem Rev*107:486–513.

Ruff SE, Arnds J, Knittel K, Amann R, Wegener G, *et al*. (2013) Microbial communities of deep-Sea methane seeps at Hikurangi continental margin (New Zealand). *PLoS One* 8:e72627.

Ruff SE, Biddle JF, Teske AP, Knittel K, Boetius A, Ramette A (2015) Global dispersion and local diversification of the methane seep microbiome. *Proc Natl Acad Sci U S A* 112:4015–4020.

Scheller S, Goenrich M, Boecher R, Thauer RK, Jaun B (2010) The key nickel enzyme of methanogenesis catalyses the anaerobic oxidation of methane. *Nature* 465:606–608.

Schreiber L, Holler T, Knittel K, Meyerdierks A, Amann R (2010) Identification of the dominant sulfate-reducing bacterial partner of anaerobic methanotrophs of the ANME-2 clade. *Environ Microbiol* 12:2327–2340.

Shen Y, Buick R, Canfield DE (2001) Isotopic evidence for microbial sulphate reduction in the early Archaean era. *Nature* 410:77–81.

Slobodkin AI, Reysenbach A-L, Slobodkina GB, Baslerov RV, Kostrikina NA, *et al*. (2012) *Thermosulfurimonas dismutans* gen. nov., sp. nov., an extremely thermophilic sulfur-disproportionating bacterium from a deep-sea hydrothermal vent. *Int J Syst Evol Microbiol* 62:2565–2571.

Slobodkin AI, Reysenbach A-L, Slobodkina GB, Kolganova TV, Kostrikina NA, Bonch-Osmolovskaya EA (2013) *Dissulfuribacter thermophilus* gen. nov., sp. nov., a thermophilic, autotrophic, sulfur-disproportionating, deeply branching deltaproteobacterium from a deep-sea hydrothermal vent. *Int J Syst Evol Microbiol* 63:1967–1971.

Sorokin DY, Tourova TP, Henstra AM, Stams AJM, Galinski EA, Muyzer G (2008) Sulfidogenesis under extremely haloalkaline conditions by *Desulfonatronospira thiodismutans* gen. nov., sp. nov., and *Desulfonatronospira delicata* sp. nov. – a novel lineage of *Deltaproteobacteria* from hypersaline soda lakes. *Microbiology* 154:1444–1453.

Spang A, Saw JH, Jørgensen SL, Zaremba-Niedzwiedzka K, Martijn J, *et al*. (2015) Complex archaea that bridge the gap between prokaryotes and eukaryotes. *Nature* 521:173–179.

Stokke R, Roalkvam I, Lanzen A, Haflidason H, Steen IH (2012) Integrated metagenomic and metaproteomic analyses of an ANME-1-dominated community in marine cold seep sediments. *Environ Microbiol* 14:1333–1346.

Takai K, Horikoshi K (1999) Genetic diversity of archaea in deep-sea hydrothermal vent environments. Genetics 152:1285–1297.

Tang K, Baskaran V, Nemati M (2009) Bacteria of the sulphur cycle: an overview of microbiology, biokinetics and their role in petroleum and mining industries. Biochem Eng J 44:73–94

Tarpgaard IH, Røy H, Jørgensen BB (2011) Concurrent low-and high-affinity sulfate reduction kinetics in marine sediment. Geochim Cosmochim Acta 75:2997–3010.

Thamdrup B, Finster K, Hansen JW, Bak F (1993) Bacterial disproportionation of elemental sulfur coupled to chemical reduction of iron or manganese. *Appl Environ Microbiol* 59:101–108.

Thauer RK (1998) Biochemistry of methanogenesis: a tribute to Marjory Stephenson. *Microbiology* 144:2377–2406.

Treude T, Krüger M, Boetius A, Jørgensen BB (2005) Environmental control on anaerobic oxidation of methane in the gassy sediments of Eckernförde Bay (German Baltic). *Limnol Oceanogr* 50:1771–1786.

Treude T, Krause S, Maltby J, Dale AW, Coffin R, Hamadan LJ (2014) Sulfate reduction and methane oxidation activity below the sulfate-methane transition zone in Alaskan-Beaufort continental margin sediments: Implications for deep sulfur cycling. *Geochim Cosmochim Acta* 144:217–237.

Valentine DL, Reeburgh WS (2000) New perspectives on anaerobic methane oxidation. *Environ Microbiol* 2:477–484.

Vetriani C, Jannasch HW, MacGregor BJ, Stahl DA, Reysenbach A-L (1999) Population structure and phylogenetic characterization of marine benthic Archaea in deep-sea sediments. *Appl Environ Microbiol* 65:4375–4384.

Wallmann K, Pinero E, Burwicz E, Haeckel M, Dale A, Ruepke L (2012) The global inventory of methane hydrate in marine sediments: A theoretical approach. *Energies* 5:2449–2498.

Wang F-P, Zhang Y, Chen Y, He Y, Qi J, *et al*. (2014) Methanotrophic archaea possessing diverging methane-oxidizing and electron-transporting pathways. *ISME J* 8:1069–1078.

Warthmann R, Vasconcelos C, Sass H, McKenzie JA (2005) *Desulfovibrio brasiliensis* sp. nov., a moderate halophilic sulfate-reducing bacterium from Lagoa Vermelha (Brazil) mediating dolomite formation. *Extremophiles* 9:255–261.

Webster G, Rinna J, Roussel EG, Fry JC, Weightman AJ, Parkes RJ (2010) Prokaryotic functional diversity in different biogeochemical depth zones in tidal sediments of the Severn Estuary, UK, revealed by stable‐isotope probing. *FEMS Microbiol Ecol* 72:179–197.

Wegener G, Krukenberg V, Riedel D, Tegetmeyer HE, Boetius A (2015) Intercellular wiring enables electron transfer between methanotrophic archaea and bacteria. *Nature* 526:587–590.

Whiticar MJ (1999) Carbon and hydrogen isotope systematics of bacterial formation and oxidation of methane. Chemical Geol 161:291–314.

Chapter II:

A long-term cultivation of an anaerobic methane-oxidizing microbial community from deep-sea methane-seep sediment using a continuous-flow bioreactor

Originally published in PLoS ONE 9:e105356.

Chapter II

2.1 Introduction

The microbially mediated anaerobic oxidation of methane (AOM) in marine sediments is a globally important microbial process in carbon cycling (Reeburgh *et al*., 2007). AOM-associated microorganisms have been extensively studied using biogeochemical and microbiological approaches. A consensus in the field of AOM studies is that euryarchaeal anaerobic methanotrophs (ANMEs) oxidize methane either solely or in syntrophic association with deltaproteobacterial sulfate-reducing bacteria (SRB) (Knittel *et al*., 2009). ANMEs are phylogenetically closely related to known methanogenic *Archaea* and can be classified into three distinct phylogenetic lineages called ANME-1, -2, and -3 (Knittel *et al*., 2009). Several groups of SRB partners have been identified, including, SEEP-SRB1, SEEP-SRB2 (also known as the Eel-2 group), HotSeep-1, seepDBB and *Desulfobulbus* relatives (Niemann *et al*., 2006; Schreiber *et al*., 2010; Holler *et al*., 2011; Kleindienst *et al*., 2012; Green-Saxena *et al*., 2014). In addition, some previous reports have suggested the possible involvement of other uncharacterized microorganisms in AOM (Knittel *et al*., 2005; Biddle *et al*., 2006; Inagaki *et al*., 2006; Sørensen *et al*., 2006; Harrison *et al*., 2009). Pernthaler *et al*. (2008) found that not only deltaproteobacterial SRB partners but also uncharacterized bacteria belonging to *Alpha*- and *Beta-proteobacteria* formed aggregates with ANME-2c cells. Metagenomic, metatranscriptomic, and metaproteomic studies have indicated that AOM is catalyzed by a reverse methanogenesis pathway (Pernthaler *et al*., 2008; Meyerdierks *et al*., 2010; Stokke *et al*., 2012; Wang *et al*., 2013; Hallam *et al*., 2004). However, neither the ANMEs nor their potential syntrophic partners have been isolated, and thus their detailed physiological properties remain poorly understood.

To gain a deeper understanding of carbon cycling in methane-seep sediments, the cultivation of AOM-associated microbial communities is a significant challenge. Cultivation results provide critical information about the active AOM microbial entities in the environment. Several research groups have employed continuous-flow bioreactor systems for the activation and enrichment of AOM microbial communities (Girguis *et al*., 2003; Meulepas *et al*., 2009; Wegener *et al*., 2009; Deusner *et al*., 2010; Zhang *et al*., 2010; Steeb *et al*., 2014). In addition to the bioreactor enrichments, a few enrichment cultures have been obtained using batch-type cultivation methods, following long-term incubation (Nauhaus *et al*., 2007; Schreiber *et al*., 2010; Holler *et al*., 2011). However, due to the extremely slow growth rate of AOM microbial communities (*i.e.*, the estimated doubling time is several months) (Girguis *et al*., 2005; Nauhaus *et al*., 2007; Meulepas *et al*., 2009; Zhang *et al*., 2011), the cultivation of AOM microbial communities is laborious, and knowledge of AOM enrichment cultures remains limited. To effectively cultivate AOM-associated microorganisms, a continuous-flow bioreactor technique was employed. The bioreactor used in this study is a down-flow hanging sponge (DHS) bioreactor (**Fig. 2-1**) originally developed for municipal wastewater treatment (Agrawal *et al*., 1997; Uemura *et al*., 2010). A distinctive feature of the DHS bioreactor is the use of polyurethane sponges, providing an enlarged surface for microbial habitats and an increased cell residence time. In addition, the sponge carriers are not submerged in the medium but are hanging freely in gaseous substrates (*e.g.*, methane), and thus the gaseous substrates effectively diffuse inside the sponge carriers as

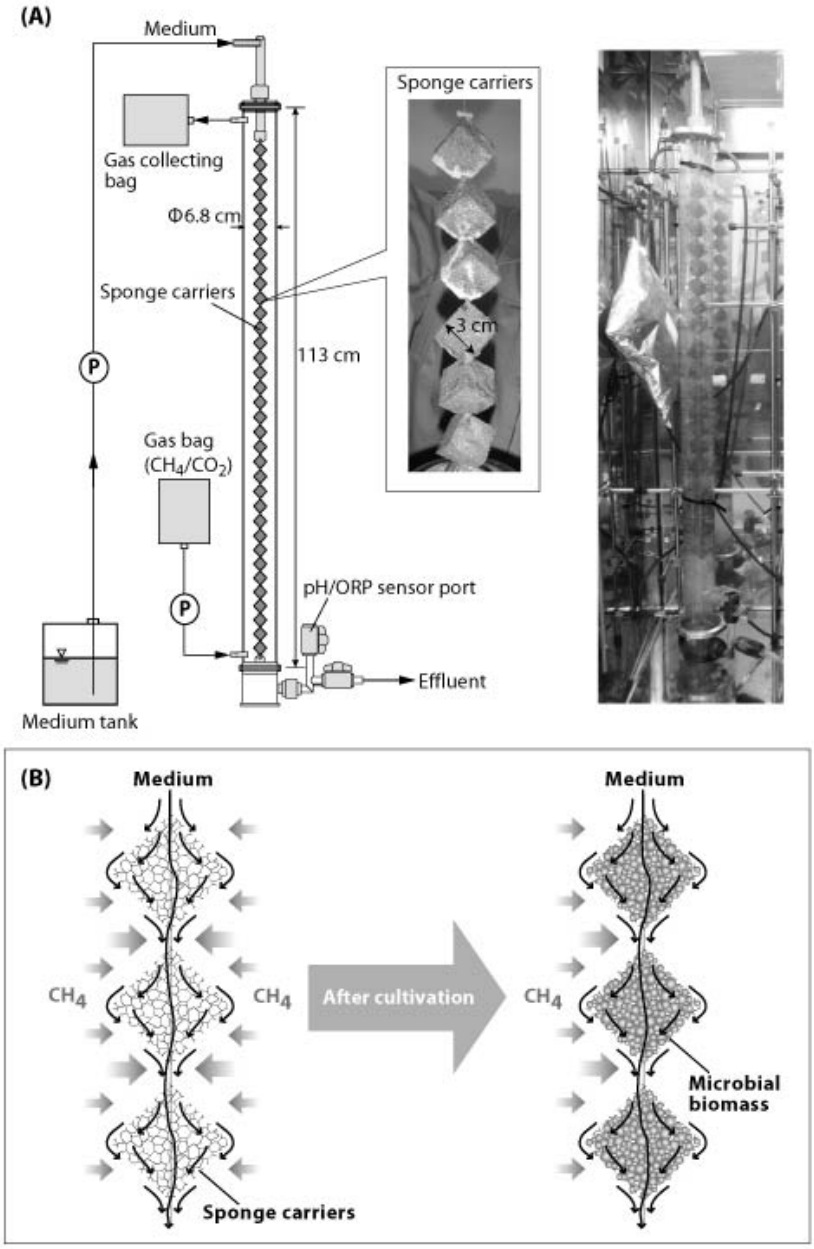

Figure 2-1. The DHS bioreactor system. (A) Schematic diagram and photographs of the DHS bioreactor used in this study. (B) The concept of cultivation of an AOM microbial community using the DHS bioreactor. Sponge carriers hang freely, suspended with string, in gaseous methane. Thus, the gaseous methane effectively diffuses not only to the surface but also inside the sponge carriers as the seawater medium flows down into the sponge carriers. The pore space in the sponge carriers serves as the habitat for microbial life.

the influent medium flows through them. Moreover, continuous flow allows the outflow of metabolic products such as hydrogen sulfide (in the case of sulfate-dependent AOM), which may inhibit microbial growth if allowed to accumulate. These properties of DHS bioreactors allow slow-glowing microorganisms to thrive and yield a greater biomass than that observed when other bioreactor systems are used (Onodera *et al*., 2013). In this study, deep-sea methane-seep sediment collected from the Nankai Trough, Japan was incubated anaerobically for 2,013

days in a newly designed DHS bioreactor system, in order to cultivate AOM-associated microorganisms. The main aim of this study was to investigate the applicability of DHS bioreactor to cultivate an AOM microbial community and identification of active AOM-associated entities in the methane-seep sediment of the Nankai Trough. In the methane-seep sediment, ANME-associated 16S rRNA gene sequences have been detected in the previous studies (Nunoura *et al*., 2013), but none of the cellular and molecular ecological evidences for active AOM microbial entities was reported. Following long-term incubation in the bioreactor, an AOM microbial community that consisted of ANMEs and phylogenetically diverse yet-to-be cultured microorganisms was successfully enriched from the methane-seep sediment.

2.2 Materials and Methods

2.2.1 Sediment core sample

An active methane-seep sediment core (named 949C3) was collected from the Omine Ridge, Nankai Trough off Kumano area, Japan (33° 7.23′ N, 136° 28.67′ E), at 2,533 m below the sea surface, via the manned submersible '*Shinkai 6500*' (cruise YK06-03, dive no. 6K949, 6 May 2006). The sediment consisted of blackish-gray, sandy silt and contained hydrogen sulfide. The sediment core was 25 cm in length and was subsampled using sterilized top-cut syringes and spatulas at 5-cm intervals on board. The subsampled sediments were used for interstitial water geochemical analysis and for culture-independent molecular analyses. The geochemical data showed that the sediment contained more than 5.4×10^2 μmol kg^{-1} methane throughout the sediment core and that sulfate concentrations in the core decreased as the depth increased (Toki *et al*., personal communication). The results of the culture independent molecular analyses (i.e., quantitative real-time PCR and 16S rRNA gene tag-sequencing) have been reported by Nunoura *et al*. (2012). In this study, the sediment that remained after the subsampling was used. The sediment sample was stored anaerobically under nitrogen gas at 4°C in the dark, until further experiments were performed.

2.2.2 DHS bioreactor and incubation of sediment

A schematic diagram of the DHS bioreactor is shown in **Fig. 2-1**. The bioreactor was constructed from a closed polyvinyl chloride (PVC) column (interior volume of 4.4 L) with polyurethane sponge cubes (3 cm × 3 cm × 3 cm, pore size of 0.83 mm) as the carrier material for cultivating the microbial cells. The 22 sponge cubes were hung vertically using a nylon string. The total volume of the sponges was 0.59 L, and this value was used for calculating the hydraulic retention time (HRT). The inoculum sediment was mixed with an anaerobic medium (described below) and the sponge carriers were soaked with the mixed sediment slurry. This inoculation procedure was performed in a cold room maintained at 4°C, and the sediment slurry and PVC column were constantly flushed with nitrogen gas. Following the inoculation, the PVC column was tightly closed and installed in an incubator (M-600FN, TAITECH, Koshigaya, Japan) in the dark at 10°C. The composition of the supplied medium was as follows (L^{-1}): Daigo's artificial seawater SP for marine microalgae medium (Nihon Pharmaceutical, Tokyo, Japan),

36 g; NH_4Cl, 0.54 g; KH_2PO_4, 0.14 g; $NaHCO_3$, 2.5 g; glucose, 0.01 g; $Na_2S \cdot 9H_2O$, 0.11 g; trace element solution (Imachi *et al*., 2008), 1 mL; vitamin solution (Imachi *et al*., 2009), 1 mL; and titanium (III)-nitrilotriacetic acid solution (Moenchi and Zeikus, 1983), 5 mL. The medium contained 24.7 mM sulfate. The medium was purged with nitrogen gas, and the pH was adjusted to 7.5. A total of 5 L of media was prepared at a time. The medium was stored at 5°C and was supplied into the bioreactor through the top inlet port using a peristaltic pump (Masterflex L/S tubing pump 7550-50, Cole-Parmer, Vernon Hills, IL, USA) and Viton tubing (Cole-Parmer). The medium then flowed down, passing through the sponge carriers by gravity, and was finally pumped out of the PVC column. The HRT in the bioreactor was set at 20 h. A gas mixture of methane and carbon dioxide (95:5, vol./vol.) was prepared in an aluminum bag (AAK-5, ASONE, Osaka, Japan) and supplied to the lower part of the bioreactor. The medium and CH_4/CO_2 gas were supplied intermittently at 1 min/9 min (on/off), regulated by an automatic on/off timer (FT-011, Tokyo Glass Kikai Co. Ltd., Tokyo, Japan) connected to the peristaltic pump. The effluent gas was collected in an aluminum bag, via Viton tubing, from the top portion of the bioreactor. The bioreactor was operated under atmospheric pressure.

2.2.3 Chemical analysis and sampling from the DHS bioreactor

The pH and oxidation-reduction potential (ORP) of the effluent medium were measured using a pH and redox electrode (InPro3250SG, Mettler-Toledo, Greifensee, Switzerland) connected to a modular transmitter (M700, Mettler-Toledo). The sulfate concentration of the influent/effluent medium was measured using a turbidimetric method (Hach Method 8051) by using subsamples diluted to 100-fold with Milli-Q water. For microbial community analyses, sediment slurry samples attached to the sponge carriers were sampled at 285, 903, 1,376, 1,529, 1,732, and 2,013 days of operation. At each sampling, several sponge carriers were randomly selected from 3 portions (upper, middle, and lower) of the bioreactor. The sediment slurry samples were removed from the selected sponges by manual rubbing in anaerobic seawater medium. Nitrogen gas was flushed during the sampling procedure.

2.2.4 Measurement of potential AOM activity

A tracer experiment using ^{13}C-labelled methane was used to estimate potential AOM activity, as described by Yoshioka *et al*. (2010). To measure activity, approximately 30 mL of the bioreactor incubation samples collected on day 1,529 was aliquotted into four 70-mL vials. After flushing with nitrogen gas, the vials were sealed with butyl rubber stoppers and aluminum crimp seals. During the incubation procedure, all samples were maintained under anaerobic conditions; this was confirmed by the clear color of the resazurin in the samples. Thirty milliliters of non-labeled methane taken from a tank [$\delta^{13}C = -36.6$ % (PDB)] was injected into 2 of the vials with a glass syringe, while 27 mL of the non-labeled methane and 3 mL of 100% ^{13}C-labeled methane (Sigma-Aldrich/ISOTEC, St. Louis, MO, USA) were injected into the other 2 vials. All the vials were incubated at 10°C in the dark. To monitor the differences in the stable carbon isotope compositions of dissolved inorganic carbon (DIC), 1 mL of solution was collected from each vial after 1, 14, 29, and 42 days of incubation. The stable

carbon isotope compositions of the DIC in the solutions were measured using a Thermoquest-Finnigan Gas Bench linked to a DeltaPlus XL mass spectrometer (Thermo Finnigan Inc., Austin, TX, USA). ^{13}C-enrichment of the DIC in the $^{13}CH_4$-amended vials relative to the non-amended vials was calculated and the methane oxidation rate was estimated by calculating the ^{13}C-enrichment in the total DIC.

2.2.5 Nucleic acid extraction, PCR, cloning, and phylogenetic analysis

DNA extraction, PCR amplification, clone library construction, and sequencing were performed as described previously (Miyashita *et al*., 2009). The PCR primers used in this study are shown in **Table S2-1**. The PCR primer pairs Arch21F/Ar912r and EUB338F/1492R were used for the construction of 16S rRNA gene-based archaeal and bacterial clone libraries, respectively. For the construction of the *mcrA* gene-based clone library, the primer pair MLf/MLr was used. PCR was performed under the following conditions: initial denaturation at 95°C for 9 min, followed by 20 to 35 cycles of denaturation at 95°C for 40 s, annealing at 50°C for 30 s, and extension at 72°C for 1 min. To reduce possible bias caused by PCR amplification, PCR products obtained following the minimal number of PCR cycles, ranging from 20 to 35 cycles at five-cycle intervals, were used. Total RNA extraction was performed immediately following sampling from the bioreactor, using a previously described method (Sekiguchi *et al*., 2005). The remaining DNA was digested with RNase-free DNase I (Promega, Madison, WI, USA). The absence of genomic DNA contamination in the RNA extracts was confirmed by PCR, using the same PCR primer pairs. The concentration of RNA was quantified spectrophotometrically using a Quant-iT RNA assay kit (Invitrogen, Carlsbad, CA, USA). Reverse transcription (RT)-PCR was performed using a SuperScript III One-Step RT-PCR System with Platinum Taq DNA polymerase (Invitrogen), according to the manufacturer's instructions. The RT-PCR primers and subsequent procedures were identical to those employed in the 16S rRNA gene-based clone analysis presented above. Recovered clone sequences were classified into phylotypes using a threshold of 97% sequence identity. The representative sequences of the phylotypes were subjected to BLASTN analysis (Altschul *et al*., 1997). 16S rRNA gene sequence-based phylogenetic tree construction was performed using the neighbor-joining method with the Jukes-Cantor correction, as described previously (Imachi *et al*., 2006). A deduced McrA amino acid sequence-based phylogenetic tree was constructed using the neighbor-joining method, implemented in the ARB program, version 5.2 (Ludwig *et al*., 2004) using 137 amino acid positions and PAM distance correction. The sequences reported in this study have been deposited in the GenBank/EMBL/DDBJ database under the accession numbers AB831260–AB831537.

2.2.6 Statistical analyses

Chao1 species richness and the Shannon diversity index were calculated using the EstimateS software, version 8.2 (http:// viceroy.eeb.uconn.edu/estimates/). Clone library coverage was calculated using the equation $[1-(n_1/N)]\times100$, where n_1 is the number of single-occurrence phylotypes within a library and N is the total number of clones in the library (Good, 1953). Evenness was calculated using the equation $H/\ln R$, where H is the Shannon diversity index and R is the number of phylotypes observed within a library (Magurran, 2004). Rarefaction curves

were calculated using the Analytic Rarefaction software, version 2.0 (http://www. huntmountainsoftware.com).

2.2.7 Terminal restriction fragment length polymorphism (T-RFLP) analysis

Archaeal and bacterial 16S rRNA gene fragments for T-RFLP analysis were amplified by PCR using the primer pairs 5′ FAM-labeled Arch21F/Ar912r and 5′ FAM-labeled EUB338F/1492R, respectively. PCR was performed under the conditions described above. The PCR products were digested with HaeIII and HhaI (TaKaRa Bio Inc., Otsu, Japan) separately. The labeled fragments were analyzed by electrophoresis on an ABI 31306l Genetic Analyzer (Applied Biosystems, CA, USA). GeneScan 1200 LIZ (Applied Biosystems) was used as a size standard.

2.2.8 Quantitative real-time PCR

Quantitative real-time PCR of archaeal and bacterial 16S rRNA genes was performed with a 7500 Real-Time PCR System (Applied Biosystems) using a SYBR Premix Ex Taq II (Perfect Real Time) kit (TaKaRa Bio Inc.). For archaeal and bacterial 16S rRNA gene quantification, the primer pairs 340F/932R and EUB338F/907R, respectively, were used (**Table S2-1**). The reaction mixture for real-time PCR was prepared according to the manufacturer's instructions. For the construction of template standards for each primer set, dilution series of 16S rRNA gene fragments of *Methanobacterium* sp. strain MO-MB1 (Imachi *et al*., 2011) and *Escherichia coli* strain K12 (DSM 5911), which were obtained using the archaeal primer pair Arch21F/1492R and the bacterial primer pair 27F/1492R, were used, respectively. These PCR products were used in each real-time PCR to calculate the 16S rRNA gene copy number. Template DNA was quantified spectrofluorometrically using a Quant-iT PicoGreen dsDNA Assay Kit (Invitrogen). The optimal PCR conditions, including the annealing temperature, were empirically determined for each primer pair. PCR was performed under the following conditions: initial denaturation at 95°C for 10 s, followed by 40 cycles of denaturation at 95°C for 5 s, 30 s of annealing (54°C for Archaea; 50°C for Bacteria), and extension at 72°C for 34 s. To verify the specificity of the real-time PCR assay, the PCR products were subjected to melting curve analysis (60–90°C) and subsequent gel electrophoresis. All assays were performed in triplicate.

2.2.9 Fluorescence *in situ* hybridization (FISH)

Subsamples for FISH were fixed with 2% paraformaldehyde in anaerobic medium excluding glucose for 12 to 16 h at 4°C and stored in a 1:1 mix of phosphate-buffered saline (PBS): ethanol at –20°C. The FISH samples used in this study were not dispersed by homogenization or ultrasonication prior to *in situ* hybridization procedures. The 16S rRNA-targeted oligonucleotide probes used in this study are listed in **Table S2-2**. The 5′ ends of the oligonucleotide probes were labeled with Alexa Fluor 488 or horseradish peroxidase (HRP). Standard FISH was performed according to previously described methods (Sekiguchi *et al*, 1999) with minor modifications. In brief, hybridizations were carried out in hybridization buffer (20 mM Tris–HCl [pH 7.2], 0.9 M NaCl, 0.01% sodium dodecyl sulfate, 1% [wt./vol.] blocking reagent [Roche Diagnostics, Mannheim, Germany], 0 to 65% formamide) with 0.5 mM of probe overnight at 46°C in the dark. The washing step was performed at 48°C for 15 min with

washing buffer containing the same components as the hybridization buffer, except for the blocking reagent and probes. Catalyzed reporter deposition (CARD)-FISH (Pernthaler *et al*., 2002) with HRP-labeled probes was performed based on a previously described method (Kubota *et al*., 2006). To inactivate endogenous peroxidase activity, the fixed samples were incubated in H_2O_2 solution (final concentration, 0.3% [vol./vol.] in methanol) for 30 min at room temperature. An HRP-labeled negative control probe, NON338, was used as the negative control. For the multi-color CARD-FISH using the probes ANME-2c-760 and EUB338, 0.01 M HCl solution (10 min at room temperature) was used for the inactivation of HRP in the initial hybridization. Hybridization conditions were controlled by varying the formamide concentrations in the hybridization and washing buffers. The hybridization conditions for six of the uncultured group-specific probes (ANME-1-350, ANME-2a-647, ANME-2c-760, MBGD-318, MBGB-380, and UncGam731) were determined by Clone-FISH (Schramm *et al*., 2002). The Clone-FISH samples were prepared as described in Kubota et al. (Kubota *et al*., 2006). The clonal sequences used for Clone-FISH were AB598074, AB598076, and AB831534 to AB831537. Four of the clonal sequences (AB831534 to AB831537) were obtained by 16S rRNA gene cloning with the primer pair Arch21F/1492R or 27F/1492R from the bioreactor incubation sample collected at day 903. The FISH samples were finally counterstained with 4', 6-diamidino-2-phenylindole (DAPI; 1 μg mL^{-1} for 5 min at room temperature) after all of the in situ hybridization steps had been performed. An Olympus microscope (BX51F, Olympus, Tokyo, Japan) with a color CCD camera system (DP72, Olympus) was used for microscopic observations.

2.3 Results

2.3.1 DHS bioreactor operation and potential AOM activity in the bioreactor

The DHS bioreactor (**Fig. 2-1**) was operated at 10°C for a total of 2,013 days. During the initial period of bioreactor operation (~365 days), the bioreactor could not adequately maintain reductive conditions, likely due to molecular oxygen contamination (**Fig. 2-2A**). When a medium containing resazurin, a redox indicator, was fed into the bioreactor, the medium at the top of the PVC column was very faintly pink in color. Therefore, to maintain more reductive conditions, all the joints in the tubing lines from the medium storage bottle to the bottom of the PVC column were sealed. Moreover, a tiny amount of glucose (0.01 g mL^{-1}) was added to the medium after day 365, with the intention that the contaminated molecular oxygen would be consumed by the activity of existing aerobic microorganisms in the bioreactor. Following these improvements, the ORP values of the effluent medium indicated that reductive conditions were maintained in the bioreactor (**Fig. 2-2A**). The average pH value of the effluent medium was 7.5 (SD ± 0.1, n = 1,441) (**Fig. 2-2B**). To confirm the occurrence of sulfate-dependent AOM reactions in the bioreactor, the sulfate concentrations of the influent and effluent medium was measured several times until 1,500 days using turbidimetric analysis. However, the sulfate concentrations in the effluent medium did not differ from those in the influent medium (*i.e.*, approximately 25 mM sulfate). This result may be explained by the relatively higher sulfate loading rate (30 mmol L^{-1} day^{-1}) compared to the AOM activity in the DHS bioreactor.

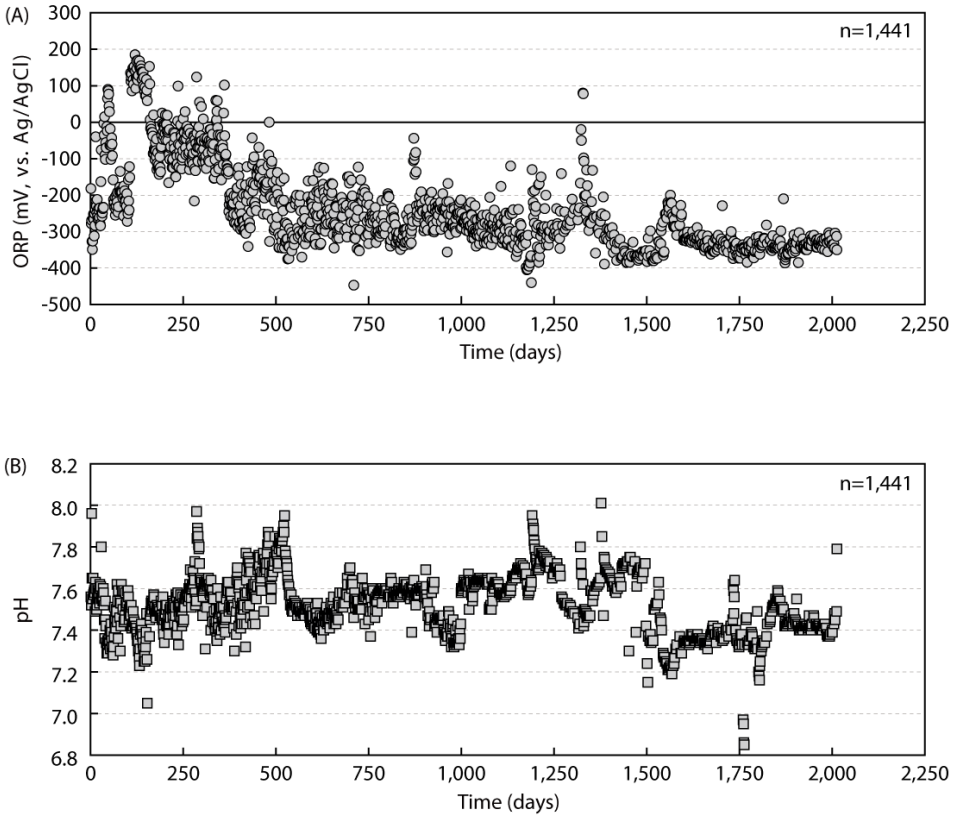

Figure 2-2. Time-course changes in (A) ORP and (B) pH values of DHS bioreactor effluent.

Therefore a tracer experiment using ^{13}C-labelled methane was conducted to measure potential AOM activity using a sample collected at day 1,529. Throughout the experiment, an increase in the ^{13}C content of the DIC was observed (**Fig. 2-3**). In the case that only AOM occurred, the potential AOM rate would have been 375 nmol g-dry weight (dw)$^{-1}$ day^{-1} (mean value, n = 2). However, recent studies have shown that AOM and methane production occur simultaneously in AOM systems (Holler *et al*., 2011; Bertram *et al*., 2013). If methane production had proceeded in the tracer experiment, the increased δ^{13}C values of DIC could have included the effect of methane production activity (Meulepas *et al*., 2010). On the other hand, the δ^{13}C values of DIC in the $^{13}CH_4$-non-amended sample, which showed a decreasing trend in the incubation (**Fig. 2-3**). The decreasing trend supports that ^{12}C was enriched in the carbon dioxide/bicarbonate pool through AOM. Although the exact AOM/methane production activity ratio in the DHS bioreactor enrichment is unclear, the tracer experiment indicated that an active AOM microbial community had been established in the bioreactor.

2.3.2 Abundance of archaeal and bacterial populations estimated by quantitative real-time PCR

To examine the changes in the abundance of archaeal and bacterial populations during the DHS bioreactor incubation, archaeal and bacterial 16S rRNA gene copy numbers were quantified (**Fig. 2-4**). In the inoculum sediment, the archaeal and bacterial 16S rRNA gene copy numbers were 4.0×10^7 and 8.2×10^8 copies g-wet weight (ww)$^{-1}$, respectively. Following incubation in the bioreactor, the bacterial 16S rRNA gene copy number

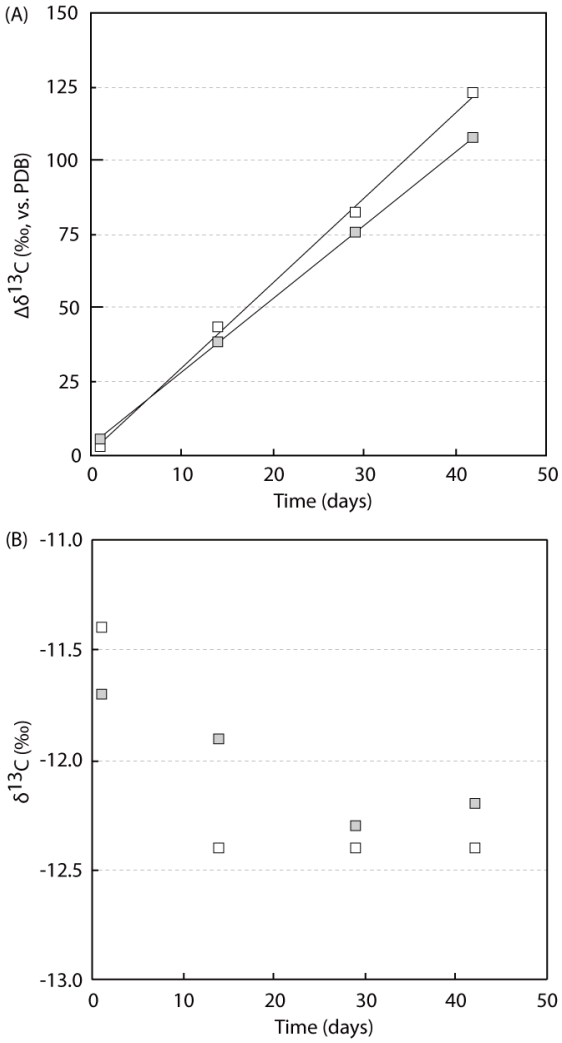

Figure 2-3. The traces of the difference in $\delta^{13}C$ values of dissolved inorganic carbon between the 1,529-day sample supplemented with ^{13}C-labelled methane and that supplemented with non-labeled methane. Values of duplicate experiments are shown.

increased approximately tenfold, to 5.7×10^9 copies g-ww^{-1} at day 285; the copy number was maintained at 10^9 copies g-ww^{-1} for the duration of the reactor operation. In contrast, archaeal 16S rRNA gene copy numbers remained at 10^7 copies g-ww^{-1} throughout the 2,013 days of incubation, although notable shifts were observed in the archaeal community, as mentioned below.

2.3.3 Composition of the microbial community in the DHS bioreactor

To characterize the composition of the AOM microbial community and any shifts in the community during the DHS bioreactor incubation, clone libraries targeting archaeal and bacterial 16S rRNA genes were constructed for the bioreactor incubation samples (**Fig. 2-5** and **S2-1**–**S2-3**). To identify the active microbial components in the bioreactor, 16S rRNA clone libraries from the total RNA extracts prepared from the 903- and 2,013-day samples were also constructed via RT-PCR. The archaeal phylotypes detected in the inoculum sediment (i.e., the 0-day sample in **Fig. 2-5A**) were closely related to the sequences of ANME-2a, ANME-2c, Deep-Sea Archaeal Group

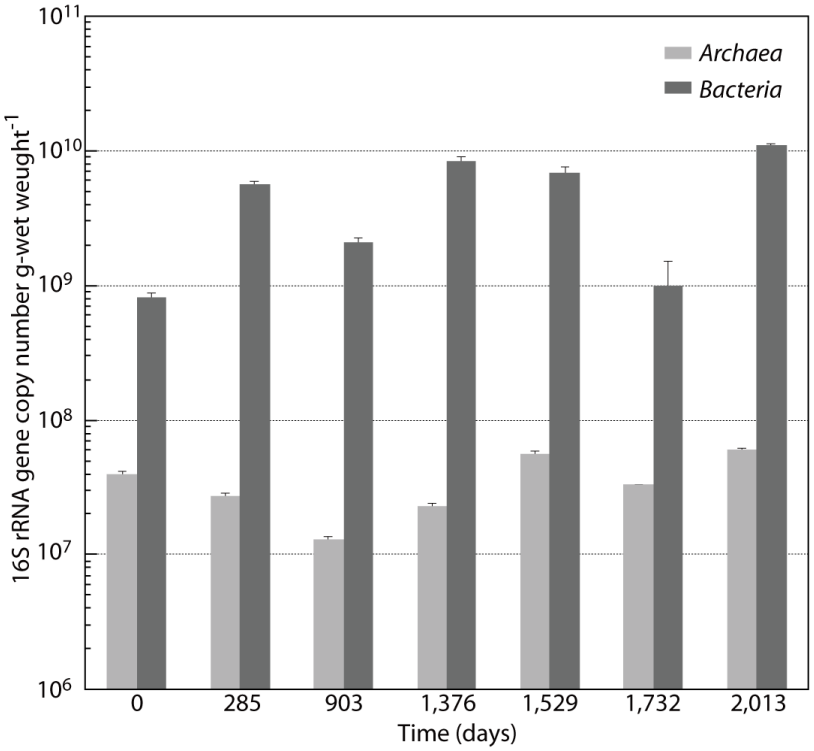

Figure 2-4. Archaeal and bacterial 16S rRNA gene copy numbers in the DHS bioreactor as determined by quantitative real-time PCR. Values are mean ± SD (n = 3).

(DSAG; also known as Marine Benthic Group-B), Marine Benthic Group-D (MBG-D), Thermoplasmata Group E2, Miscellaneous Crenarchaeotic Group (MCG), and Marine Group-I (MG-I) *Thaumarchaeota*, which are frequently observed in marine subsurface sediments. The relative abundance of ANME-related clones (*i.e.*, ANME-2a and -2c) in the archaeal 16S rRNA gene clone library of the inoculum sediment was 23.7%. During incubation in the bioreactor, the archaeal composition gradually shifted. The total clonal abundance of ANMEs in the archaeal 16S rRNA gene and 16S rRNA clone libraries gradually increased, and phylotypes representing the three ANME groups (i.e., ANME- 1, -2, and -3) were identified, although ANME-1 and -3 phylotypes were not detected in the inoculum sediment by the 16S rRNA gene clone analysis. The archaeal phylotype MK0D_A9, affiliated with ANME-2a, was the most abundant archaeal phylotype on day 2,013 (25.7% and 66.0% of the clones examined in the 2,013-day 16S rRNA gene and 16S rRNA libraries, respectively). Interestingly, the methylotrophic methanogen genus *Methanococcoides* phylotype MK903D_A2 was predominantly detected in the 903-day 16S rRNA library, although no potential methylotrophic substrates for *Methanococcoides*, such as methanol or methylamines (Sowers, 2001), were supplied in the bioreactor. Conceivably, the methylotrophic substrates were eluted as secondary products from the inoculum sediment (Liu *et al*., 2008). Indeed, methylotrophic methanogens also grew in a previously reported DHS bioreactor for the cultivation of a subseafloor methanogenic community, although no methylotrophic substrate was provided to the bioreactor (Imachi *et al*, 2011). These methanotrophic/methanogenic archaeal components were also confirmed by

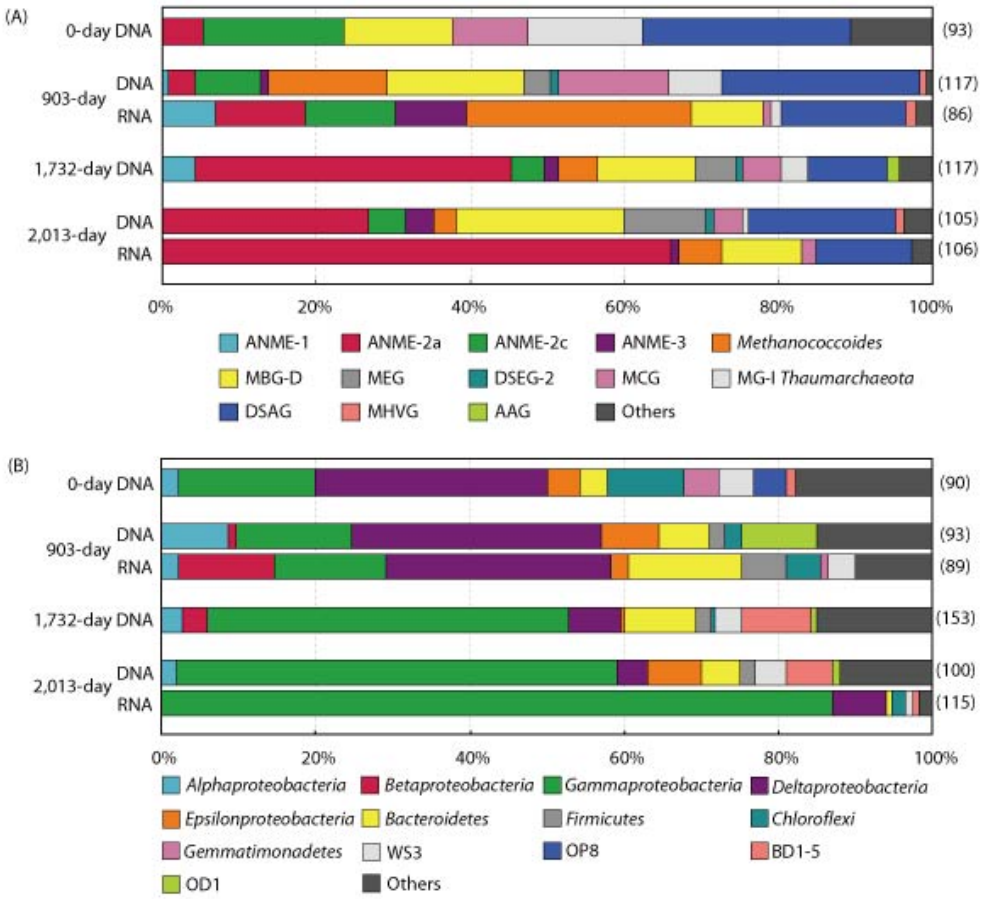

Figure 2-5. Microbial community structures based on 16S rRNA gene sequence-based clone libraries. Phylogenetic affiliations based on (A) archaeal and (B) bacterial 16S rRNA genes and 16S rRNA. The 16S rRNA clone libraries were constructed from the 903-day and 2,013-day samples only. The numbers in parentheses are the total number of sequenced clones.

methyl-coenzyme M reductase alpha-subunit gene (*mcrA*; a key gene in methane-oxidation/production) sequence-based clone analysis of the 2,013-day sample, and the results were generally consistent with those of the archaeal 16S rRNA gene sequence-based clone analysis **(Fig. S2-4)**. One remarkable inconsistency was noted between the *mcrA* gene and 16S rRNA gene sequence-based clone libraries: phylotypes related to *Methanococcoides* were the dominant component in the *mcrA* mRNA-based library (65.3% of the clones examined), whereas the ANME-2a phylotype was the dominant component in the 2,013-day archaeal 16S rRNA gene and 16S rRNA libraries. This inconsistency may have been caused by the biases associated with PCR amplification and cloning, but the potential involvement of *Methanococcoides* members in AOM could not be excluded. Co-occurrence of AOM and methanogenesis by *Methanococcoides* may be one of the conceivable explanations for the highly expressed *Methanococcoides*-related *mcrA* mRNA in the bioreactor. In addition to the methanotrophic/methanogenic archaeal phylotypes, many phylotypes related to other diverse uncultured archaeal lineages were also identified in the bioreactor enrichment. The 16S rRNA gene and 16S rRNA phylotypes related to DSAG and MBG-D were relatively abundant, comprising 10.3–25.6% and 9.3–21.9% of the archaeal 16S

rRNA gene sequence based clone libraries, respectively. Other uncultured archaeal lineages, such as MCG, Miscellaneous Euryarchaeotic Group (MEG), Deep-Sea Euryarchaeotic Group-2 (DSEG-2), Marine Hydrothermal Vent Group (MHVG), and Ancient Archaeal Group (AAG), were detected as minor components following the long-term incubation. The dominant bacterial components in the inoculum sediment (i.e., the 0-day sample in **Fig. 2-5B**) were related to members of the *Deltaproteobacteria*, *Gammaproteobacteria*, and *Chloroflexi*, which have been frequently detected as dominant bacterial components in subseafloor sediments, including methane seeps and mud volcanoes (Inagaki *et al*., 2004; Heijs *et al*., 2007; Orcutt *et al*., 2010; Pachiadaki *et al*., 2010). Putative sulfate-reducing deltaproteobacterial partners of ANMEs (SEEP-SRB1, SEEP-SRB2, *Desulfobacteraceae*, and *Desulfobulbaceae*; **Fig. S2-3B**) were detected in the inoculum sediment (30.0% of the clones examined). During incubation in the DHS bioreactor, the bacterial community gradually shifted. The putative SRB partners were the dominant bacterial populations until day 903, and then gammaproteobacterial phylotypes became the dominant population. The bacterial phylotype MK903D_B5, which is affiliated with an uncultured gammaproteobacterial lineage, was the dominant bacterial phylotype on day 2,013 (**Fig. S2-3C**; 20.0% and 50.4% of the clones examined in the 2,013-day 16S rRNA gene and 16S rRNA clone libraries, respectively). This gammaproteobacterial phylotype was not detected in the inoculum sediment, but its population gradually increased during the bioreactor operation period. The second most abundant bacterial phylotype on day 2,013, MK903D_B19, is also affiliated with the *Gammaproteobacteria* and is closely related to the aerobic methanotrophic genus *Methylobacter* (**Fig. S2-3C**; 16.0% and 32.2% of the clones examined in the 2,013-day 16S rRNA gene and 16S rRNA clone libraries, respectively). Other gammaproteobacterial aerobic methanotrophic genera, such as *Methylomonas* and *Methylophaga*, were also detected in small numbers (**Fig. S2-3C**). The occurrence of these aerobic methanotrophs indicated the contamination of a small amount of molecular oxygen in the bioreactor. In fact, some minor bacterial phylotypes (MK903D_B6, MK903D_B31, MK903D_B42, MK903R_B71, MK903R_B75, MK1732D_B15, MK1732D_B55, and MK2013D_B26) were shown to be closely related to aerobic bacterial isolates (97.0% 16S rRNA gene sequence identity in the National Center for Biotechnology Information 16S Microbial database; data not shown). In addition to the delta- and gamma-proteobacterial phylotypes, other phylogenetically diverse bacterial phylotypes were detected following incubation, and the overall bacterial diversity spanned 24 bacterial phyla/lineages (**Fig. S2-3**). As described above, the 16S rRNA gene and *mcrA* gene sequence-based clone analyses demonstrated that the microbial community shifted during operation of the bioreactor, and phylogenetically diverse yet-to-be-cultured microorganisms were successfully cultivated in the DHS bioreactor. The changes in the composition of the microbial community were further confirmed by archaeal and bacterial 16S rRNA gene-based T-RFLP analysis of bioreactor incubation samples collected at days 285, 1,376, 1,529, in addition to the samples used for clone analysis, as mentioned above (**Fig. S2-5** and **S2-6**). The detection of unassigned TRFs indicated the presence of microbial components that could not be identified by the 16S rRNA gene sequence-based clone analysis.

Table 2-1. Statistical analysis of clone libraries.

Clone library	Total clone number	Phylotype [a] number	Chao1 species richness [b]	Shannon diversity index	Evenness	Coverage (%)
Archaeal 16S rRNA gene						
0-day DNA	93	22	26 (23–41)	2.71	0.88	92
903-day DNA	117	26	42 (30–84)	2.58	0.79	89
903-day RNA	86	23	45 (29–110)	2.55	0.81	86
1,732-day DNA	117	37	83 (53–169)	2.63	0.73	79
2,013-day DNA	105	31	58 (39–121)	2.76	0.80	84
2,013-day RNA	106	13	24 (15–67)	1.34	0.52	93
Bacterial 16S rRNA gene						
0-day DNA	90	62	135 (95–223)	3.98	0.96	51
903-day DNA	93	45	99 (65–190)	3.49	0.92	70
903-day RNA	89	54	115 (80–197)	3.76	0.94	58
1,732-day DNA	153	53	89 (68–143)	3.33	0.84	80
2,013-day DNA	100	35	56 (42–97)	2.92	0.82	80
2,013-day RNA	115	15	27 (18–69)	1.43	0.53	92
mcrA gene						
2,013-day DNA	80	12	15 (13–34)	1.78	0.72	94
2,013-day RNA	121	6	6 (6–6)	1.14	0.64	99

[a] A phylotype was defined as ≥ 97% sequence identity.

[b] Numbers in parentheses indicate the 95% confidence interval.

2.3.4 Microbial diversity and richness in the DHS bioreactor incubation samples

To evaluate the diversity and richness of the DHS bioreactor incubation samples, Chao1 species richness, Shannon diversity index, Evenness, clone library coverage, and rarefaction curves were calculated for all clone libraries (**Table 2-1** and **Fig. 2-6**). The rarefaction curves for the bioreactor incubation samples, except the *mcrA* mRNA-based clone library, did not plateau (**Fig. 2-6**), and the coverage values did not reach 100% in any of the clone libraries (51–99%; **Table 2-1**). These results indicated that additional archaeal and bacterial phylotypes would be found in the incubation samples with additional sequencing. Interestingly, the Chao1 species richness, Shannon diversity index, and rarefaction curves for the archaeal 16S rRNA gene clone libraries indicated that the archaeal diversity of the 2,013-day incubation sample was higher than that of the inoculum sediment (**Table 2-1** and **Fig. 2-6A**). These results suggest that the abundance of minor archaeal components, which could not be detected in the inoculum sediment, increased in the bioreactor. The existence of minor and diverse archaeal components in the same sediment core sample has been revealed by 16S rRNA gene tag-sequencing analysis (Nunoura *et al*., 2012). In contrast to the results obtained from analysis of the archaeal clone libraries, statistical analyses of the bacterial clone libraries suggested that the bacterial diversity gradually decreased during the bioreactor operation period (**Table 2-1** and **Fig. 2-6B**).

2.3.5 Detection of microbial cells in the DHS bioreactor using FISH

The presence of active microorganisms in the DHS bioreactor was further confirmed by standard FISH and CARD-FISH analyses of the 903- and 2,013-day samples (**Fig. 2-7** and **Table 2-2**). The ANME-1-350

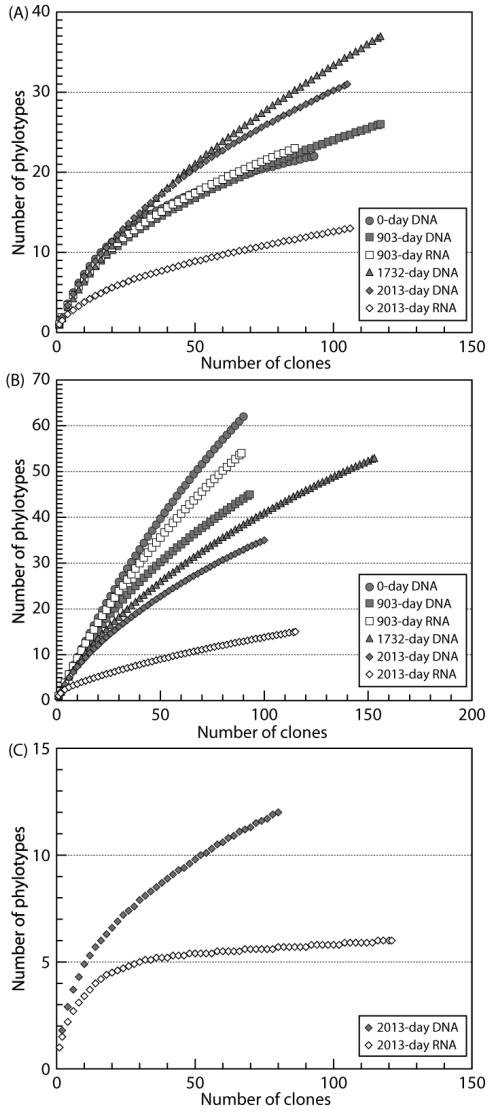

Figure 2-6. Rarefaction curves for (A) archaeal and (B) bacterial 16S rRNA genes and 16S rRNA, and (C) *mcrA* genes and mRNA.

probe-stained cells had a typical ANME-1-like rectangular morphology and formed chains of two or three cells (**Fig. 2-7A**). All ANME-2a cells visualized with the ANME-2a-647 probe occurred as single cells without any bacterial partners (**Fig. 2-7B**). The cells of ANME-2a were small cocci of approximately 0.4–0.6 μm in diameter. The ANME-2c cells stained with the ANME-2c-760 probe in the 903-day sample formed aggregates with bacterial partners, which were stained with the EUB338 probe (**Fig. 2-7C**), or occurred as aggregates without bacterial cells (**Fig. 2-7D**). Most of the ANME-2c aggregates detected did not occur with bacterial cells (11 of 15 aggregates examined in this experiment). In the 2,013-day sample, no signals of the ANME-2c-760 probe were identified in the triplicate CARD-FISH experiments. All of the MBGB-380-stained cells were small coccoid-shaped cells with a size of approximately 0.4–0.6 μm (**Fig. 2-7E**), and the cell morphology and size were consistent with those of DSAG archaeal cells detected in Black Sea microbial mats (Knittel *et al*., 2005). The

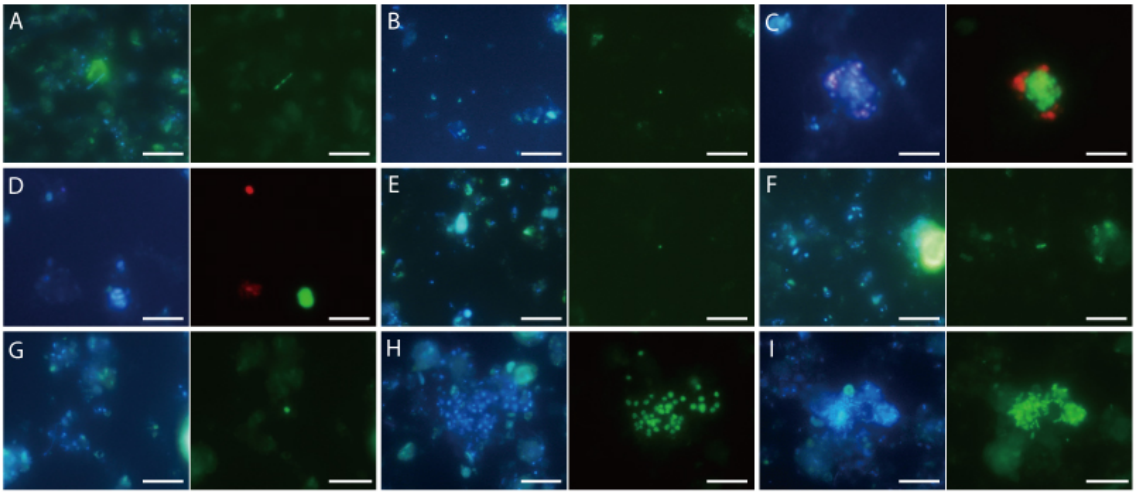

Figure 2-7. (A and G–I) FISH and (B–F) CARD-FISH images of microbial cells cultivated in the DHS bioreactor. Photomicrographs of DAPI-stained cells (left) and epifluorescence (right) showing identical fields. (A) Chain-forming ANME-1-350-stained cells in the 2,013-day sample (Alexa Fluor 488, green). (B) An ANME-2a-647-stained coccoid-shaped cell in the 2,013-day sample (Fluorescein, green). (C and D) Color overlay of ANME-2c-760 (Fluorescein, green) and EUB338-stained cells (Alexa Fluor 594, red) in the 903-day sample. (E) A MBGB-380-stained coccoid-shaped cell in the 2,013-day sample (Fluorescein, green). (F) A MBGD-318-stained rod-shaped cell in the 2,013-day sample (Fluorescein, green). (G) A MCOCID442-stained coccoid-shaped cell in the 2,013-day sample. (H) Mγ669-stained coccoid-shaped cells in the 2,013-day sample (Alexa Fluor 488, green). (I) UncGAM731-stained irregular rod-shaped cells in the 2,013-day sample (Alexa Fluor 488, green). Bars represent 10 μm.

Table 2-2. Summary of FISH and CARD-FISH results.

Probe	Target group	Sample/Detection method			
		903-day sample		2,013-day sample	
		FISH	CARD-FISH	FISH	CARD-FISH
ARC915	Most *Archaea*	+	+	+	+
ANME-1-350	ANME-1	+	NT	+	NT
ANME-2a-647	ANME-2a	-	+	-	+
ANME-2c-760	ANME-2c	-	+	-	-
ANME-3-1249	ANME-3	-	NT	-	NT
MBGD-318	MBG-D	-	+	-	+
MBGB-380	DSAG	-	+	-	+
MCOCID442	*Methanococcoides*	+	NT	+	NT
EUB338	Most *Bacteria*	+	+	+	+
Mγ669	*Methylobacter* and *Methylomonas*	+	NT	+	NT
UncGam731	Gammaproteobacterial phylotype MK903D_B5	+	NT	+	NT

+: detected, -: not detected, NT: not tested.

MBG-D archaeal cells detected by the MBGD-318 probe were straight rods (approximately 2–3 μm long and 0.5–1 μm wide) with blunt ends and a sheath-like structure (**Fig. 2-7F**). Almost all of the cells stained by the Mγ669 probe morphologically resembled *Methylobacter* species (**Fig. 2-7H**) and formed cysts that are normally found under conditions of oxygen deprivation and desiccation (Bowman, 2005). The UncGAM731 probe-positive cells were irregular rod-shaped cells (**Fig. 2-7I**; approximately 1–2 μm long and 0.5–1 μm wide). These uncultured

gammaproteobacterial cells formed monospecies aggregates (**Fig. 2-7I**) and did not form aggregates with ANME cells.

2.4 Discussion

A continuous-flow DHS bioreactor system was used to cultivate an AOM microbial community from deep-sea methane-seep sediment collected from the Nankai Trough, Japan. In this study, 24.7 mM sulfate was fed as the dominant electron acceptor for the AOM microbial community. The potential AOM activity in the DHS bioreactor is in the range of seep and mud volcano samples (Knittel *et al*., 2009). However, it was probably low compared to what could be achieved in high-pressure bioreactors (Deusner *et al*., 2010; Zhang *et al*., 2010) (**Table 2-3**). Due to the extremely low energy yield of the net AOM reaction ($\Delta G^{\circ\prime} = -16$ kJ mol^{-1} in the case of sulfate-dependent AOM (Knittel *et al*., 2009), the reaction is strongly influenced by substrate and product concentrations. In terms of the poor solubility of methane in solution at ambient pressure (~2 mM CH_4 at 10°C; Yamamoto *et al*., 1976), high pressure-type cultivation systems have the advantages of *in vitro* stimulation of AOM (Nauhaus *et al*., 2002; Deusner *et al*., 2010; Zhang *et al*., 2010). In other words, effective methane supply is thought to be an important factor for the cultivation of AOM microbial communities when using ambient-pressure type bioreactor systems. Meulepas *et al*. (2009) used an ambient-pressure submerged-membrane bioreactor system and achieved significantly higher potential AOM activity (286 μmol g-dw^{-1} day^{-1}) after 884 days of operation. In the submerged-membrane bioreactor system, the AOM microbial community was continuously sparged by methane gas bubbles for an ideal methane supply, but the gas-sparging method may expose microorganisms to relatively high shear forces. In contrast, the DHS bioreactor has a good gas-exchange capability because of a relatively large gas-liquid interface and a relatively short substrate transportation distance between the gas-liquid interface and the center of sponges. This unique feature of the DHS bioreactor may have enabled the successful long-term cultivation of the AOM microbial community under a non-turbulent ambient methane pressure condition.

Interestingly, the 16S rRNA gene-based quantitative real-time PCR data showed that the archaeal and bacterial populations in the DHS bioreactor responded differently to the incubation. The bacterial 16S rRNA gene copy number increased approximately tenfold during the period of incubation, whereas the archaeal 16S rRNA gene copy numbers remained roughly the same throughout the 2,013 days of incubation (**Fig. 2-4**). Additionally, statistical analyses of the 16S rRNA gene clone libraries showed that archaeal diversity after 2,013 days of incubation was higher than in the inoculum sediment, whereas the bacterial diversity decreased during the period of bioreactor operation (**Table 2-1** and **Fig. 2-6**). These different behaviors may have resulted from differences in survival mechanisms between the archaeal and bacterial communities, such as membrane structure and energy conversion efficiency (Valentine, 2007).

Table 2-3. Comparison of AOM enrichments in different types of continuous-flow bioreactors.

Incubation technique name	CH_4 pressure	Influent sulfate concentration	Incubation temperature	Sediment (water depth)	Maximum AOM rate	Involved ANMEs[d]	Reference
Down-flow hanging sponge (DHS) bioreactor	Ambient	25 mM	10°C	Nankai Trough (2,533 m)	375 nmol g-dw^{-1} day^{-1}	ANME-1, **ANME-2a**, ANME-2c and ANME-3	This study
Anaerobic sediment incubator system (AMIS)	Ambient	28 mM[b]	5°C	Monterey Bay (962 m)[b]	138 nmol g-dw^{-1} day^{-1}[b]	**ANME-1** and ANME-2c[b]	Girguis *et al*. (2003), Girguis *et al*. (2005)
Submerged membrane bioreactor	Ambient	21 mM	15°C	Eckernförde Bay (28 m)	286 µmol g-dw^{-1} day^{-1}	**ANME-2a**	Jagersma et al. (2009); Meulepas *et al*. (2009)
Flow-through system	Ambient[a]	28 mM[a]	4–6°C	Black Sea (326 m)	0.65 µmol g-dw^{-1} day^{-1}[a]	NR	Wegener and Boetius (2009)
				Hydrate Ridge (776 m)	0.55 µmol g-dw^{-1} day^{-1}[a]	NR	Wegener and Boetius (2009)
				Gullfaks (150 m)	0.12 µmol g-dw^{-1} day^{-1}[a]	NR	Wegener and Boetius (2009)
Sediment flow-through (SLOT) system	Ambient	19 mM[c]	10°C	Eckernförde Bay (28 m)	5.32 nmol cm^{-3} day^{-1}[c]	NR	Steeb *et al*. (2014)
Continuous high-pressure bioreactor	8 MPa	9 mM	15°C	Gulf of Cadiz (1,200 m)	9.22 µmol g-dw^{-1} day^{-1}	**ANME-2a** and ANME-3	Zhang *et al*. (2010), Zhang *et al*. (2011)
High-pressure continuous incubation system (HP-CI system)	10 MPa	8 mM	20°C	Black Sea (213 m)	0.37 mmol g-dw^{-1} day^{-1}	NR	Deusner *et al*. (2010)

NR: not reported.
[a]Data from long-term incubations with short columns described in Wegener and Boetius (2009).
[b]Data from high-flow experiments with NON-SEEP sediments described in Girguis *et al*. (2005).
[c]Data from new high flow core experiments described in Steeb *et al*. (2014).
[d]Dominant ANME type is shown in bold.

The 16S rRNA gene sequence-based molecular analyses suggest that ANME-2a is the dominant anaerobic methane oxidizer in the DHS bioreactor. In contrast, the relative abundance of ANME-2c-related clones decreased during the period of bioreactor operation, and ANME-2c cells could not be detected by CARD-FISH in the 2,013-day sample. ANME-2a and -2c are both categorized as members of ANME-2 (Knittel *et al*., 2005), but ANME-2a and -2c are phylogenetically distinct at the genus and family levels (*e.g.*, the predominant ANME-2a phylotype MK0D_A9 has 89.8% 16S rRNA gene sequence identity to the ANME-2c phylotype MK0D_A1). Thus, ANME-2a and -2c may differ in their physiological properties, and the physical-chemical conditions in the DHS bioreactor cultivation appear to favor enrichment of ANME-2a. The physical-chemical conditions potentially controlling the occurrence of specific ANME groups are still under debate (Knittel *et al*., 2005; Girguis *et al*., 2005; Nauhaus *et al*., 2005; Rossel *et al*., 2011; Yanagawa *et al*., 2011), but the environmental distributions of intact polar membrane lipids, and *mcrA* gene and 16S rRNA gene sequences have indicated that

ANME-2 dominates in relatively sulfate-rich or high-sulfate-flux environments (Rossel *et al*., 2011; Yanagawa *et al*., 2011; Nunoura *et al*., 2006; Vigneron *et al*., 2013). The dominance of ANME-2a populations has also been confirmed in a submerged-membrane bioreactor system fed with high concentrations of sulfate (**Table 2-3**) (Jagersma *et al*., 2009; Meulepas *et al*., 2009). In

addition to the sulfate concentration, the redox potential is thought to be a significant variable affecting the occurrence of ANME-2a. The habitats typically dominated by ANME-2 and -3 members are characterized by higher dissolved oxygen (DO) contents (*i.e.*, higher redox environments) than ANME-1-dominated habitats (Knittel *et al*., 2005; Rossel *et al*., 2011. A high-pressure continuous-flow AOM bioreactor was also reported to be dominated by ANME-2a and gammaproteobacterial aerobic methanotroph populations (Zhang *et al*., 2010; Zhang *et al*., 2011). Therefore, assuming that contamination with a small amount of molecular oxygen is inevitable in continuous-flow bioreactor systems, the preferred enrichment of ANME-2a may be explained by the combination of high-sulfate and relatively more oxidative conditions. The effect of the incubation temperature (*i.e*., 10°C) on the predominance of ANME-2a is unlikely to be significant because some ANME-1 and -2 members are metabolically active at ~10°C (Nauhaus *et al*., 2005).

FISH and 16S rRNA clone analyses revealed that active ANME-1 cells also thrived in the DHS bioreactor. ANME-1 members are frequently observed in the deeper zones of subseafloor sediments and in the internal section of microbial mats (Nunoura *et al*., 2006; Krüger *et al*., 2008; Yanagawa *et al*., 2011; Vigneron *et al*., 2013), indicating that members of ANME-1 prefer to inhabit highly reductive environments. Considering these previous observations and the possible occurrence of DO concentration gradients in the sponge carriers (Araki *et al*., 1999; Machdar *et al*., 2000), the ANME-1 cells may colonize the interior portion of the sponge carriers and/or the lower portion of the DHS bioreactor, where redox potentials are comparatively low. In addition, the coexistence of three ANME groups (*i.e.*, ANME-1, -2, and -3) in the DHS bioreactor is interesting because their co-occurrence has only been reported in some marine sediments (Knittel *et al*., 2009; Vigneron *et al*., 2013). This co-occurrence may have resulted from physical-chemical gradients along bioreactor height and/or sponge carrier depth. It should be noted that the composition of the ANME groups in inoculum sediments would significantly affect the cultivation results, along with physical-chemical factors.

The presence of ANME-1, -2a, and most ANME-2c cells without close physical interaction with bacterial cells (**Fig. 2-7**) is intriguing because ANMEs may require a close physical interaction with their syntrophic SRB partners to perform AOM (Hoehler *et al*., 1994; Boetius *et al*., 2000; Orphan *et al*., 2001). AOM without syntrophic SRB partners is still largely unknown, but a bacteria-independent AOM mechanism has been recently proposed by Milucka *et al*. (2012). In contrast, the involvement of SRB in AOM cannot be denied because some potential sulfate-reducing deltaproteobacterial phylotypes (*i.e.*, *Desulfobacteraceae* and SEEP-SRB1) were detected, even after 2,013 days of enrichment (**Fig. S2-3B**). Further enrichment and multicomponent investigations may shed more light on the mechanisms of AOM.

In addition to ANMEs, other diverse uncultured archaeal lineages, such as DSAG, MBG-D, MEG, DSEG-2, MCG, MHVG, and AAG, were also identified in the DHS bioreactor incubation samples. DSAG members are known to be a predominant archaeal component of subseafloor sediments (Fry *et al*., 2008; Teske *et al*., 2008; Durbin *et al*., 2012). Metabolically active DSAG members have frequently been detected within sulfate-methane

transition zones, where AOM is prominent (Biddle *et al*., 2006; Sørensen *et al*., 2006). A previous study of the stable carbon isotopic composition of archaeal lipids/cells suggested that DSAG might assimilate sedimentary organic matter as a carbon source while performing AOM for energy generation (Biddle *et al*., 2006). The occurrence of active DSAG phylotypes in the bioreactor provides further evidence that DSAG may be sustained by AOM. However, current studies based on the co-variation of DASG archaeal 16S rRNA gene abundance and geochemical data suggest that members of DSAG are heterotrophic and involved in the iron and/or manganese cycle (Jorgensen *et al*., 2012; Jørgensen *et al*., 2013). In the bioreactor, we supplied iron and manganese compounds as trace elements. DHS bioreactor systems are also known to possess the ability to maintain a relatively large biomass (Onodera *et al*., 2013). Therefore, the presence of iron, manganese, and a higher concentration of biomass-derived organic compounds may enhance the growth of DSAG phylotypes. MBG-D, a *Thermoplasmata*-related uncultured archaeal lineage, is globally distributed in marine sediments (Lloyd *et al*., 2013) and has been co-detected with ANME-2a in some AOM enrichment cultures (Girguis *et al*., 2003; Jagersma *et al*., 2009; Zhang *et al*., 2011). Recent single-cell genomic sequencing has revealed that members of MBG-D are likely anaerobic protein-degrading microorganisms (Lloyd *et al*., 2013). Thus, active MBG-D phylotypes may utilize dead biomass produced in the bioreactor and/or extracellular organic matrix, which may be excreted by ANME populations (Krüger *et al*., 2008; Knittel *et al*., 2009). Other uncultured archaeal lineages, such as MEG, DSEG-2, MCG, MHVG, and AAG, may be metabolically less active in the DHS bioreactor because their sequences either were not retrieved or were less abundant in the 16S rRNA clone libraries (**Fig. 2-5A**, **S2-1**, and **S2-2**). In contrast, the detection of such previously uncultured archaeal lineages after long-term cultivation indicates that these archaeal lineages can be cultured under laboratory conditions mimicking methane-seep environments.

At the end of the long-term cultivation, gammaproteobacterial phylotypes were the dominant bacterial population. The dominant gammaproteobacterial phylotype, MK903D_B5, is phylogenetically similar to a chemoautotrophic sulfur-oxidizing endosymbiont group (e.g., 91.7% 16S rRNA gene sequence identity to an endosymbiont of *Alviniconcha* sp.; **Fig. S2-3C**). However, the physiological characteristics of this phylotype remain largely unknown because no closely related isolate exists. Thus, further analyses are needed to clarify the ecological roles of this phylotype. Detection of the *Methylococcales*, *Methylophaga*, and other aerobic bacterial phylotypes indicates that molecular oxygen may have contaminated the medium through the Viton tubing before entering the PVC column. However, the reducing condition of the effluent medium indicates removal of the dissolved molecular oxygen. The dissolved oxygen was likely reduced by these bacterial lineages during retention of the medium in the sponge carriers. An alternative explanation for the significant increase in the *Methylococcales* phylotypes in the oxygen-limited DHS bioreactor is that they might gain energy by methane-based fermentation metabolism, as recently shown by Kalyuzhnaya *et al*. (2013). Among the other diverse bacterial lineages, WS3, BD1-5, and OD1 were relatively abundant phylum-level uncultured bacterial lineages in the incubation samples

(**Fig. 2-5B**). These bacterial lineages have also been detected in marine sediments, including methane seeps and mud volcanoes (Li *et al*., 1999; Orcutt *et al*., 2010; Pachiadaki *et al*., 2010; Yanagawa *et al*., 2011), and metagenomic studies of acetate-amended aquifers revealed that members of OD1 and BD1-5 play an important role in molecular hydrogen production, sulfur cycling, and anaerobic fermentation of sedimentary carbon (Wrighton *et al*., 2012; Kantor *et al*., 2013). The biogeochemical roles of these bacterial lineages in marine environments are not yet fully understood, but these lineages probably contribute to the cycling of methane-derived carbon in methane-seep ecosystems.

2.5 Summary of this chapter

The results obtained in this study show that potential AOM entities phylogenetically affiliated with ANME-1, -2a, -2c, and -3 in the Nankai Trough methane-seep sediment would be active and might involve *in situ* AOM activity in the methane-seep sediment. The selective enrichment of ANME-2a in the coexistence of phylogenetically distinct ANME lineages supported the hypothesis that the existence of certain physical-chemical condition(s) controls the ANME community structure. The existence of ANME-1 and -2a, and that most ANME-2c cells occurred without close physical interaction with potential bacterial partners, implies that these archaeal components can perform AOM independently of potential bacterial partners. The detection of diverse yet-to-be-cultured microorganisms (*e.g.*, DSAG, MBG-D, and an uncultured gammaproteobacterial lineage) in addition to the ANMEs in the enrichment demonstrate that the DHS bioreactor system offers an initiative step to obtain a pure culture of ANMEs and other elusive uncultured microbes. Further multicomponent investigations (*e.g.*, subsequent isolation, (meta)genomic sequencing, and stable isotope labeling experiments) using DHS bioreactor enrichment cultures will enable the physiological characterization of the cryptic microorganisms in methane-seep ecosystems.

2.6 References

Agrawal LK, Ohashi Y, Mochida E, Okui H, Ueki Y, *et al*. (1997) Treatment of raw sewage in a temperate climate using a UASB reactor and the hanging sponge cubes process. *Wat Sci Technol* 36: 433–440.

Altschul SF, Madden TL, Schäffer AA, Zhang J, Zhang Z, *et al*. (1997) Gapped BLAST and PSI-BLAST: a new generation of protein database search programs. *Nucleic Acids Res* 25: 3389–3402.

Araki N, Ohashi A, Machdar I, Harada H (1999) Behaviors of nitrifiers in a novel biofilm reactor employing hanging sponge-cubes as attachment site. *Wat Sci Technol* 39: 23–31.

Bertram S, Blumenberg M, Michaelis W, Siegert M, Krüger M, Seifert R (2013) Methanogenic capabilities of ANME-archaea deduced from ^{13}C-labelling approaches. *Environ Microbiol* 15: 2384–2393.

Biddle JF, Lipp JS, Lever MA, Lloyd KG, Sørensen KB, *et al*. (2006) Heterotrophic Archaea dominate sedimentary subsurface ecosystems off Peru. *Proc Natl Acad Sci U S A* 103: 3846–3851.

Boetius A, Ravenschlag K, Schubert CJ, Rickert D, Widdel F, *et al*. (2000) A marine microbial consortium apparently mediating anaerobic oxidation of methane. *Nature* 407: 623–626.

Bowman JP (2005) Order VII. *Methylococcales* ord. nov. *In* Brenner DJ, Krieg NR, Staley JR, Garrity GM (eds.),

Bergey's Manual of Systematic Bacteriology (2nd edition), Springer, pp. 248–252.
Deusner C, Meyer V, Ferdelman TG (2010) High-pressure systems for gas-phase free continuous incubation of enriched marine microbial communities performing anaerobic oxidation of methane. *Biotechnol Bioeng* 105: 524–533.
Durbin AM, Teske A (2012) Archaea in organic-lean and organic-rich marine subsurface sediments: an environmental gradient reflected in distinct phylogenetic lineages. *Front Microbiol* 3:168.
Fry JC, Parkes RJ, Cragg BA, Weightman AJ, Webster G (2008) Prokaryotic biodiversity and activity in the deep subseafloor biosphere. *FEMS Microbiol Ecol* 66:181–196.
Girguis PR, Orphan VJ, Hallam SJ, DeLong EF (2003) Growth and methane oxidation rates of anaerobic methanotrophic archaea in a continuous-flow bioreactor. *Appl Environ Microbiol* 69:5472–5482.
Girguis PR, Cozen AE, DeLong EF (2005) Growth and population dynamics of anaerobic methane-oxidizing archaea and sulfate-reducing bacteria in a continuous-flow bioreactor. *Appl Environ Microbiol* 71:3725–3733.
Good IJ (1953) The population frequencies of species and the estimation of population parameters. *Biometrika* 40:237–264.
Green-Saxena A, Dekas AE, Dalleska NF, Orphan VJ (2014) Nitrate-based niche differentiation by distinct sulfate-reducing bacteria involved in the anaerobic oxidation of methane. *ISME J* 8:150–163.
Hallam SJ, Putnam N, Preston CM, Detter JC, Rokhsar D, *et al*. (2004) Reverse methanogenesis: testing the hypothesis with environmental genomics. *Science* 305:1457–1462.
Harrison BK, Zhang H, Berelson W, Orphan VJ (2009) Variations in archaeal and bacterial diversity associated with the sulfate-methane transition zone in continental margin sediments (Santa Barbara Basin, California). *Appl Environ Microbiol* 75:1487–1499.
Heijs SK, Haese RR, van der Wielen PW, Forney LJ, van Elsas JD (2007) Use of 16S rRNA gene based clone libraries to assess microbial communities potentially involved in anaerobic methane oxidation in a Mediterranean cold seep. *Microb Ecol* 53:384–398.
Hoehler TM, Alperin MJ, Albert DB, Martens CS (1994) Field and laboratory studies of methane oxidation in an anoxic marine sediment: Evidence for a methanogen-sulfate reducer consortium. *Glob Biogeochem Cycles* 8:451–463.
Holler T, Widdel F, Knittel K, Amann R, Kellermann MY, *et al*. (2011) Thermophilic anaerobic oxidation of methane by marine microbial consortia. *ISME J* 5:1946–1956.
Imachi H, Sekiguchi Y, Kamagata Y, Loy A, Qiu YL, *et al*. (2006) Non-sulfate-reducing, syntrophic bacteria affiliated with *Desulfotomaculum* cluster I are widely distributed in methanogenic environments. *Appl Environ Microbiol* 72:2080–2091.
Imachi H, Sakai S, Hirayama H, Nakagawa S, Nunoura T, *et al*. (2008) *Exilispira thermophila* gen. nov., sp. nov., an anaerobic, thermophilic spirochaete isolated from a deep-sea hydrothermal vent chimney. *Int J Syst Evol Microbiol* 58:2258–2265.
Imachi H, Sakai S, Nagai H, Yamaguchi T, Takai K (2009) *Methanofollis ethanolicus* sp. nov., an ethanol-utilizing methanogen isolated from a lotus field. *Int J Syst Evol Microbiol* 59:800–805.
Imachi H, Aoi K, Tasumi E, Saito Y, Yamanaka Y, *et al*. (2011) Cultivation of methanogenic community from subseafloor sediments using a continuous-flow bioreactor. *ISME J* 5:1913–1925.
Inagaki F, Tsunogai U, Suzuki M, Kosaka A, Machiyama H, *et al*. (2004) Characterization of C_1-metabolizing prokaryotic communities in methane seep habitats at the Kuroshima Knoll, southern Ryukyu Arc, by analyzing *pmoA*, *mmoX*, *mxaF*, *mcrA*, and 16S rRNA genes. *Appl Environ Microbiol* 70:7445–7455.
Inagaki F, Nunoura T, Nakagawa S, Teske A, Lever M, *et al*. (2006) Biogeographical distribution and diversity of microbes in methane hydrate-bearing deep marine sediments on the Pacific Ocean Margin. *Proc Natl Acad Sci U S A* 103:2815–2820.
Jagersma GC, Meulepas RJ, Heikamp-de Jong I, Gieteling J, Klimiuk A, *et al*. (2009) Microbial diversity and community structure of a highly active anaerobic methane-oxidizing sulfate-reducing enrichment. *Environ Microbiol* 11:3223–3232.
Jorgensen SL, Hannisdal B, Lanzén A, Baumberger T, Flesland K, *et al*. (2012) Correlating microbial community profiles with geochemical data in highly stratified sediments from the Arctic Mid-Ocean Ridge. *Proc Natl Acad Sci U S A* 109:E2846–2855.
Jørgensen SL, Thorseth IH, Pedersen RB, Baumberger T, Schleper C (2013) Quantitative and phylogenetic study of the Deep Sea Archaeal Group in sediments of the Arctic mid-ocean spreading ridge. *Front Microbiol* 4:299.
Kalyuzhnaya MG, Yang S, Rozova ON, Smalley NE, Clubb J, *et al*. (2013) Highly efficient methane biocatalysis revealed in a methanotrophic bacterium. *Nat Commun* 4:2785.
Kantor RS, Wrighton KC, Handley KM, Sharon I, Hug LA, *et al*. (2013) Small genomes and sparse metabolisms of sediment-associated bacteria from four candidate phyla. *MBio* 4:e00708–00713.
Kleindienst S, Ramette A, Amann R, Knittel K (2012) Distribution and *in situ* abundance of sulfate-reducing

bacteria in diverse marine hydrocarbon seep sediments. *Environ Microbiol* 14:2689–2710.
Knittel K, Lösekann T, Boetius A, Kort R, Amann R (2005) Diversity and distribution of methanotrophic archaea at cold seeps. *Appl Environ Microbiol* 71:467–479.
Knittel K, Boetius A (2009) Anaerobic oxidation of methane: progress with an unknown process. Annu Rev Microbiol 63:311–334.
Krüger M, Blumenberg M, Kasten S, Wieland A, Kanel L, *et al*. (2008) A novel, multi-layered methanotrophic microbial mat system growing on the sediment of the Black Sea. *Environ Microbiol* 10:1934–1947.
Kubota K, Ohashi A, Imachi H, Harada H (2006) Visualization of *mcr* mRNA in a methanogen by fluorescence *in situ* hybridization with an oligonucleotide probe and two-pass tyramide signal amplification (two-pass TSA-FISH). *J Microbiol Methods* 66:521–528.
Li L, Kato C, Horikoshi K (1999) Bacterial diversity in deep-sea sediments from different depths. *Biodivers Conserv* 8: 659–677.
Liu Y, Whitman WB (2008) Metabolic, phylogenetic, and ecological diversity of the methanogenic archaea. *Ann N Y Acad Sci* 1125:171–189.
Lloyd KG, Schreiber L, Petersen DG, Kjeldsen KU, Lever MA, *et al*. (2013) Predominant archaea in marine sediments degrade detrital proteins. *Nature* 496:215–218.
Ludwig W, Strunk O, Westram R, Richter L, Meier H, *et al*. (2004) ARB: a software environment for sequence data. *Nucleic Acids Res* 32:1363–1371.
Machdar I, Sekiguchi Y, Sumino H, Ohashi A, Harada H (2000) Combination of a UASB reactor and a curtain type DHS (downflow hanging sponge) reactor as a cost-effective sewage treatment system for developingcountries. *Wat Sci Technol* 42:83–88.
Magurran AE (2004) Measuring biological diversity, Blackwell Publishing.
Meulepas RJW, Jagersma CG, Gieteling J, Buisman CJ, Stams AJ, *et al*. (2009) Enrichment of anaerobic methanotrophs in sulfate-reducing membrane bioreactors. *Biotechnol Bioeng* 104:458–470.
Meulepas RJW, Jagersma CG, Zhang Y, Petrillo M, Cai H, *et al*. (2010) Trace methane oxidation and the methane dependency of sulfate reduction in anaerobic granular sludge. *FEMS Microbiol Ecol* 72:261–271.
Meyerdierks A, Kube M, Kostadinov I, Teeling H, Glöckner FO, *et al*. (2010) Metagenome and mRNA expression analyses of anaerobic methanotrophic archaea of the ANME-1 group. *Environ Microbiol* 12:422–439.
Milucka J, Ferdelman TG, Polerecky L, Franzke D, Wegener G, *et al*. (2012) Zero-valent sulphur is a key intermediate in marine methane oxidation. *Nature* 491:541–546.
Miyashita A, Mochimaru H, Kazama H, Ohashi A, Yamaguchi T, *et al*. (2009) Development of 16S rRNA gene-targeted primers for detection of archaeal anaerobic methanotrophs (ANMEs). *FEMS Microbiol Lett* 297:31–37.
Moench TT, Zeikus JG (1983) An improved preparation method for a titanium(III) media reductant. *J Microbiol Methods* 1: 199–202.
Nauhaus K, Boetius A, Krüger M, Widdel F (2002) *In vitro* demonstration of anaerobic oxidation of methane coupled to sulphate reduction in sediment from a marine gas hydrate area. *Environ Microbiol* 4:296–305.
Nauhaus K, Treude T, Boetius A, Krüger M (2005) Environmental regulation of the anaerobic oxidation of methane: a comparison of ANME-I and ANME-II communities. *Environ Microbiol* 7:98–106.
Nauhaus K, Albrecht M, Elvert M, Boetius A, Widdel F (2007) *In vitro* cell growth of marine archaeal-bacterial consortia during anaerobic oxidation of methane with sulfate. *Environ Microbiol* 9:187–196.
Niemann H, Lösekann T, de Beer D, Elvert M, Nadalig T, *et al*. (2006) Novel microbial communities of the Haakon Mosby mud volcano and their role as a methane sink. *Nature* 443:854–858.
Nunoura T, Oida H, Toki T, Ashi J, Takai K, *et al*. (2006) Quantification of *mcrA* by quantitative fluorescent PCR in sediments from methane seep of the Nankai Trough. *FEMS Microbiol Ecol* 57:149–157.
Nunoura T, Takaki Y, Kazama H, Hirai M, Ashi J, *et al*. (2012) Microbial diversity in deep-sea methane seep sediments presented by SSU rRNA gene tag sequencing. Microbes Environ 27: 382–390.
Onodera T, Matsunaga K, Kubota K, Taniguchi R, Harada H, *et al*. (2013) Characterization of the retained sludge in a down-flow hanging sponge (DHS) reactor with emphasis on its low excess sludge production. *Bioresour Technol* 136:169–175.
Orcutt BN, Joye SB, Kleindienst S, Knittel K, Ramette A, *et al*. (2010) Impact of natural oil and higher hydrocarbons on microbial diversity, distribution, and activity in Gulf of Mexico cold-seep sediments. *Deep-Sea Res Pt II* 57:2008–2021.
Orphan VJ, House CH, Hinrichs KU, McKeegan KD, DeLong EF (2001) Methane-consuming archaea revealed by directly coupled isotopic and phylogenetic analysis. *Science* 293:484–487.
Pachiadaki MG, Lykousis V, Stefanou EG, Kormas KA (2010) Prokaryotic community structure and diversity in the sediments of an active submarine mud volcano (Kazan mud volcano, East Mediterranean Sea). *FEMS*

Microbiol Ecol 72:429–444.
Pernthaler A, Pernthaler J, Amann R (2002) Fluorescence in situ hybridization and catalyzed reporter deposition for the identification of marine bacteria. *Appl Environ Microbiol* 68:3094–3101.
Pernthaler A, Dekas AE, Brown CT, Goffredi SK, *et al.* (2008) Diverse syntrophic partnerships from deep-sea methane vents revealed by direct cell capture and metagenomics. *Proc Natl Acad Sci U S A* 105:7052–7057.
Reeburgh WS (2007) Oceanic methane biogeochemistry. *Chem Rev* 107:486–513.
Rossel PE, Elvert M, Ramette A, Boetius A, Hinrichs K-U (2011) Factors controlling the distribution of anaerobic methanotrophic communities in marine environments: Evidence from intact polar membrane lipids. *Geochim Cosmochim Acta* 75:164–184.
Schramm A, Fuchs BM, Nielsen JL, Tonolla M, Stahl DA (2002) Fluorescence *in situ* hybridization of 16S rRNA gene clones (Clone-FISH) for probe validation and screening of clone libraries. *Environ Microbiol* 4:713–720.
Schreiber L, Holler T, Knittel K, Meyerdierks A, Amann R (2010) Identification of the dominant sulfate-reducing bacterial partner of anaerobic methanotrophs of the ANME-2 clade. *Environ Microbiol* 12:2327–2340.
Sekiguchi Y, Kamagata Y, Nakamura K, Ohashi A, Harada H (1999) Fluorescence in situ hybridization using 16S rRNA-targeted oligonucleotides reveals localization of methanogens and selected uncultured bacteria in mesophilic and thermophilic sludge granules. *Appl Environ Microbiol* 65:1280–1288.
Sekiguchi Y, Uyeno Y, Sunaga A, Yoshida H, Kamagata Y (2005) Sequence-specific cleavage of 16S rRNA for rapid and quantitative detection of particular groups of anaerobes in bioreactors. *Wat Sci Technol* 52:107–113.
Sørensen KB, Teske A (2006) Stratified communities of active Archaea in deep marine subsurface sediments. *Appl Environ Microbiol* 72:4596–4603.
Sowers KR (2001) Genus II. *Methanococcoides*. *In* Boone DR, Castenholz RW, Garrity G (eds.), Bergey's Manual of Systematic Bacteriology (2nd edition), Springer, pp. 276–278.
Steeb P, Linke P, Treude T (2014) A sediment flow-through system to study the impact of shifting fluid and methane flow regimes on the efficiency of the benthic methane filter. *Limnol Oceanogr Methods* 12:25–45.
Stokke R, Roalkvam I, Lanzen A, Haflidason H, Steen IH (2012) Integrated metagenomic and metaproteomic analyses of an ANME-1-dominated community in marine cold seep sediments. *Environ Microbiol* 14:1333–1346.
Teske A, Sørensen KB (2008) Uncultured archaea in deep marine subsurface sediments: have we caught them all? *ISME J* 2:3–18.
Uemura S, Harada H (2010) Application of UASB technology for sewage treatment with a novel post-treatment process. *In* HHP Fang (ed.), Environmental Aanaerobic Technology, Imperial College Press, pp. 91–112.
Valentine DL (2007) Adaptations to energy stress dictate the ecology and evolution of the Archaea. *Nat Rev Microbiol* 5:316–323.
Vigneron A, Cruaud P, Pignet P, Caprais JC, Cambon-Bonavita MA, *et al*. (2013) Archaeal and anaerobic methane oxidizer communities in the Sonora Margin cold seeps, Guaymas Basin (Gulf of California). *ISME J* 7:1595–1608.
Wang FP, Zhang Y, Chen Y, He Y, Qi J, *et al*. (2013) Methanotrophic archaea possessing diverging methane-oxidizing and electron-transporting pathways. *ISME J* 8: 1069–1078.
Wegener G, Boetius A (2009) An experimental study on short-term changes in the anaerobic oxidation of methane in response to varying methane and sulfate fluxes. *Biogeosciences* 6:867–876.
Wrighton KC, Thomas BC, Sharon I, Miller CS, Castelle CJ, *et al*. (2012) Fermentation, hydrogen, and sulfur metabolism in multiple uncultivated bacterial phyla. *Science* 337: 1661–1665.
Yamamoto S, Alcauskas JB, Crozier TE (1976) Solubility of methane in distilled water and seawater. *J Chem Eng Data* 21:78–80.
Yanagawa K, Sunamura M, Lever MA, Morono Y, Hiruta A, *et al*. (2011) Niche separation of methanotrophic archaea (ANME-1 and -2) in methane-seep sediments of the Eastern Japan Sea offshore Joetsu. *Geomicrobiol J* 28:118–129.
Yoshioka H, Maruyama A, Nakamura T, Higashi Y, Fuse H, *et al*. (2010) Activities and distribution of methanogenic and methane-oxidizing microbes in marine sediments from the Cascadia Margin. Geobiology 8:223–233.
Zhang Y, Henriet JP, Bursens J, Boon N (2010) Stimulation of *in vitro* anaerobic oxidation of methane rate in a continuous high-pressure bioreactor. *Bioresour Technol* 101:3132–3138.
Zhang Y, Maignien L, Zhao X, Wang F, Boon N (2011) Enrichment of a microbial community performing anaerobic oxidation of methane in a continuous high-pressure bioreactor. *BMC Microbiol* 11:137.

2.7 Supplementary Information

Figure S2-1. Phylogenetic tree showing the affiliations of *Euryarchaeota*-related 16S rRNA gene and 16S rRNA phylotypes obtained in this study. The phylotypes obtained in this study are shown in red, bold type. The initial tree was constructed with sequences that were longer than 1,000 nucleotides, using the neighbor-joining method. Shorter sequences were subsequently inserted into the tree using the parsimony insertion tool in the ARB program. Three crenarchaeotal sequences (*Aeropyrum pernix* K1 [D83259], *Sulfolobus acidocaldarius* ATCC 33909 [D14876], and *Thermofilum pendens* DSM 2475 [X14835]) were used as the outgroups (not shown). The numbers in parentheses indicate the number of phylotypes in each clone library and their frequency in each library in the following order: 16S rRNA gene clone library at day 0 (the inoculum sample), 16S rRNA gene clone library at day 903, 16S rRNA clone library at day 903, 16S rRNA gene clone library at day 1,732, 16S rRNA gene clone library at day 2,013, and 16S rRNA clone library at day 2,013. The scale bar represents the estimated number of nucleotide changes per sequence position. The symbols at the nodes show the bootstrap values (only those > 75% are indicated) obtained after 1,000 resamplings.

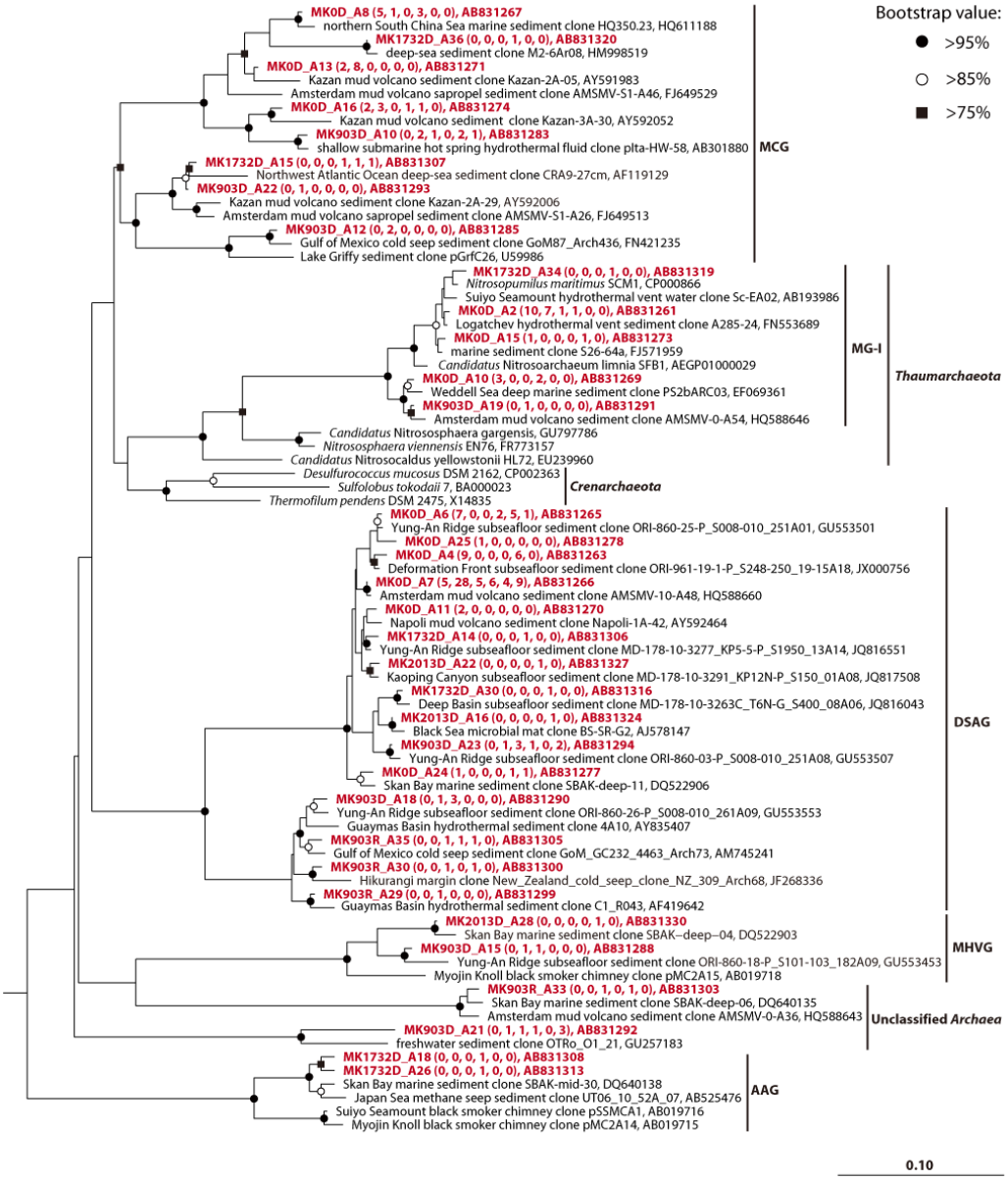

Figure S2-2. Phylogenetic tree showing the phylogenetic affiliations of *Crenarchaeota*, *Thaumarchaeota*, and deeply branching archaea-related 16S rRNA gene and 16S rRNA phylotypes obtained in this study. The tree was constructed in the same manner as the *Euryarchaeota*-related 16S rRNA gene and 16S rRNA phylotypes (**Fig. S2-1**). Three bacterial sequences (*Bacillus subtilis* subsp. *subtilis* NCIB 3610 [ABQL01000001], *Escherichia coli* ATCC 11775 [X80725], and *Aquifex pyrophilus* Kol5a [M83548]) were used as the outgroups (not shown). The scale bar represents the estimated number of nucleotide changes per sequence position. The bold and colored sequences, symbols at the nodes, and numbers in the parentheses indicate the same meanings as in **Fig. S2-1**.

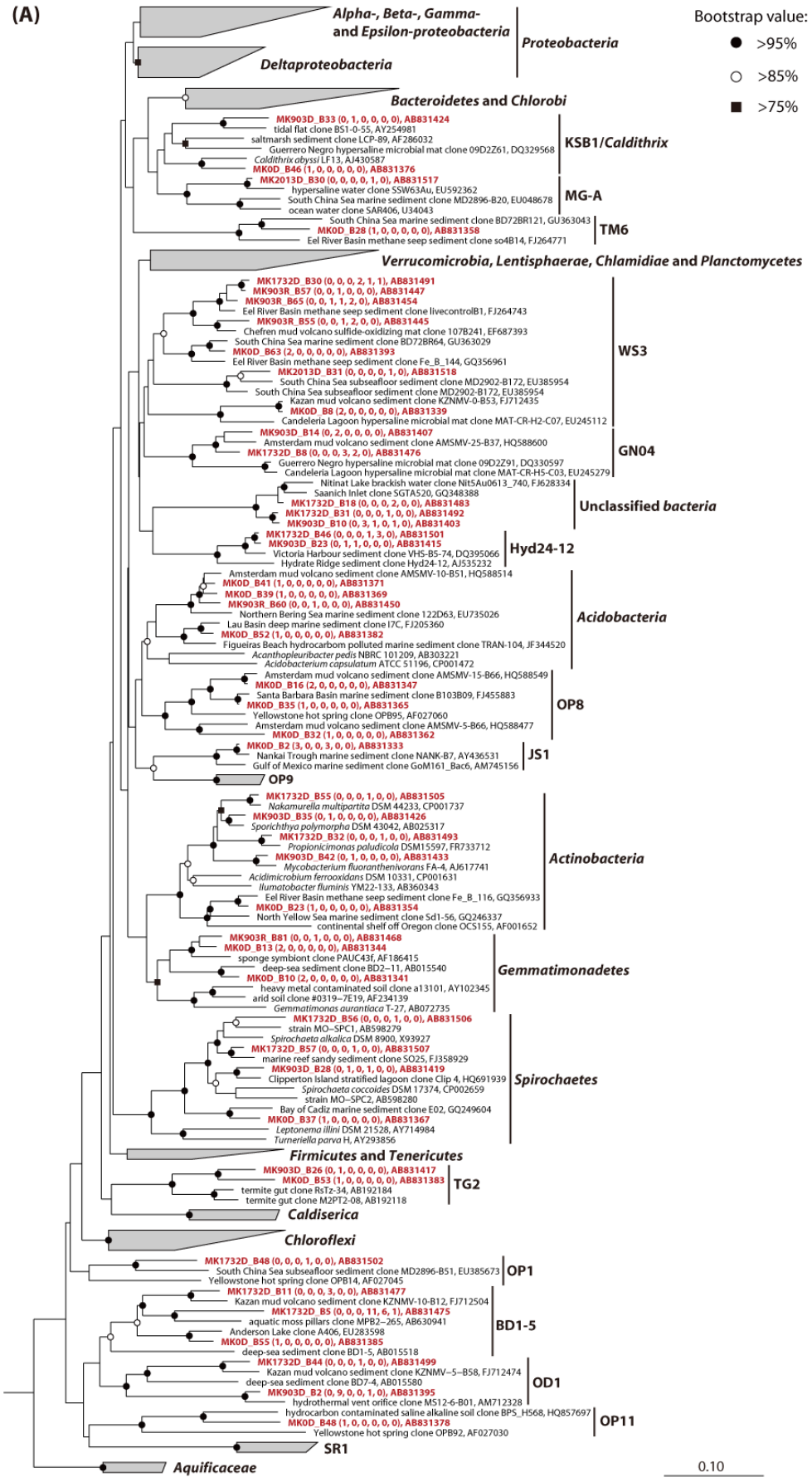
(A)
Alpha-, Beta-, Gamma- and Epsilon-proteobacteria
Proteobacteria
Deltaproteobacteria
Bacteroidetes and Chlorobi
KSB1/Caldithrix
MG-A
TM6
Verrucomicrobia, Lentisphaerae, Chlamidiae and Planctomycetes
WS3
GN04
Unclassified bacteria
Hyd24-12
Acidobacteria
OP8
JS1
OP9
Actinobacteria
Gemmatimonadetes
Spirochaetes
Firmicutes and Tenericutes
TG2
Caldiserica
Chloroflexi
OP1
BD1-5
OD1
OP11
SR1
Aquificaceae
Bootstrap value:
>95%
>85%
>75%
0.10

(See figure on previous page.)

Figure S2-3. Phylogenetic tree showing the phylogenetic affiliations of bacterial 16S rRNA gene and 16S rRNA phylotypes obtained in this study. The initial tree was constructed with sequences longer than 1,200 nucleotides, using the neighbor-joining method. Shorter sequences were subsequently inserted into the tree using the parsimony insertion tool in the ARB program. Three archaeal sequences (*Methanosarcina acetivorans* C2A [AE010299], *Thermococcus profundus* DT5432 [Z75233], and *Nitrosopimilus maritimus* SCM1 [CP000866]) were used as the outgroups (not shown). (A) A large bacterial tree including diverse bacterial groups. (B–G) Expanded bacterial phylogenetic trees for (B) *Deltaproteobacteria*, (C) *Alphaproteobacteria*, *Betaproteobacteria*, *Gammaproteobacteria*, and *Epsilonproteobacteria*, (D) *Verrucomicrobia*, *Lentisphaerae*, *Chlamidiae*, and *Planctomycetes*, (E) *Bacteroidetes* and *Chlorobi*, (F) *Firmicutes* and *Tenericutes*, and (G) *Chloroflexi*. The scale bars represent the estimated number of nucleotide changes per sequence position. The bold and colored sequences, symbols at the nodes, and numbers in the parentheses indicate the same meanings as in **Fig. S2-1**.

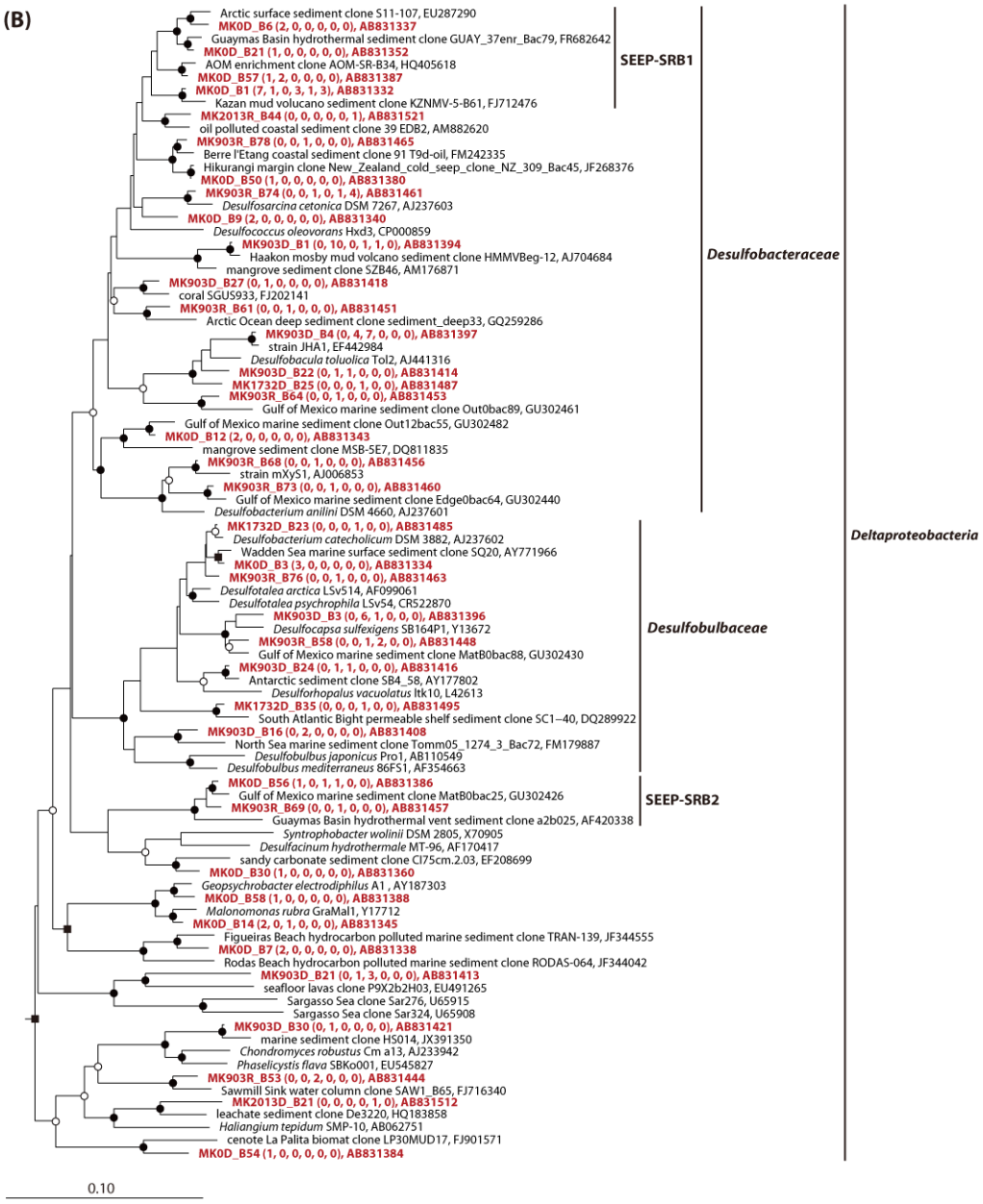

Figure S2-3—continued.

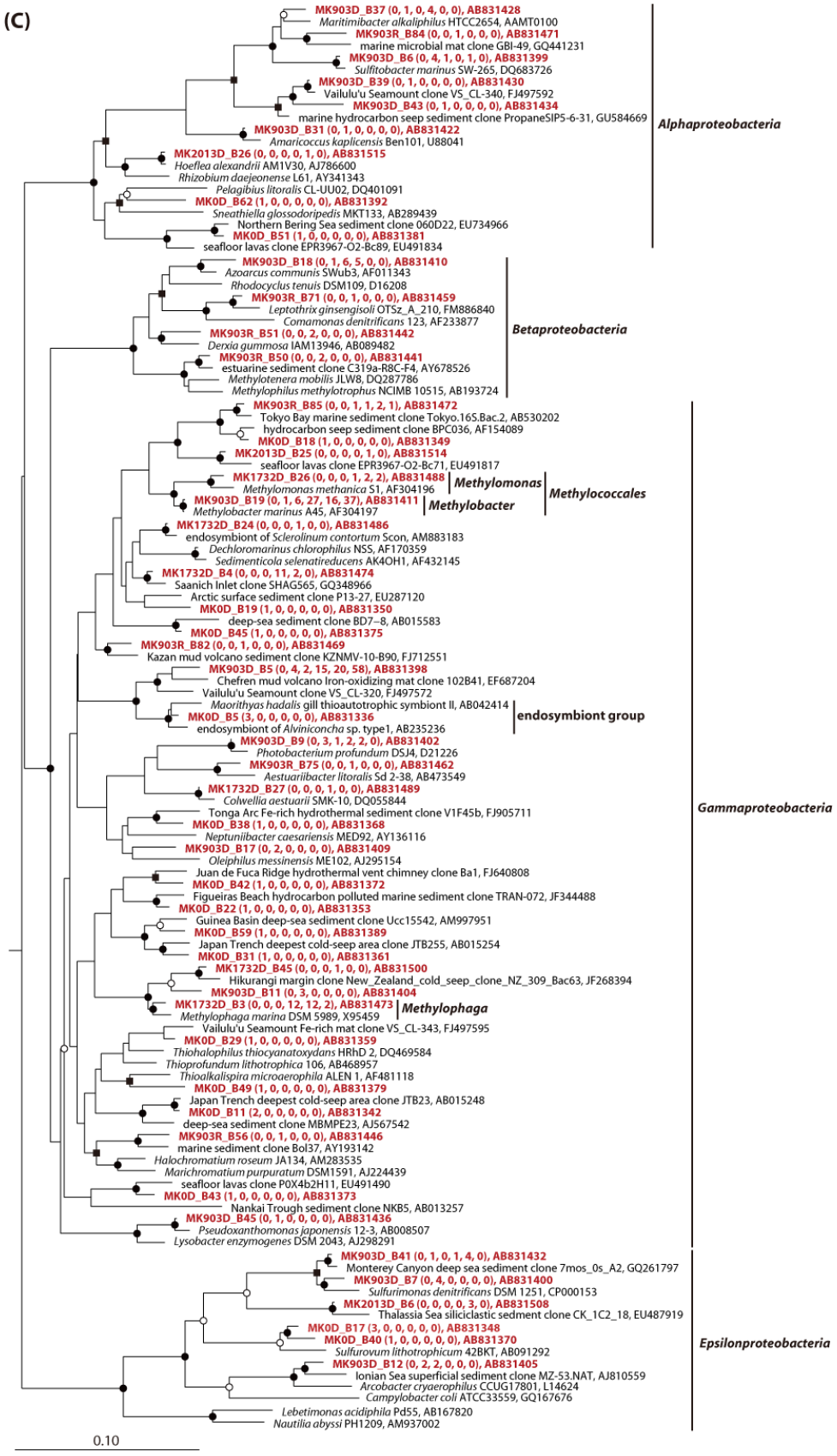

Figure S2-3—continued.

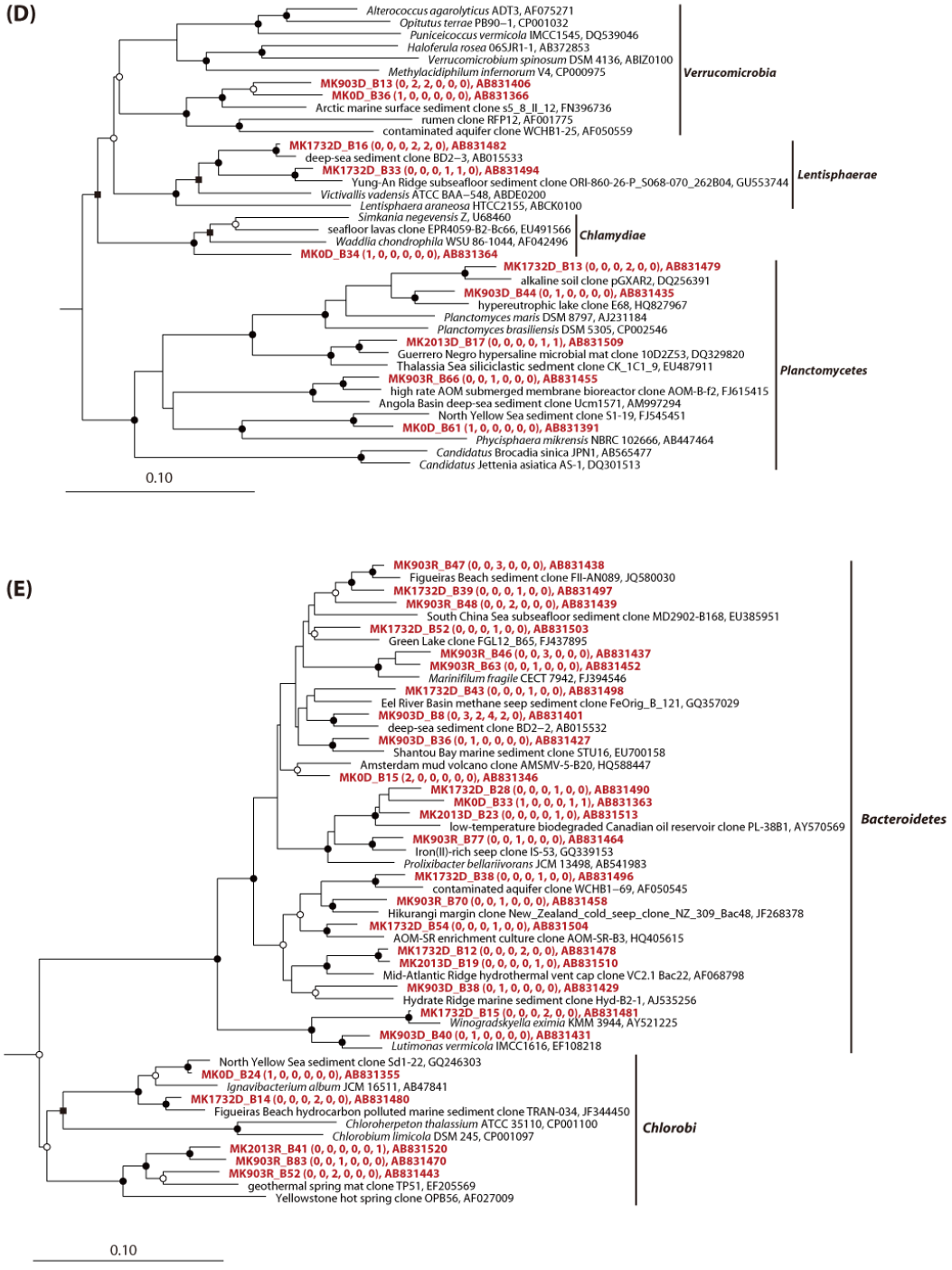

Figure S2-3—continued.

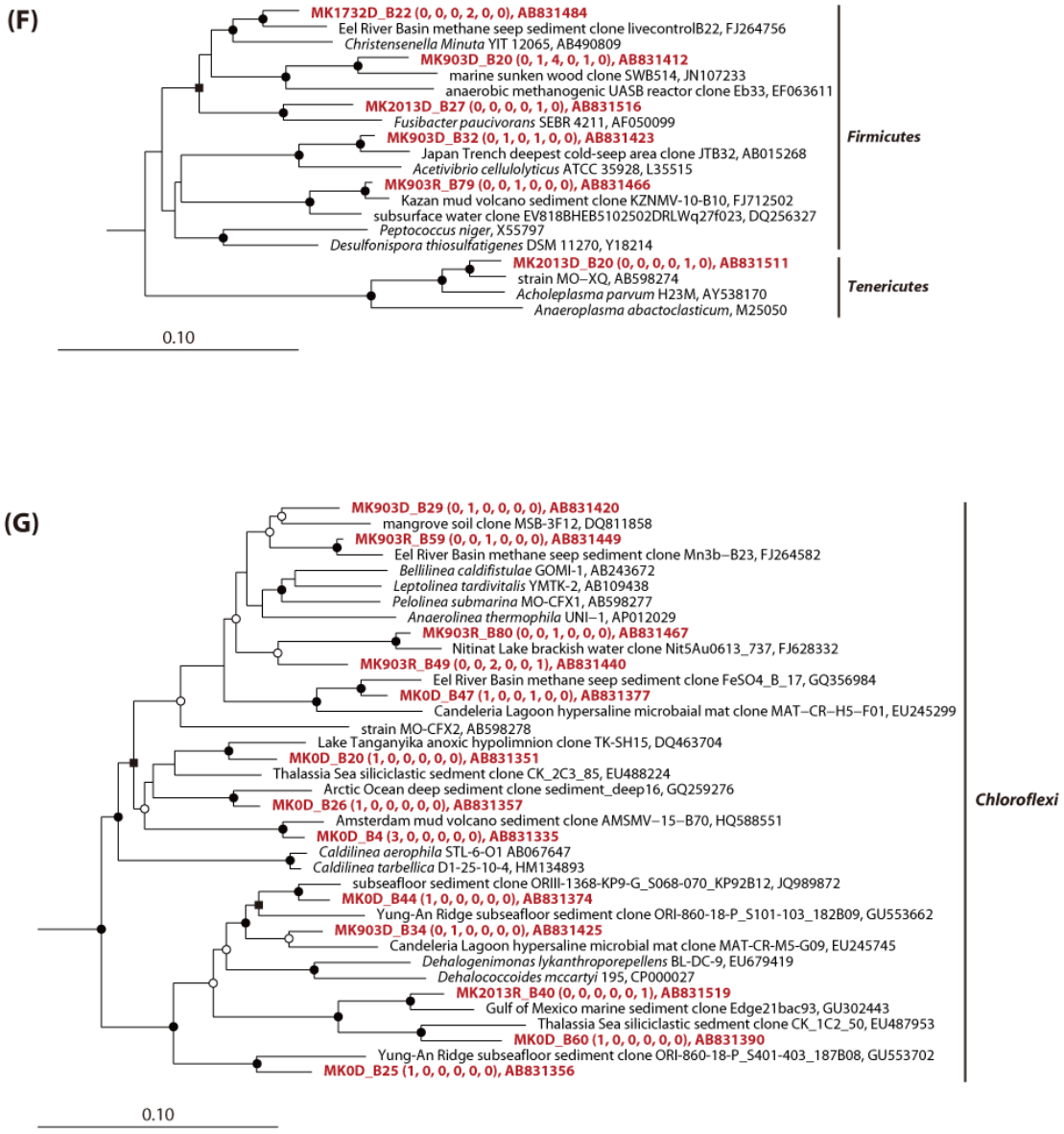

Figure S2-3—continued.

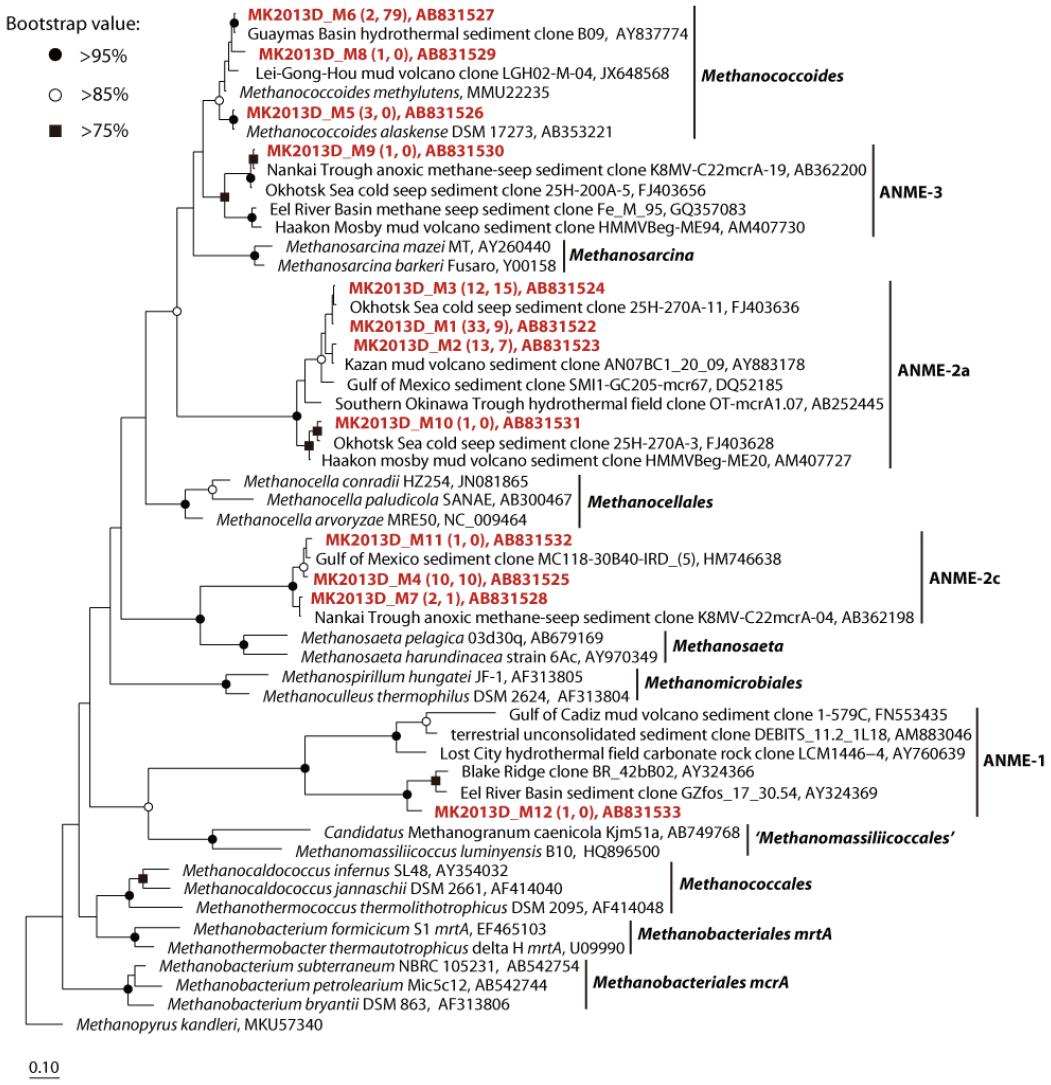

Figure S2-4. Phylogenetic tree showing the phylogenetic affiliations of deduced McrA amino acid sequences obtained in this study. The numbers in parentheses indicate the number of phylotypes in each clone library and their frequency in each library in the following order: *mcrA* gene-based clone library at day 2,013, and *mcrA* mRNA-based clone library at day 2,013. The scale bar indicates 10% estimated sequence divergence. The meanings of the bold and colored sequences, and symbols at the nodes are the same as in **Fig. S2-1**.

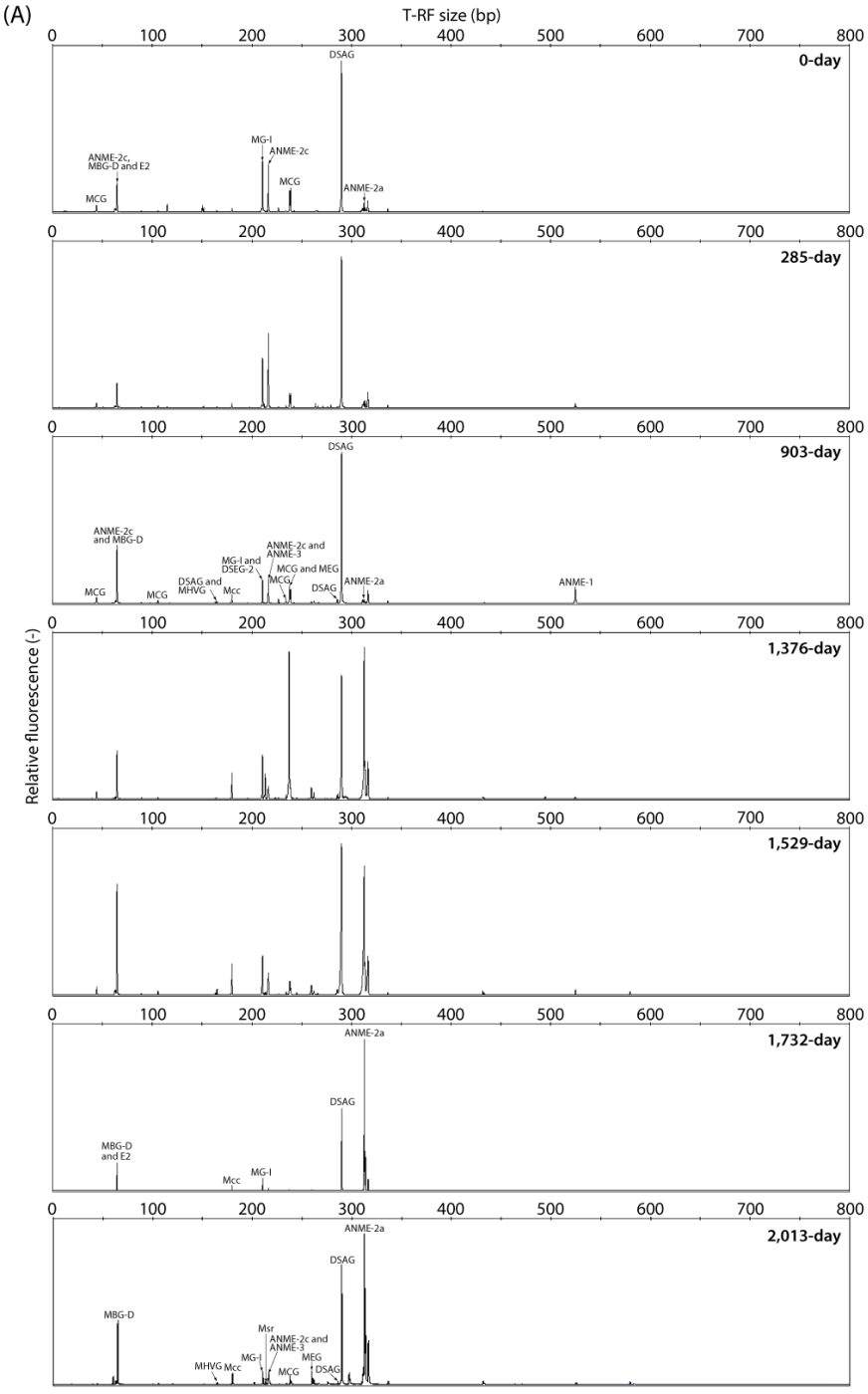

Figure S2-5. T-RFLP profiles of archaeal 16S rRNA genes digested with (A) HaeIII or (B) HhaI. The phylogenetic affiliations of each T-RF were identified using the archaeal 16S rRNA gene and 16S rRNA clone sequences obtained in this study. The abbreviations for some peaks are as follows: Mcc, *Methanococcoides*; Msr, uncultured *Methanosarcinaceae*; UE, unclassified *Euryarchaeota*; and UA, unclassified *Archaea*.

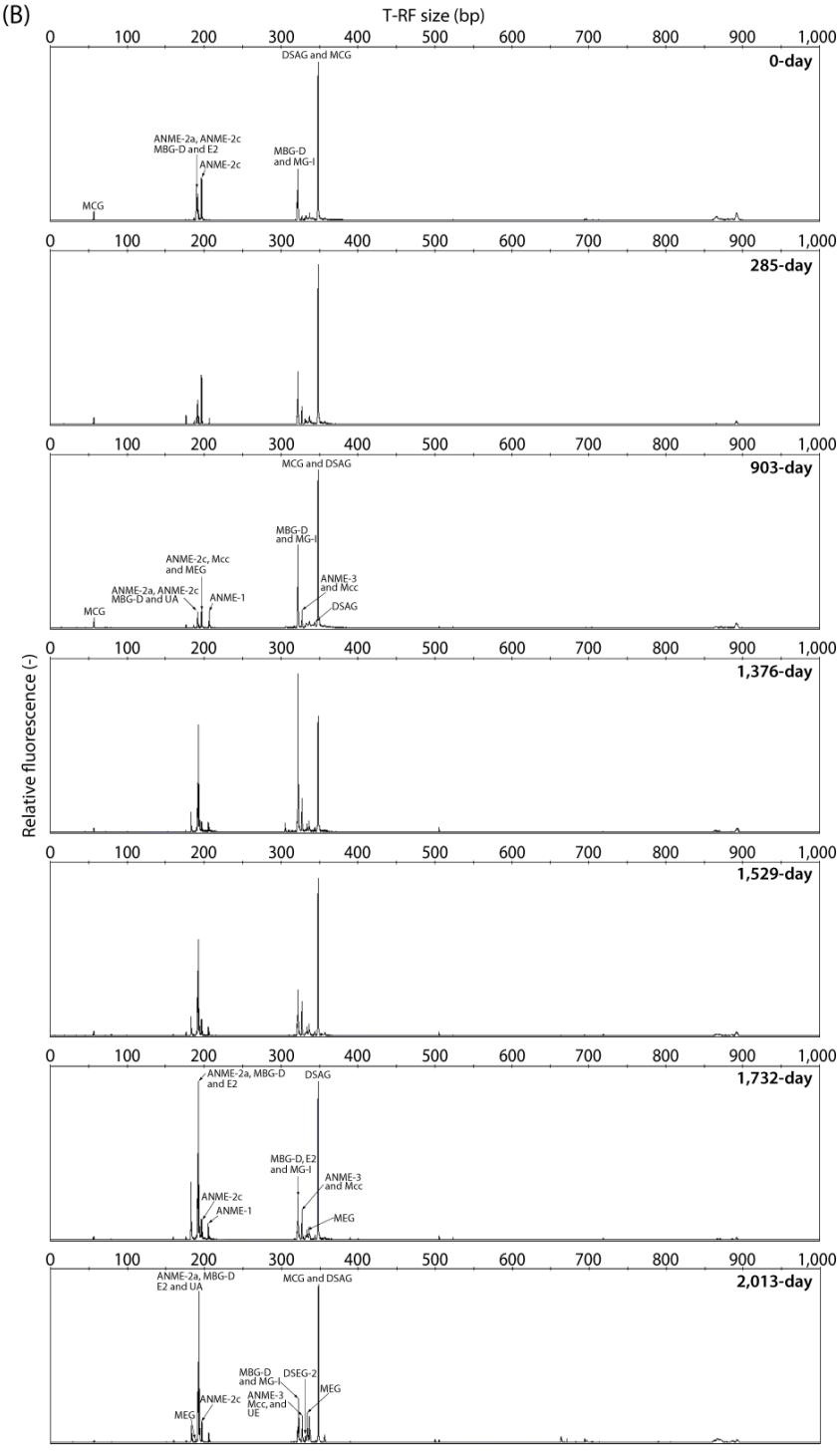

Figure S2-5—continued.

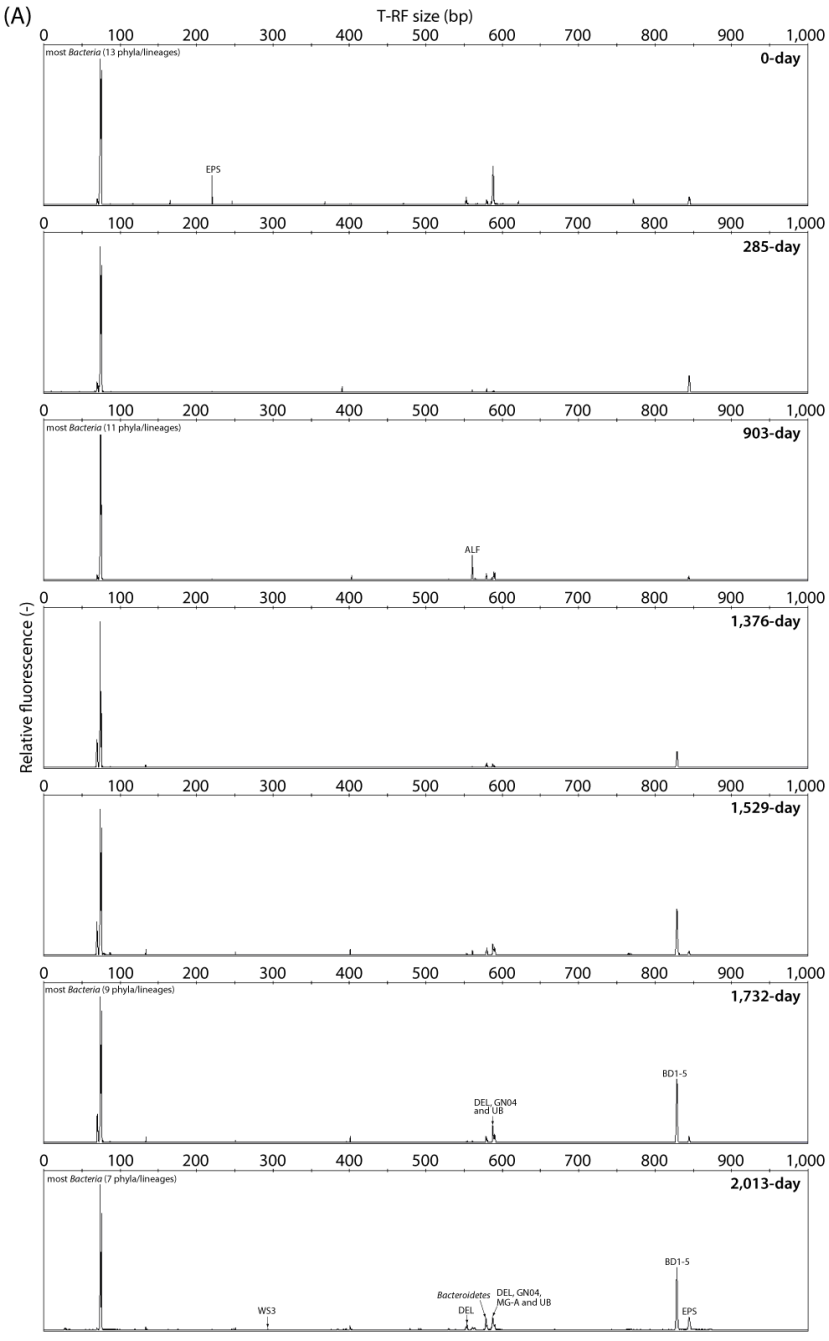

Figure S2-6. T-RFLP profiles of bacterial 16S rRNA genes digested with (A) HaeIII or (B) HhaI. The phylogenetic affiliations of each T-RF were identified using the bacterial 16S rRNA gene and 16S rRNA clone sequences obtained in this study. The abbreviations for some peaks are as follows: ALF, *Alphaproteobacteria*; BET, *Betaproteobacteria*; GAM, *Gammaproteobacteria*; DEL, *Deltaproteobacteria*; EPS, *Epsilonproteobacteria*; and UB, unclassified *Bacteria*.

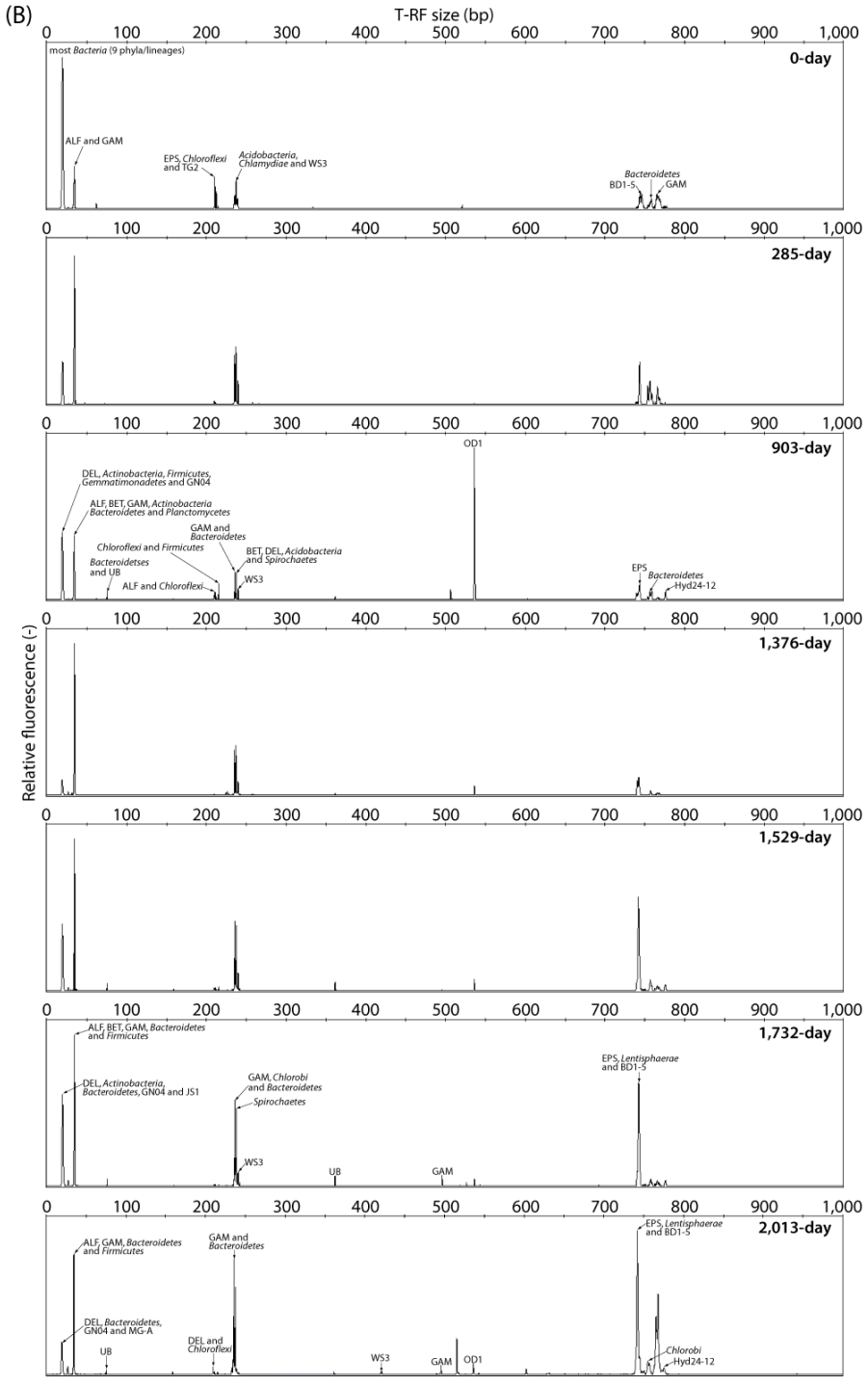

Figure S2-6—continued.

Table S2-1. Oligonucleotide primers used in this study.

primer	Target	Primer sequence (5' to 3')	Reference
Arch21F	Archaeal 16S rRNA gene	TTC CGG TTG ATC CYG CCG GA	DeLong (1992)
340F[a]	Archaeal 16S rRNA gene	CCY TAY GRG GYG CAS CAG G	Gantner *et al*. (2011)
Ar912r[a]	Archaeal 16S rRNA gene	CCC CCG CCA ATT CCT TTA A	Großkopf *et al*. (1998); Lueders and Friedrich (2000)
932R	Archaeal 16S rRNA gene	GCY CYC CCG CCA ATT CMT TTA	Murakami *et al*. (2012)
27F	Bacterial 16S rRNA gene	AGA GTT TGA TCM TGG CTC AG	Lane (1991)
EUB338F[b]	Bacterial 16S rRNA gene	ACT CCT ACG GGA GGC AGC	Amann *et al*. (1990)
		ACT CCT ACG GGA GGC TGC	Daims *et al*. (1999)
		ACA CCT ACG GGT GGC TGC	Daims *et al*. (1999)
		ACA CCT ACG GGT GGC AGC	Daims *et al*. (1999)
907R[a]	Bacterial 16S rRNA gene	CCG TCA ATT CMT TTR AGT T	Lane (1991)
1492R[a]	Archaeal and bacterial 16S rRNA gene	GGH TAC CTT GTT ACG ACT T	Lane (1991)
MLf	*mcrA* gene	GGT GGT GTM GGA TTC ACA CAR TAY GCW ACA GC	Luton *et al*. (2002)
MLr	*mcrA* gene	TTC ATT GCR TAG TTW GGR TAG TT	Luton *et al*. (2002)

[a]These primers are a slightly modified version of the original designed primers.

[b]This primer consisted of a mixture of four primers at an equal amount (mol).

References

Amann RI, Binder BJ, Olson RJ, Chisholm SW, Devereux R, *et al*. (1990) Combination of 16S rRNA-targeted oligonucleotide probes with

Daims H, Brühl A, Amann R, Schleifer K-H, Wagner M (1999) The domain-specific probe EUB338 is insufficient for the detection of all *Bacteria*: development and evaluation of a more comprehensive probe set. *Syst Appl Microbiol* 22:434–444.

DeLong EF (1992) Archaea in coastal marine environments. *Proc Natl Acad Sci U S A* 89:5685–5689.

Gantner S, Andersson AF, Alonso-Sáez L, Bertilsson S (2011) Novel primers for 16S rRNA-based archaeal community analyses in environmental samples. *J Microbiol Methods* 84:12–18.

Großkopf R, Janssen PH, Liesack W (1998) Diversity and structure of the methanogenic community in anoxic rice paddy soil microcosms as examined by cultivation and direct 16S rRNA gene sequence retrieval. *Appl Environ Microbiol* 64:960–969.

Lane DJ (1991) 16S/23S rRNA sequencing. *In* Stackebrandt E, Goodfellow M (eds.). Nucleic acid techniques in bacterial systematics, John Wiley & Sons, pp. 115–175.

Lueders T, Friedrich M (2000) Archaeal population dynamics during sequential reduction processes in rice field soil. *Appl Environ Microbiol* 66:2732–2742.

Luton PE, Wayne JM, Sharp RJ, Riley PW (2002) The *mcrA* gene as an alternative to 16S rRNA in the phylogenetic analysis of methanogen populations in landfill. *Microbiology* 148:3521–3530.

Murakami S, Fujishima K, Tomita M, Kanai A (2012) Metatranscriptomic analysis of microbes in an Oceanfront deep-subsurface hot spring reveals novel small RNAs and type-specific tRNA degradation. *Appl Environ Microbiol* 78:1015–1022.

Table S2-2. 16S rRNA-targeted oligonucleotide probes used in this study.

Probe	Target group	Probe sequence (5' to 3')	%FA[f]	Reference
ARC915	Most *Archaea*	GTG CTC CCC CGC CAA TTC CT	35 (60)	Stahl and Amann (1991)
ANME-1-350	ANME-1	AGT TTT CGC GCC TGA TGC	20[g]	Boetius *et al*. (2000)
ANME-2a-647[a]	ANME-2a	TCT TCC GGT CCC AAG CCT	10[g] (50)[g]	Knittel *et al*. (2005)
ANME-2c-760[b]	ANME-2c	CGC CCC CAG CTT TCG TCC	35[g] (65)[g]	Knittel *et al*. (2005)
ANME-3-1249[c]	ANME-3	TCG GAG TAG GGA CCC ATT	20[h]	Niemann *et al*. (2006)
ANME-3-1249H3	Helper probe for ANME-3-1249	GTC CCA ATC ATT GTA GCC GGC		Lösekann *et al*. (2007)
ANME-3-1249H5	Helper probe for ANME-3-1249	TTA TGA GAT TAC CAT CTC CTT		Lösekann *et al*. (2007)
MBGD-318[a]	MBG-D	GAT ATC GTG TCT CAG ATA	5[g] (15)[g]	Imachi *et al*. (2011)
MBGB-380[d]	DSAG	GTA ACC CCG TCA CAC TTT	10[g] (30)[g]	Knittel *et al*. (2005)
MCOCID442[e]	*Methanococcoides*	ACA CAT GCC GTT TAC ACA TG	20	Imachi *et al*. (2011)
EUB338	Most *Bacteria*	GCT GCC TCC CGT AGG AGT	20 (20)	Amann *et al*. (1990)
Mγ669	*Methylobacter* and *Methylomonas*	GCT ACA CCT GAA ATT CCA CTC	20	Eller *et al*. (2001)
UncGam731	Gammaproteobacterial phylotype MK903D_B5	AAT GTT AAC CCA GAC AGT CGC	20[g]	This study
NON338	Negative control for CARD-FISH	ACT CCT ACG GGA GGC AGC	(15–65)	Wallner *et al*. (1993)

[a]Permeabilization pretreatment with 0–2 μg ml^{-1} proteinase K (room temperature, 10 min) was used for CARD-FISH.

[b]Permeabilization pretreatment with 0.1–1.0 M HCl (room temperature, 1 min) was used for CARD-FISH.

[c]Used together with the unlabeled helper probes ANME-3-1249H3 and ANME-3-1249H5.

[d]Permeabilization pretreatment with 100–150 μg ml^{-1} proteinase K (room temperature, 10 min) was used for CARD-FISH.

[e]To avoid *Methanococcoides* cell losses, the sodium dodecyl sulfate concentration in hybridization and washing buffers was lowered from 0.01 to 0.0001% when using the probe MCOCID442.

[f]Numbers in parentheses are the formamide (FA) concentration of hybridization and washing buffers in CARD-FISH.

[g]These FA concentarions were determined by Clone-FISH (Schramm *et al*., 2002).

[h]Since a nearly full-length of ANME-3 16S rRNA gene sequence for Clone-FISH was not retrieved from the 903-day sample, the optimal FA concentration reported by Lösekann *et al*. (2007) was used.

References

Amann RI, Binder BJ, Olson RJ, Chisholm SW, Devereux R, *et al*. (1990) Combination of 16S rRNA-targeted oligonucleotide probes with flow cytometry for analyzing mixed microbial populations. *Appl Environ Microbiol* 56:1919–1925.

Boetius A, Ravenschlag K, Schubert CJ, Rickert D, Widde F, *et al*. (2000) A marine microbial consortium apparently mediating anaerobic oxidation of methane. *Nature* 407:623–626.

Eller G, Stubner S, Frenzel P (2001) Group-specific 16S rRNA targeted probes for the detection of type I and type II methanotrophs by fluorescence in situ hybridisation. *FEMS Microbiol Lett* 198:91–97.

Imachi H, Aoi K, Tasumi E, Saito Y, Yamanaka Y, *et al*. (2011) Cultivation of methanogenic community from subseafloor sediments using a continuous-flow bioreactor. *ISME J* 5:1913–1925.

Knittel K, Lösekann T, Boetius A, Kort R, Amann R (2005) Diversity and distribution of methanotrophic archaea at cold seeps. *Appl Environ Microbiol* 71:467–479.

Lösekann T, Knittel K, Nadalig T, Fuchs B, Niemann, *et al*. (2007) Diversity and abundance of aerobic and anaerobic methane oxidizers at the Haakon Mosby Mud Volcano, Barents Sea. *Appl Environ Microbiol* 73:3348–3362.

Niemann H, Lösekann T, de Beer D, Elvert M, Nadalig T, *et al*. (2006) Novel microbial communities of the Haakon Mosby mud volcano and their role as a methane sink. *Nature* 443:854–858.

Schramm A, Fuchs BM, Nielsen JL, Tonolla M, Stahl DA (2002) Fluorescence *in situ* hybridization of 16S rRNA gene clones (Clone-FISH) for probe validation and screening of clone libraries. *Environ Microbiol* 4:713–720.

Stahl DA, Amann R (1991) Development and application of nucleic acid probes. *In* Stackebrandt E, Goodfellow M (eds.), Nucleic acid techniques in bacterial systematics, John Wiley & Sons, pp. 205–248.

Wallner G, Amann R, Beisker W (1993) Optimizing fluorescent in situ hybridization with rRNA-targeted oligonucleotide probes for flow cytometric identification of microorganisms. *Cytometry* 14:136–143.

Chapter III:

Possible effect of redox potential on methane-seep sediment microbial community structure development

Chapter III

3.1 Introduction

As indicated by massively parallel tag sequencing of 16S rRNA genes, methane seeps show moderate levels of microbial richness compared with other marine sedimentary ecosystems (Ruff *et al*., 2015). Also, the methane-seep ecosystems possess the microbes involves in biogeochemically important microbial processes, such as anaerobic oxidation of methane (AOM) and sulfate reduction relevant to carbon and sulfur cycling. It is also known that the occurrence of local variation of methane-seep microbial community structure within same sediment core (Nunoura *et al*., 2012; Ruff *et al*., 2015). Oxygen, methane, and sulfate contents and temperature have been proposed as the key environmental parameter(s) affecting the anaerobic methanotroph (ANME) community structures (Girguis *et al*., 2005; Knittel *et al*. 2005; Rossel *et al*., 2011; Yanagawa *et al*., 2011). In contrast, knowledge regarding factor(s) controlling the methane-seep microbial community structure development remains limited.

Microbes with anaerobic metabolism are particularly sensitive to the changes in the redox potential of the surrounding environment (Hirano *et al*., 2013). It has been suggested that the growth of *Methanothermobacter thermautotrophicus* and *Desulfovibrio desulfuricans* is influenced by the redox potential of cultivation medium, which is controlled by the ratio of the oxidized/reduced form of anthraquinone-2, 6-disulfonate (AQDS; a model quinone compound) using a bio-electrochemical reactor (BER) (Hirano *et al*., 2008; Hirano *et al*., 2013). Quinone compounds are widely distributed in natural ecosystems and act as electron shuttles (Kappler *et al*., 2004), and thus, these compounds would significantly contribute the changes in the redox potential of the natural ecosystems. These previous findings suggested that quinone compound-mediated anaerobic redox potential differences might affect the growth of certain microbes, resulting in distinct microbial community structure development in natural ecosystems. In the present study, a methane-seep sediment-associated microbial community originally obtained from the methane-seep sediment of the Nankai Trough (Aoki *et al.*, 2014) was cultivated using a BER. The aim of this study was to reveal possible effect of the quinone compound-mediated anaerobic redox potential difference on AOM-associated community structure development in the methane-seep sediment of the Nankai Trough.

3.2 Materials and Methods

3.2.1 Inoculum culture and the culture medium

Methane-seep sediment from Omine Ridge, Nankai Trough off Kumano area, Japan (33°7.2253' N, 136°28.6672' E; 2,533 m water depth) was collected during the cruise YK06-03, 6 May 2006. Following the collection of sediment, the sediment was incubated on a continuous-flow bioreactor under an AOM condition (Aoki *et al*., 2014). The inoculum culture used in this study was sampled 7 years after the initiation of the bioreactor operation and the sample was stored anaerobically under nitrogen gas at 4°C in the dark until further experiments were performed. The composition of the synthetic seawater medium used in this study was as follows (L^{-1}): Daigo's artificial seawater SP for marine microalgae medium (Nihon Pharmaceutical, Tokyo, Japan), 36 g;

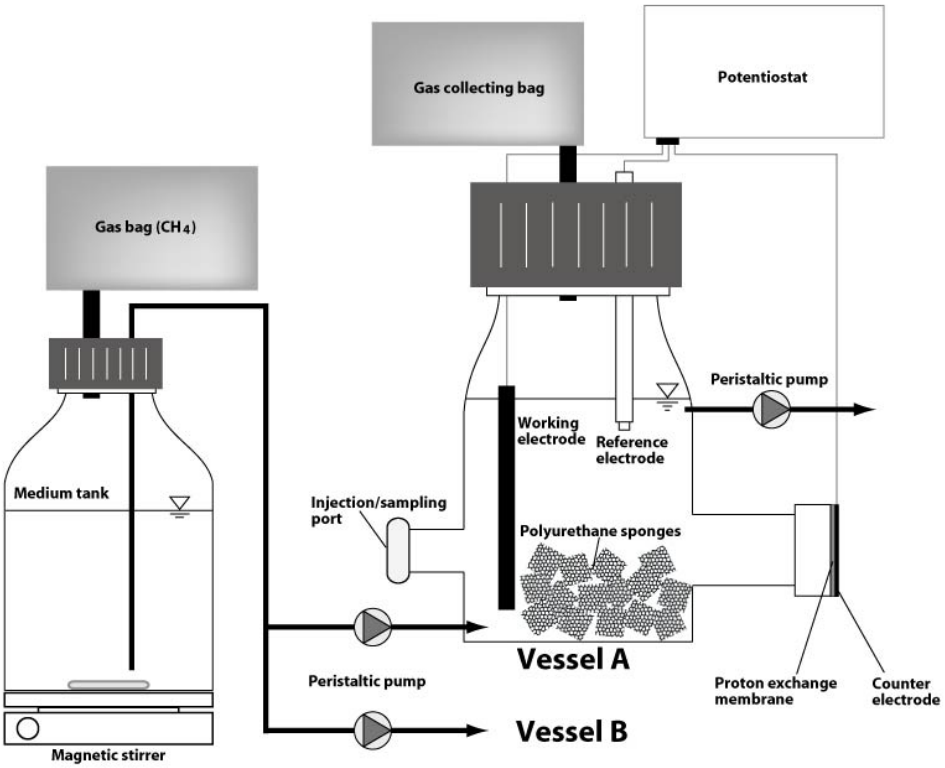

Figure 3-1. Schematic diagram of the continuous-flow type BER used in this study.

NH_4Cl, 0.54 g; KH_2PO_4, 0.14 g; $NaHCO_3$, 2.5 g; trace element solution, 1 mL (Imachi *et al*., 2008); vitamin solution (Imachi *et al*., 2009), 1 mL; neutralized 0.3 M Na_2S solution, 2 mL; and titanium (III)-nitrilotriacetic acid solution (Moench and Zeikus, 1983), 5 mL. The cultivation medium supplied to the BER also contained 0.12 g L^{-1} AQDS. The cultivation medium was purged with nitrogen gas to remove dissolved oxygen, and then the gas phase of a 5-L medium tank was replaced with pure methane gas. The pH of the cultivation medium was adjusted to 7.5 ± 0.1 by adding hydrochloric acid to the cultivation medium.

3.2.2 BER used in this study

The schematic diagram of the continuous-flow type BER used in this study is shown in **Fig. 3-1**. The BER was a modified version of previously reported single-chamber BER systems (Jeon *et al*., 2009; Hirano *et al*., 2013). The volume of medium in each cultivation vessel was 110 mL. A carbon felt (40 mm × 35 mm × 5 mm), a Teflon-coated carbon cloth (35 mm in diameter; EC-CC1-060T, ElectroChem, Inc., MA, USA), and a Ag/AgCl type electrode (saturated KCl, RE-1, EC FRONTIER, Inc., Kyoto, Japan) were used as the working, counter, and reference electrodes, respectively. The working, counter, and reference electrodes were connected to a potentiostat (PS-08, Toho Giken, Tokyo, Japan). All reported voltages are with respect to the Ag/AgCl reference electrode (+199 mV vs. a standard hydrogen electrode at 25°C). The cultivation vessel and counter electrode were separated by a proton exchange membrane (35 mm in diameter; Nafion N117, Sigma-Aldrich, St. Louis, MO, USA). A total

of 15 hydrophilic polyurethane sponges (10 mm × 10 mm × 10 mm, APG CC-10B, Nisshinbo Chemical Inc., Tokyo, Japan) were packed into each cultivation vessel as microbe-bound carriers. The cultivation medium in a 5-L medium tank was continuously mixed using a magnetic stirrer at 150 rpm. A peristaltic pump (Masterflex L/S tubing pump 7550-50, Cole-Parmer, Vernon Hills, IL, USA) and Viton tubing (Cole-Parmer) were used for the cultivation medium supply. The cultivation medium was supplied intermittently at 1/59 min (on/off), regulated by an automatic on/off timer (FT-011, Tokyo Glass Kikai Co. Ltd., Tokyo, Japan). The flow rate of cultivation medium was 5.5 ml min^{-1}, yielding hydraulic retention time of 20 h. The working electrode potential in the cultivation vessels A and B were regulated to −0.4 and −0.6 V, respectively. Following 5 hours of regulated working electrode potential, 2.5 g-wet weight of the inoculum culture was injected into each cultivation vessel from the sampling/injection port. The BER was installed in a 10°C incubator in the dark. The cultivation vessels were manually shaken once a week to improve mixing of substrates.

3.2.3 Total DNA extraction, PCR, cloning, and phylogenetic analysis

For microbial community analyses, enrichment cultures were sampled from the sampling port of each cultivation vessel at 112, 182, and 266 days of operation. Before sampling, the cultivation medium in the cultivation vessels was flushed with nitrogen gas. Extraction of total DNA from 1 mL each of enrichment cultures was performed using an ISOIL for Beads Beating kit (Nippon Gene, Tokyo, Japan) according to the manufacturer's instructions. The concentration of template DNA was measured using a Quant-iT PicoGreen dsDNA assay kit (Invitrogen, Carlsbad, CA, USA). PCR amplification of archaeal and bacterial 16S rRNA genes was performed using the TaKaRa Ex Taq (TaKaRa Bio Inc., Shiga, Japan). The PCR reaction mixtures were prepared according to the manufacturer's instruction. The PCR primer pairs of Arch340F/932R and EUB338F/907R were used for archaeal and bacterial 16S rRNA gene amplification, respectively (Aoki *et al*., 2014). PCR was performed under the following conditions: initial denaturation at 95°C for 2 min, followed by 25 (for bacterial 16S rRNA gene) or 35 (for archaeal 16S rRNA gene) cycles of denaturation at 95°C for 40 s, annealing at 50°C for 30 s, and extension at 72°C for 45 s. The PCR products were checked by 1−2% agarose gel electrophoresis, and then, PCR products were purified using a MinElute PCR purification kit (Qiagen, Venlo, Netherlands). Following purification, the PCR products were cloned with a pCR 2.1 TOPO TA cloning kit (Invitrogen). The cloned 16S rRNA gene sequences were determined using a BigDye Terminator v3.1 cycle sequencing kit (Applied Biosystems, CA, USA) and 3730xl Genetic Analyzer (Applied Biosystems). The obtained 16S rRNA gene sequences were aligned using ARB (version 6.0; Ludwig *et al*., 2004). The calculated distance matrix using ARB was inputted into mothur (version 1.33; Schloss *et al*., 2009) and the obtained sequences were grouped into phylotypes at 97% sequence identity based on the distance matrix. Putative chimeric sequences were detected and removed using the "chimera.uchime" command in mothur. The taxonomic classification was done by the "wang" kmer-based method via the "classify.seqs" command applied to the SILVA 119 reference database (http://www.mothur.org/wiki/Silva_reference_files), with a confidence cut-off value of 0.5. Epsilonproteobacterial

16S rRNA gene sequence-based phylogenetic tree construction was performed using the neighbor-joining method in ARB with the Jukes-Cantor correction, as described previously (Aoki *et al*., 2014).

3.2.4 Quantitative real-time PCR

Quantitative real-time PCR (qPCR) of archaeal and bacterial 16S rRNA genes was performed as shown by Aoki *et al*. (2014). The archaeal and bacterial PCR primers used in the qPCR were the same as those used in the clone library construction described above. Each sample was analyzed in triplicate.

3.2.5 Potential AOM activity measurement

A tracer experiment using ^{14}C-labelled methane was performed to estimate potential AOM activity. To measure the potential AOM activity, 1 mL aliquots of each of enrichment culture were dispensed into 30-mL serum vials containing 9 mL of anaerobic seawater medium. The headspace of the vials was replaced by pure methane gas, and then 1 mL of ^{14}C-labeled methane was injected into the vials. After 1 month of incubation, ^{14}C-labeling was terminated by injecting 1 mL of 1 M sodium hydroxide into the vials. Subsequently, the samples were shaken vigorously for 1 min and incubated for 30 min at room temperature to absorb CO_2 gas completely into the liquid phase. After flushing the headspace of the vials using pure helium gas, CO_2 was degassed from the liquid phase again by injecting 2 mL of 1 M nitric acid. The radioactivity of $^{14}CO_2$ gas in the headspace of the vials was measured by a radio-gas-chromatograph system composed of Raga Star radioactivity flow detector (Raytest, Straubenhardt, Germany) and a GC-2014 gas chromatograph (Shimadzu, Kyoto, Japan) equipped with a Shincarbon ST ZT-15 stainless steel column (Shinwa Chemical Ltd., Kyoto, Japan) under the following conditions: carrier gas, helium at 15 mL min^{-1}; column oven temperature, 75ºC; injection temperature, 100ºC; and counting gas, methane at 43 mL min^{-1}. Potential AOM rates were calculated by the equation $(^{14}CO_2 \times CH_4)/(^{14}CH_4 \times v \times t)$, where $^{14}CO_2$ is the activity of the produced radioactive carbon dioxide, CH_4 is the total amount of methane in the sample, $^{14}CH_4$ is the activity of the radioactive methane, v is the volume of sample, and t is the incubation time (Treude *et al*., 2003). Each sample was analyzed in triplicate.

3.3 Results and Discussion

In the present study, a methane-seep sediment-associated microbial community was cultivated using a BER to reveal possible effect of the quinone compound-mediated anaerobic redox potential difference on AOM-associated community structure development in the methane-seep sediment of the Nankai Trough. A small amount of AQDS (0.3 mM), an electrochemically active quinone compound, was added to the cultivation medium for the regulation of the redox potential of cultivation medium using a BER (Hirano *et al*., 2013).

Over the 0-day-182-day period, the working electrode potential was poised at −0.4 and −0.6 V in cultivation vessels A and B, respectively. The negative potential applied in the present study (−0.4 or −0.6 V) was comparatively high compared to −0.8 V for significant H_2 evolution by proton reduction (Su *et al*., 2012; Lohner *et al*., 2014). Current densities (mean value ± standard deviation) in the cultivation vessels A and B were −82 ± 80

Table 3-1. Quantitative data of 16S rRNA gene copy numbers.

Sample		copies ml-culture^{-1}	
		Archaea	Bacteria
Inoculum (0-day sample)		1.1×10^8 (7.4×10^6)	1.3×10^{10} (5.8×10^{10})
Vessel A	112-day	5.3×10^5 (4.8×10^4)	1.1×10^8 (1.0×10^7)
	182-day	3.4×10^6 (5.8×10^5)	1.3×10^9 (2.2×10^8)
	266-day	4.5×10^6 (1.2×10^6)	4.6×10^9 (7.7×10^8)
Vessel B	112-day	6.4×10^6 (6.5×10^5)	1.3×10^9 (4.9×10^7)
	182-day	2.4×10^6 (4.1×10^5)	1.3×10^9 (2.4×10^8)
	266-day	1.0×10^6 (2.8×10^5)	1.7×10^9 (2.8×10^8)

[a]The figures in ( ) parentheses are standard errors.

Table 3-2. Potential AOM activity as determined using $^{14}CH_4$.

Sample		Potential AOM activity [nmol ml-culture^{-1} day^{-1}]
Inoculum (0-day sample)		4.2 (0.2)[a]
Vessel A	182-day	1.3 (0.1)
	266-day	3.6 (0.1)
Vessel B	182-day	1.9 (0.8)
	266-day	2.7 (0.7)

[a]The figures in parentheses are standard deviation.

and −183 ± 94 μA electrode^{-1}, respectively. Following 182 days of operation, the regulation of working electrode potential was stopped, and then the BER was subsequently operated for 3 months (*i.e.*, days 183-266) without the poised working electrode potential. During the period, the redox potential (mean value ± standard deviation) of the cultivation medium in the cultivation vessels A and B were −376 ± 13 and −363 ± 22 mV, respectively.

To examine the changes in the abundance of archaeal and bacterial populations in the BER, archaeal and bacterial 16S rRNA gene copy numbers were quantified (**Table 3-1**). Before cultivation, the archaeal and bacterial 16S rRNA gene copy numbers were 1.1×10^8 and 1.3×10^{10} copies ml-culture^{-1}, respectively. Following 182 days of incubation in the presence of the working electrode potential (*i.e.*, −0.4 V or −0.6 V), the archaeal and bacterial 16S rRNA gene copy numbers in the both of cultivation vessels were decreased to 10^6 and 10^9 copies mL-culture^{-1}, respectively. Following the subsequent 3-month BER operation without the regulation of working electrode potential, the archaeal and bacterial 16S rRNA gene copy numbers were also on the order of 10^6 and 10^9 copies mL-culture^{-1}, respectively, To reveal the behaviors of AOM-associated microbes in the BER, the potential AOM rates were measured using ^{14}C-labeled methane. The potential AOM rates observed in cultivation vessels A and B were of the same order of magnitude as during the BER operation (**Table 3-2**). As previous studies demonstrated, the growth of some anaerobes can be stimulated in the lower redox cultivation conditions that can be achieved by BER cultivation methods (Hirano *et al*., 2008; Hirano *et al*., 2013). In contrast, considering that the potential AOM

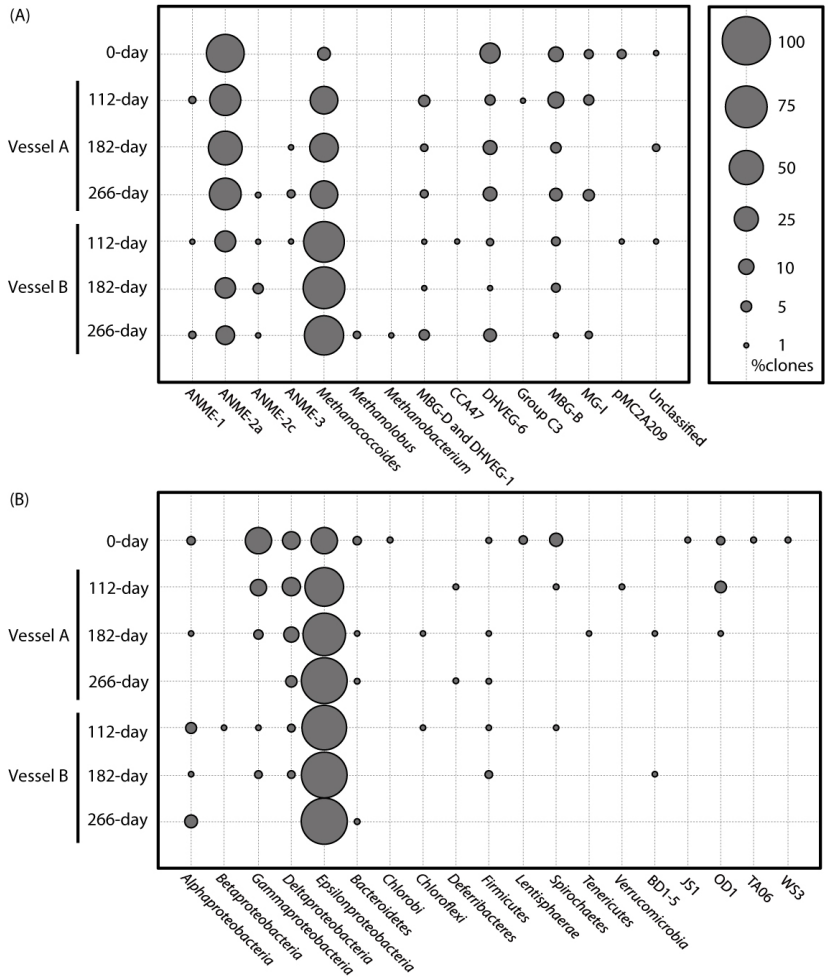

Figure 3-2. Community structures based on (a) archaeal and (b) bacterial 16S rRNA gene clone libraries. The size of each dot indicates the percentage of identified 16S rRNA gene sequences falling within a particular taxonomic group. The numbers of obtained clones in each library are shown in parentheses.

activity observed in the BER and the 1-4 months of doubling time of ANMEs (Girguis *et al*., 2005; Nauhaus *et al*., 2007; Meulepas *et al*., 2009; Zhang *et al*., 2011), it seems that the BER cultivation method does not have the potential to stimulate the growth of AOM-associated microbes in the cultivation condition presented here.

Archaeal and bacterial 16S rRNA gene-based clone analysis was performed to reveal microbial community structure developed in the BER (**Fig. 3-2**, and **Table S3-1** and **S3-2**). Following 182 days of BER operation, the most predominant archaeal phylotype observed in cultivation vessel A (−0.4 V of working electrode potential) was the ANME-2a phylotype EA02 (42/88 clones; **Table S3-1**), whereas the genus *Methanococcoides* phylotype EA01 (67/92 clones; **Table S3-1**) was the most predominant archaeal phylotype in cultivation vessel B (−0.6 V of working electrode potential). The *Methanococcoides* phylotype EA01 has 100% identity to a *Methanococcoides* isolate of the *Methanococcoides alaskense* strain AK-5 (GenBank accession number NR_029122). It is known that some hydrogenotrophic methanogens are known to perform electromethanogenesis (Cheng *et al*., 2009;

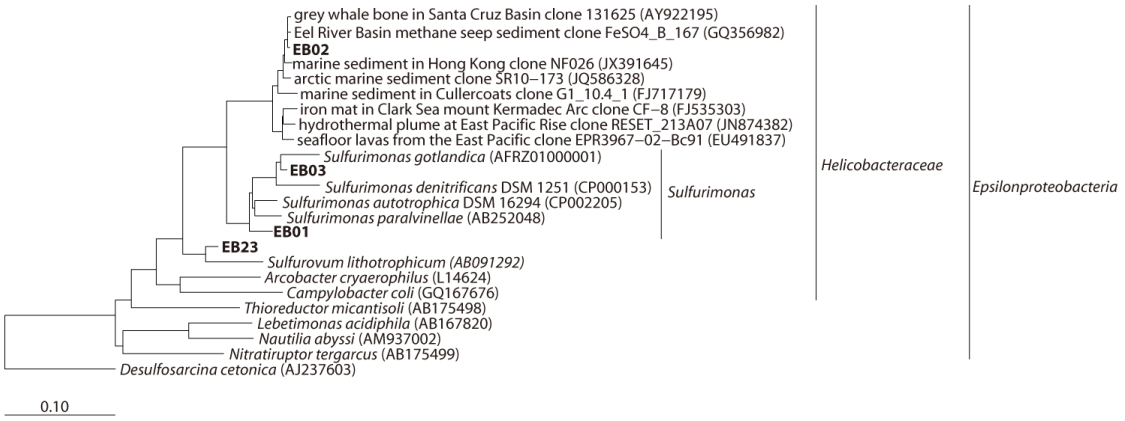

Figure 3-3. Phylogenetic tree showing the phylogenetic position of *Helicobactereace*-associated phylotypes. The 16S rRNA gene-based tree was constructed using the neighbor-joining method implemented in the ARB program. The phylotypes detected in this study are shown in bold letters. The scale bar indicates the number of nucleotide changes per sequence position.

Lohner *et al*., 2014). In contrast, all of the previously cultivated *Methanococcoides* members cannot utilize hydrogen for methanogenesis (L'Haridon *et al*., 2014). Thus, the enrichment of the *Methanococcoides* phylotype might be not due to the capability of electromethanogenesis. Considering that the long-term survival of *Methanococcoides* phylotype in the previously reported DHS bioreactor (Aoki *et al*., 2014) and the BER without the direct metabolic substrates for methanogenesis, the *Methanococcoides* phylotype might be associated with the AOM reaction and the lower redox potential preferentially selected the *Methanococcoides* phylotype in the BER.

As to bacterial phylotypes, the genus *Sulfurimonas* phylotype EB01 (42/81 clones; **Fig. 3-3** and **Table S3-2**) and the uncultivated *Helicobacteraceae* lineage-associated phylotype EB02 (62/82 clones; **Fig. 3-3** and **Table S3-2**) were dominated at 182-day in cultivation vessel A (−0.4 V of working electrode potential) and vessel B (−0.6 V of working electrode potential), respectively. None of the previously identified putative deltaproteobacterial sulfate-reducing bacterial partners of ANMEs (*e.g.*, SEEP-SRB1; Schreiber *et al*., 2010) were detected in the BER incubation samples. The bacterial phylotype EB01 has 97.7% sequence identity to *Sulfurimonas autotrophica* strain DSM16294 (GenBank accession number NR_074451), whereas the uncultivated *Helicobacteraceae* lineage-associated phylotype EB02 has 91.3% sequence identity to the strain DSM16294. Although the genus *Sulfurimonas* is known to use oxygen as an electron acceptor (Han and Perner, 2015) and trace amounts of molecular oxygen could have contaminated the BER, the lower redox potential values observed in cultivation vessels A and B in the absence of a working electrode potential (*i.e.*, −376 ± 13 in cultivation vessel A and −363 ± 22 mV in cultivation vessel B) implied that oxygen could not be the dominant electron acceptor in the BER. Although little is known about the anaerobic metabolism of the family *Helicobacteraceae* microbes and their involvement to AOM, *Sulfurimonas gotlandica* is known to grow anaerobically on thiosulfate or elemental sulfur as the sole energy substrate (Grote *et al*., 2012). Sulfide, which was added as a reducing agent, could be oxidized to sulfur compounds for sulfur compound disproportionation via the

abiotic reaction with oxidants (*e.g.*, oxygen and oxidized form AQDS). In addition, zero-valent sulfur could be produced by AOM reaction (Milucka *et al*., 2012). Thus, energy-conserving anaerobic sulfur metabolism may have sustained the growth of the dominant *Helicobacteraceae* phylotypes and the differences in the poised redox potential also affected the predominantly cultivated bacterial phylotypes within the family *Helicobacteraceae*.

Notice that the predominant archaeal and bacterial phylotypes were also detected predominantly even after the subsequent 3 months of operation without cathodic reactions (**Table S3-1** and **S3-2**). This result suggests that the presence of a working electrode potential was not necessary to sustain the growth of the predominant archaeal and bacterial phylotypes observed in the BER. Of course, the effect of non-AQDS mediated reactions, *e.g.*, trace hydrogen evolution and direct electron transfer between electrode and microbes to the microbial community structure development should be further investigated.

3.4 Summary of this chapter

The available data from this study implies that the quinone compound-mediated anaerobic redox potential difference is a factor that controls microbial community structure development in the methane-seep sediment of the Nankai Trough. In addition, the enrichment of uncultured *Helicobacteraceae* phylotype EB02 suggests that the continuous-flow BER cultivation method has potential to enrich taxonomically novel microbes. Considering that the detection of the phylotype EB02-related sequences form diverse marine sedimentary environments (**Fig. 3-3**), the phylotype EB02-related lineage might have an important function in marine sedimentary biogeochemical cycling. Further analysis is needed to clarify the detailed mechanism(s) behind the enrichment effect. The enrichment result reported here would provide valuable information about a mechanism of microbial community development in methane-seep sedimentary ecosystems and the cultivation/isolation of uncultivated microbes.

3.5 References

Aoki M, Ehara M, Saito Y, Yoshioka H, Miyazaki M, *et al*. (2014) A long-term cultivation of an anaerobic methane-oxidizing microbial community from deep-sea methane-seep sediment using a continuous-flow bioreactor. *PLoS ONE* 9:e105356.

Cheng S, Xing D, Call DF, Logan BE (2009) Direct biological conversion of electrical current into methane by electromethanogenesis. *Environ Sci Technol* 43 3953–3958.

Girguis PR, Cozen AE, DeLong EF (2005) Growth and population dynamics of anaerobic methane-oxidizing archaea and sulfate-reducing bacteria in a continuous-flow bioreactor. *Appl Environ Microbiol* 71:3725–3733.

Grote J, Schott T, Bruckner CG, Glöckner FO, Jost G, *et al*. (2012) Genome and physiology of a model epsilonproteobacterium responsible for sulfide detoxification in marine oxygen depletion zones. *Proc Natl Acad Sci U S A* 109:506–510.

Han Y, Perner M (2015) The globally widespread genus *Sulfurimonas*: versatile energy metabolisms and adaptations to redox clines. *Front Microbiol* 6:989.

Hirano S, Matsumoto N, Ohmura N (2008) Electrochemical control of bacteria (Part XI) - regulation of sulfate reducing bacteria by redox control - (in Japanese). Environmental Science Research Laboratory report:V07018, Central Research Institute of Electric Power Industry.

Hirano S, Matsumoto N, Morita M, Sasaki K, Ohmura N (2013) Electrochemical control of redox potential affects methanogenesis of the hydrogenotrophic methanogen *Methanothermobacter thermautotrophicus*. *Lett Appl Microbiol* 56:315–321.

Imachi H, Sakai S, Hirayama H, Nakagawa S, Nunoura T, *et al*. (2008) *Exilispira thermophila* gen. nov., sp. nov., an anaerobic, thermophilic spirochaete isolated from a deep-sea hydrothermal vent chimney. *Int J Syst Evol*

Microbiol 58: 2258–2265.
Imachi H, Sakai S, Nagai H, Yamaguchi T, Takai K (2009) *Methanofollis ethanolicus* sp. nov., an ethanol-utilizing methanogen isolated from a lotus field. *Int J Syst Evol Microbiol* 59: 800–805.
Imachi H, Aoi K, Tasumi E, Saito Y, Yamanaka Y, *et al*. (2011) Cultivation of methanogenic community from subseafloor sediments using a continuous-flow bioreactor. *ISME J* 5 1913–1925.
Jeon BY, Kim SY, Park YK, Park DH (2009) Enrichment of hydrogenotrophic methanogens in coupling with methane production using electrochemical bioreactor. *J Microbiol Biotechnol* 19:1665–1671.
Kappler A, Benz M, Schink B, Brune A (2004) Electron shuttling via humic acids in microbial iron(III) reduction in a freshwater sediment. *FEMS Microbiol Ecol* 47:85–92.
Knittel K, Lösekann T, Boetius A, Kort R, Amann R (2005) Diversity and distribution of methanotrophic archaea at cold seeps. *Appl Environ Microbiol* 71:467–479.
Lohner ST, Deutzmann JS, Logan BE, Leigh J, Spormann AM (2014) Hydrogenase-independent uptake and metabolism of electrons by the archaeon *Methanococcus maripaludis*. *ISME J* 8:1673–1681.
Ludwig W, Strunk O, Westram R, Richter L, Meier H, *et al*. (2004) ARB: a software environment for sequence data. *Nucleic Acids Res* 32:1363–1371.
L'Haridon S, Chalopin M, Colombo D, Toffin L (2014) *Methanococcoides vulcani* sp. nov., a marine methylotrophic methanogen that uses betaine, choline and N,N-dimethylethanolamine for methanogenesis, isolated from a mud volcano, and emended description of the genus *Methanococcoides*. *Int J Syst Evol Microbiol* 64:1978–1983.
Meulepas RJW, Jagersma CG, Gieteling J, Buisman CJ, Stams AJ, *et al*. (2009) Enrichment of anaerobic methanotrophs in sulfate-reducing membrane bioreactors. *Biotechnol Bioeng* 104: 458–470.
Milucka J, Ferdelman TG, Polerecky L, Franzke D, Wegener G, *et al*. (2012) Zero-valent sulphur is a key intermediate in marine methane oxidation. *Nature* 491:541–546.
Moench TT, Zeikus JG (1983) An improved preparation method for a titanium (III) media reductant. *J Microbiol Methods* 1: 199–202.
Nauhaus K, Albrecht M, Elvert M, Boetius A, Widdel F (2007) *In vitro* cell growth of marine archaeal-bacterial consortia during anaerobic oxidation of methane with sulfate. *Environ Microbiol* 9:187–196.
Nunoura T, Takaki Y, Kazama H, Hirai M, Ashi J, *et al*. (2012) Microbial diversity in deep-sea methane seep sediments presented by SSU rRNA gene tag sequencing. *Microbes Environ* 27:382–390.
Rossel PE, Elvert M, Ramette A, Boetius A, Hinrichs K-U (2011) Factors controlling the distribution of anaerobic methanotrophic communities in marine environments: Evidence from intact polar membrane lipids. *Geochim Cosmochim Acta* 75:164–184.
Ruff SE, Biddle JF, Teske AP, Knittel K, Boetius A, Ramette A (2015) Global dispersion and local diversification of the methane seep microbiome. *Proc Natl Acad Sci USA* 112:4015–4020.
Schloss PD, Westcott SL, Ryabin T, Hall JR, Hartmann M, *et al*. (2009) Introducing mothur: open-source, platform-independent, community-supported software for describing and comparing microbial communities. *Appl Environ Microbiol* 75:7537-7541.
Schreiber L, Holler T, Knittel K, Meyerdierks A, Amann R (2010) Identification of the dominant sulfate-reducing bacterial partner of anaerobic methanotrophs of the ANME-2 clade. *Environ Microbiol* 12:2327–2340.
Su W, Zhang L, Tao Y, Zhan G, Li D, Li D (2012) Sulfate reduction with electrons directly derived from electrodes in bioelectrochemical systems. *Electrochem Commun* 22:37–40.
Treude T, Boetius A, Knittel K, Wallmann K, Joergensen BB (2003) Anaerobic oxidation of methane above gas hydrates at Hydrate Ridge, NE Pacific Ocean. *Mar Ecol Prog Ser* 264:1–14.
Yanagawa K, Sunamura M, Lever MA, Morono Y, Hiruta A, *et al*. (2011) Niche separation of methanotrophic archaea (ANME-1 and -2) in methane-seep sediments of the eastern Japan Sea offshore Joetsu. *Geomicrobiol J* 28:118–129.
Zhang Y, Maignien L, Zhao X, Wang F, Boon N (2011) Enrichment of a microbial community performing anaerobic oxidation of methane in a continuous high-pressure bioreactor. *BMC Microbiol* 11:137.

3.6 Supplementary Information

Table S3-1. List of archaeal 16S rRNA gene phylotypes detected in this study.

Phylotype	Number of clones							Phylogenetic affiliation
	Inoculum	Vessel A			Vessel B			
	(0-day)	112-day	182-day	266-day	112-day	182-day	266-day	
EA01	6	30	30	24	65	67	58	*Methanococcoides*
EA02	53	38	42	32	17	16	13	ANME-2a
EA03	2	9	4	4	1	2	1	MBG-B
EA04	12	2	3	2	1	1	5	DHVEG-6
EA05	2	4	0	0	0	0	2	MG-I
EA06	0	5	0	2	0	1	2	MBG-D and DHVEG-1
EA07	2	1	3	1	1	0	0	DHVEG-6
EA08	0	0	0	1	1	4	1	ANME-2c
EA09	0	0	2	0	0	0	0	MBG-D and DHVEG-1
EA10	0	0	0	4	0	0	0	MG-I
EA11	3	0	0	0	0	1	0	MBG-B
EA12	0	0	1	2	1	0	0	ANME-3
EA13	3	0	0	0	1	0	0	pMC2A209
EA14	2	0	0	1	0	0	0	MBG-B
EA15	0	0	0	0	1	0	2	ANME-1
EA16	1	0	2	0	1	0	0	Unclassified *Archaea*
EA17	1	0	0	0	2	0	0	MBG-B
EA18	0	0	0	0	0	0	2	*Methanolobus*
EA19	0	0	0	0	1	0	2	MBG-D and DHVEG-1
EA20	0	0	0	3	0	0	0	DHVEG-6
EA21	0	2	0	0	0	0	0	ANME-1
EA22	0	1	0	0	0	0	0	Group C3
EA23	0	1	0	0	0	0	1	DHVEG-6
EA24	1	0	0	0	0	0	0	DHVEG-6
EA25	0	0	0	0	0	0	1	*Methanobacterium*
EA26	0	0	0	0	1	0	0	*Thermoplasmatales*-CCA47
EA27	0	0	1	0	0	0	0	DHVEG-6
EA28	1	0	0	0	0	0	0	MG-I
EA29	0	1	0	0	0	0	0	MBG-B

Table S3-2. List of bacterial 16S rRNA gene phylotypes detected in this study.

Phylotype	Number of clones							Phylogenetic affiliation
	Inoculum	Vessel A			Vessel B			
	(0-day)	112-day	182-day	266-day	112-day	182-day	266-day	
EB01	1	25	42	57	23	10	3	*Epsilonproteobacteria*
EB02	0	20	21	9	42	62	60	*Epsilonproteobacteria*
EB03	19	0	0	0	1	0	2	*Epsilonproteobacteria*
EB04	12	4	2	0	1	1	0	*Gammaproteobacteria*
EB05	0	9	4	3	1	1	0	*Deltaproteobacteria*
EB06	2	0	0	0	3	1	5	*Alphaproteobacteria*
EB07	4	0	1	0	0	0	0	*Gammaproteobacteria*
EB08	0	1	1	1	1	1	0	*Deltaproteobacteria*
EB09	1	2	1	0	0	0	0	OD1
EB10	3	0	0	0	0	0	0	*Deltaproteobacteria*
EB11	1	2	0	0	0	0	0	*Gammaproteobacteria*
EB12	3	0	0	0	0	0	0	*Deltaproteobacteria*
EB13	3	0	0	0	0	0	0	*Gammaproteobacteria*
EB14	0	0	1	1	0	0	0	*Bacteroidetes*
EB15	1	1	0	0	0	0	0	*Spirochaetes*
EB16	0	0	2	0	0	0	0	*Deltaproteobacteria*
EB17	0	0	0	0	0	2	0	*Firmicutes*
EB18	0	2	0	0	0	0	0	OD1
EB19	1	0	0	0	0	0	0	*Firmicutes*
EB20	1	0	0	0	0	0	0	WS3
EB21	1	0	0	0	0	0	0	TA06
EB22	0	0	1	0	1	0	0	*Chloroflexi*
EB23	0	0	0	0	1	0	0	*Epsilonproteobacteria*
EB24	0	0	1	0	1	0	0	*Alphaproteobacteria*
EB25	1	0	0	0	0	0	0	*Bacteroidetes*
EB26	1	0	0	0	0	0	0	JS1
EB27	2	0	0	0	0	0	0	*Spirochaetes*
EB28	0	0	1	0	0	0	0	*Tenericutes*
EB29	0	0	1	1	0	0	0	*Firmicutes*
EB30	0	0	1	0	0	0	0	*Deltaproteobacteria*
EB31	0	0	0	0	0	1	0	BD1-5
EB32	1	0	0	0	0	0	0	*Spirochaetes*
EB33	1	0	0	0	0	0	0	*Deltaproteobacteria*
EB34	1	0	0	0	0	0	0	*Chlorobi*
EB35	1	0	0	0	0	0	0	*Deltaproteobacteria*
EB36	1	0	0	0	0	0	0	*Lentisphaerae*
EB37	0	0	0	1	0	0	0	*Deferribacteres*
EB38	1	0	0	0	0	0	0	OD1
EB39	0	1	0	0	0	0	0	*Gammaproteobacteria*
EB40	0	0	0	0	0	1	0	*Gammaproteobacteria*
EB41	0	1	0	0	0	0	0	*Gammaproteobacteria*
EB42	0	0	0	0	1	0	0	*Betaproteobacteria*
EB43	0	0	1	0	0	0	0	BD1-5
EB44	1	0	0	0	0	0	0	*Spirochaetes*
EB45	0	0	0	0	0	0	1	*Bacteroidetes*
EB46	1	0	0	0	0	0	0	*Deltaproteobacteria*
EB47	1	0	0	0	0	0	0	*Bacteroidetes*
EB48	0	1	0	0	0	0	0	*Deferribacteres*
EB49	0	0	0	0	1	0	0	*Spirochaetes*
EB50	0	0	0	0	1	0	0	*Firmicutes*
EB51	0	1	0	0	0	0	0	*Verrucomicrobia*
EB52	1	0	0	0	0	0	0	*Lentisphaerae*

Chapter IV:

Phylogenetic diversity of *aprA* genes in subseafloor sediments on the northwestern Pacific margin off Japan

Originally published in Microbes and Environments 30:276–280.

4.1 Introduction

Subseafloor microbial ecosystems play significant biogeochemical roles in the transformation of sulfur compounds; approximately 11.3 Tmols of sulfate are microbially reduced each year, accounting for the oxidation of 12%–29% of the organic carbon flux to the seafloor (Bowles *et al*., 2014). Some sulfate-reducing bacteria play an important role in the mitigation of methane emissions from marine sediments because they may significantly interact with archaeal anaerobic methanotrophs (ANMEs) that mediate the anaerobic oxidation of methane (AOM) (Knittel and Boetius, 2009). Dissimilatory sulfate reduction by marine sediments largely depends on the availability of sulfate supplied from seawater or underlying basaltic aquifers (D'Hondt *et al*., 2004). Recent biogeochemical studies detected the presence of cryptic sulfur-metabolizing activity in sulfate-depleted subseafloor sediments in which methanogenesis was the favored metabolic pathway (Knab *et al*., 2009; Holmkvist *et al*., 2011; Treude *et al*., 2014). On the other hand, dissimilatory sulfur oxidation occurs where reduced inorganic sulfur compounds derived from abiotic processes or dissimilatory sulfate reduction is available. In methane-seep sediment, sulfur oxidizers have been identified as primary producers due to the high sulfide fluxes derived from AOM (Jørgensen and Boetius, 2007).

In spite of the biogeochemical significance of sulfate reduction and sulfur oxidation in subseafloor sediments, information regarding the phylogenetic diversity and distribution of functional genes relevant to the subseafloor sulfur cycle remains limited. One useful functional marker gene used to detected the microbial sulfur cycle is the adenosine-5'-phosphosulfate (APS) reductase alpha subunit (*aprA*) gene, which encodes a key enzyme for dissimilatory sulfate reduction and sulfur oxidation (Meyer and Kuever, 2007a). In the present study, the diversity of the *aprA* gene in sediment samples obtained from the northwestern Pacific margin off Japan was investigated to identify putative sulfur-metabolizing microbial components and obtain new insights into the microbial sulfur cycle in the sedimentary environment.

4.2 Materials and Methods

4.2.1 Sediment and enrichment samples

Sediment samples obtained from three distinct locations on the northwestern Pacific margin off Japan were used in this study (**Table 4-1**) (Aoike, 2007; Tsuchiya and Takahashi, 2009; Aoki *et al*., 2014; Toki *et al*., 2014). The depth profiles of sulfate and methane concentrations suggested the occurrence of AOM in the sampling sites (**Fig. 4-1**). Furthermore, a continuous-flow bioreactor enrichment culture capable of AOM, which had been established using the methane-seep sediment of Site 6K949 (hereafter called 6K949 enrichment), was also examined in order to identify active, culturable sulfur-metabolizing components (Aoki *et al*., 2014).

4.2.2 Total DNA extraction, PCR amplification, clone library construction and sequencing

Extraction of total DNA was performed using an ISOIL for Beads Beating kit (Nippon Gene, Tokyo, Japan). All the natural sediment samples for the clone library construction were subsampled from the innermost of the

Table 4-1. Summary of sediment samples used in this study.

Location	Offshore Boso Peninsula	Offshore Shimokita Peninsula	Nankai Trough
Site (hole name)	C9010 (Hole E)	C9001 (Hole C)	6K949[b]
Cruise	CK09-03	CK06-06	YK06-03
Latitude	34°33.4569'N	41°10.6380'N	33°7.2253'N
Longitude	139°53.3822'E	142°12.081'E	136°28.6672'E
Water depth [mbsl]	2,027	1,180	2,533
Sampling depth [mbsf]	3.7 and 15.4[a]	2.5, 5.1, and 48.3[a]	0–0.25[c]
Reference	Tsuchiya and Takahashi (2009)	Aoike (2007)	Aoki *et al*. (2014), Toki *et al*. (2014)

mbsl: m below sea level, mbsf: m below seafloor.

[a]These are the sampling depths of 10-cm-long whole-round cores.

[b]This is the sampling site of core 949C3 (Aoki *et al*., 2014; Toki *et al*., 2014).

[c]Subsumpled sediment analyzed in this study is same as the inoculum used for bioreactor enrichment, and the enrichment culture analyzed in this study was collected after 903 days after initiation of the bioreactor operation (Aoki *et al*., 2014)

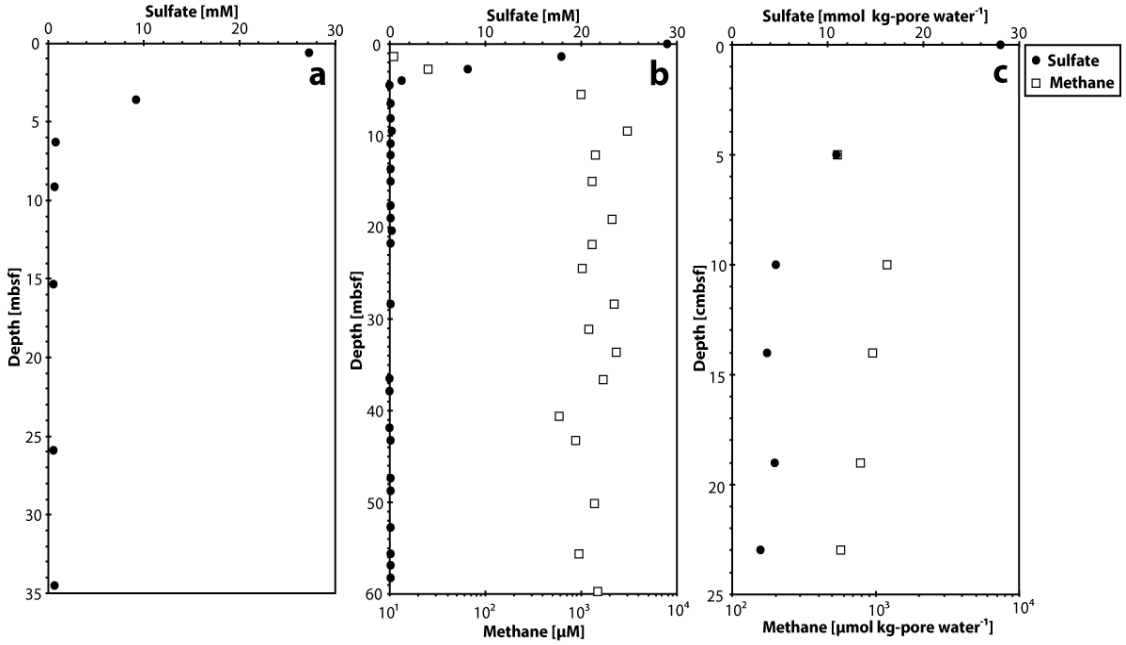

Figure 4-1. Vertical profiles of sulfate and methane concentrations in sediment core samples. (a) Site C9010, Hole E, offshore the Boso Peninsula (only shown above 35 mbsf) (10). (b) Site C9001, Hole C, offshore the Shimokita Peninsula (only shown above 60 mbsf) (Aoike, 2007; Tomaru *et al*., 2009). (c) Site 6K949 in the Nankai Trough (Nunoura *et al*., 2012; Toki *et al*., 2014). At Site C9010, methane concentrations were only measured in the deeper layer of Hole E (below about 100 mbsf), whereas an increasing trend in methane concentrations along with the increasing depth was observed in 1–15 mbsf of Hole B (34°33.4500'N, 139°53.4000'E; about 30 m away from Hole E) (Tsuchiya and Takahashi, 2009).

sediment cores. All the samples were stored at −80°C after subsampling until total DNA extraction was performed. PCR amplification was performed using the TaKaRa Ex Taq (TaKaRa Bio Inc., Otsu, Japan), and the reaction mixtures for PCR were prepared according to the manufacturer's instruction. *aprA* gene fragments were amplified using primer pair AprA-1-FW (5'-TGG CAG ATC ATG ATY MAY GG-3') and AprA-5-RV' (5'-GCG CCA ACN GGD CCR TA-3'; a slightly modified version of AprA-5-RV) (Meyer and Kuever, 2007a). PCR was

performed under the following conditions: initial denaturation at 95°C for 2 min, followed by 25, 30, or 35 cycles of denaturation at 95°C for 40 s, annealing at 55°C for 30 s, and extension at 72°C for 30 s. The final extension step was conducted at 72°C for 7 min. The annealing temperature was empirically determined using genomic DNA extracts from three sulfate-reducing bacterial strains of *Thermodesulfobacterium commune* strain DSM 2178, *Desulfotomaculum thermosapovorans* strain DSM 6562, and *Desulfovibrio vulgaris* subsp. *vulgaris* strain DSM 644 obtained from Deutsche Sammlung von Mikroorganismen und Zellkulturen GmbH, Germany. To reduce possible bias caused by PCR amplification, PCR products that had obtained the minimal number of PCR cycles were used for following experiments. The PCR products were checked on 1%–2% agarose gel electrophoresis, and the expected-size PCR products (approximately 0.4 kbp) were purified using a MinElute Gel Extraction kit (Qiagen, Venlo, the Netherlands). After purification, the purified PCR products were cloned with a pCR 2.1 TOPO TA cloning kit (Invitrogen, Carlsbad, CA, USA). The cloned *aprA* gene sequences were determined using a BigDye terminator v3.1 cycle sequencing kit (Applied Biosystems, Foster City, CA, USA) and an automated sequence analyzer (3730xl DNA Analyzer, Applied Biosystems). Clonal sequences with stop codons were excluded from this study. The *aprA* nucleotide sequences reported in this study have been deposited in the DDBJ/EMBL/GenBank database under accession numbers LC015806–LC016497.

4.2.3 Phylogenetic and statistical analyses

The obtained *aprA* gene sequences were aligned using the ClustalX program (Larkin *et al*., 2007), version 2.1, and a sequence distance matrix was generated using the ARB program (Ludwig *et al*., 2004), version 6.0. The calculated distance matrix was inputted into the mothur program (Schloss *et al*., 2009), version 1.33 and the obtained *aprA* gene sequences were grouped into operational taxonomic units (OTUs) at a 90% nucleotide sequence identity based on the matrix. Putative chimeric sequences were not detected using the "chimera.uchime" command in the mothur program and the more abundant sequences in the obtained clone libraries as a reference. Translated deduced AprA amino acid sequences were subjected to BLASTP analysis (http://blast.ncbi.nlm.nih.gov/Blast.cgi). The deduced AprA amino acid sequences (111–127 amino acid residues) used for AprA tree construction were aligned using the ClustalX program, and then manually corrected. A neighbor-joining AprA phylogenetic tree construction was performed using the MEGA program (Tamura *et al*., 2013), version 6.06. A pairwise distance matrix used for the tree construction was calculated based on the aligned AprA sequences and the Poisson model. A bootstrap analysis with 1,000 replicates was performed to assign confidence levels to the tree topology. The resulting tree was displayed using the FigTree program, version 1.4.2 (http://tree.bio.ed.ac.uk/software/figtree/). Chao1 and ACE richness estimators, Shannon diversity indices, Good's coverage values, and rarefaction curves were calculated using the mothur program.

4.3 Results and Discussion

Phylogenetically diverse *aprA* genes were detected in all the samples tested by PCR and subsequent cloning

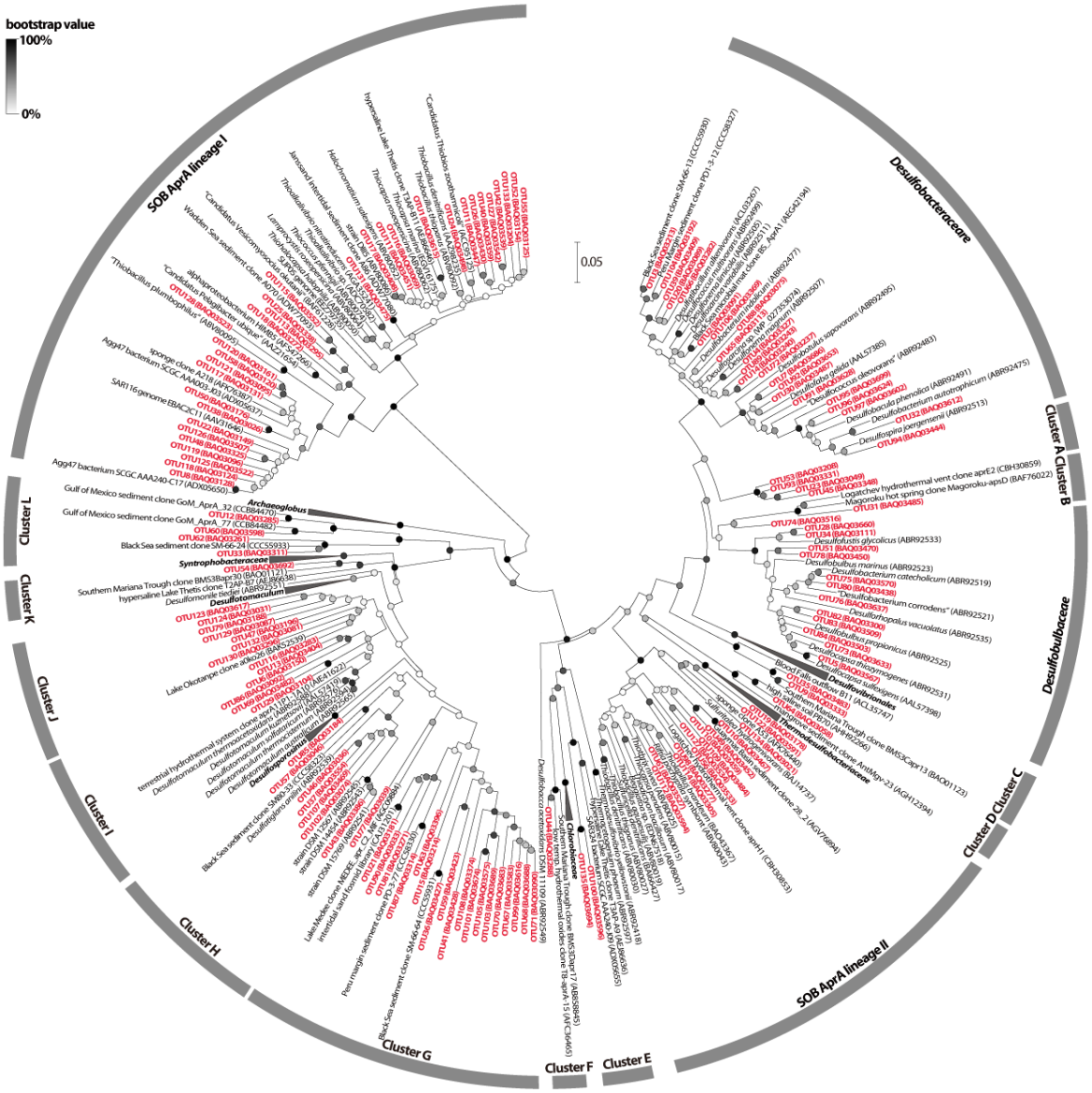

Figure 4-2. Neighbor-joining phylogenetic tree of deduced AprA amino acid sequences. Bold red letters indicate the OTUs detected in this study. The accession numbers are shown in parentheses. The scale bar represents 0.05 amino acid substitutions per sequence position. The color of circles at the branch nodes indicates the bootstrap values obtained after 1,000 resamplings.

procedures. A total of 692 *aprA* gene clones were obtained, and these genes were grouped into 135 distinct operational taxonomic units (OTUs) based on 90% nucleotide sequence identity (**Fig. 4-2** and **Table S4-1**). The rarefaction curves for all clone libraries did not plateau (**Fig. 4-3**), and the Good's coverage values did not reach 100% in any of the clone libraries (77%–93%; **Table S4-2**). Therefore, additional *aprA* OTUs may be recovered by additional sequencing efforts with the same PCR primer set in each clone library. The higher diversity observed at shallower (*i.e.*, 3.7 m below seafloor [mbsf] of Site C9010, and 2.5 and 5.1 mbsf of Site C9001) than greater sediment depths (*i.e.*, 15.4 mbsf of Site C9010 and 48.3 mbsf of Site C9001) suggested the suppression of

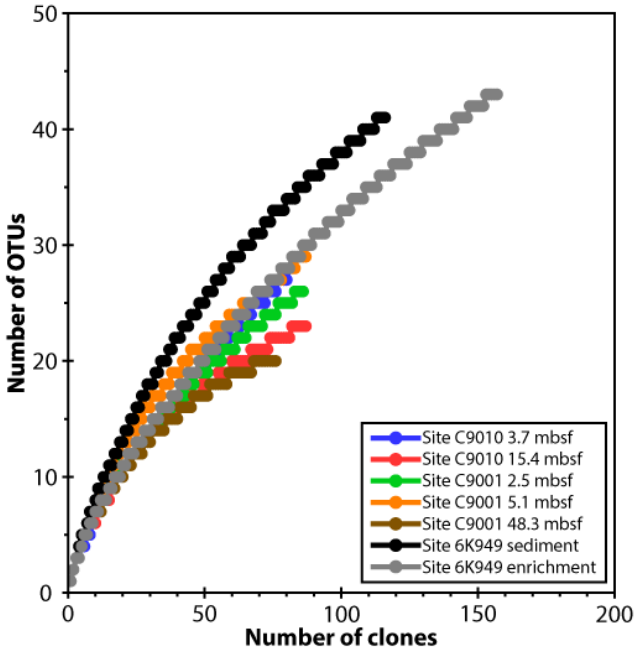

Figure 4-3. Rarefaction curves for each *aprA* gene clone library.

phylogenetic diversity at greater sediment depths of Sites C9010 and C9001 (**Fig. S4-2** and **Table 4-2**). Based on the phylogenetic positions, each OTU was assigned to one of the 16 phylogenetic groups, including tentatively classified uncultivated groups (**Fig. 4-2**). Clusters A to G and J to L did not contain any AprA sequences from pure cultures with validated names. The *aprA*-based community structures and putative function of each phylogenetic group are shown in **Fig. 4-4**. On the basis of the closest cultured relatives and AprA phylogeny (Meyer and Kuever, 2007b), 87 and 45 OTUs were assigned to putative sulfate-reducing and sulfur-oxidizing functional groups, respectively. All 45 putative sulfur-oxidizing OTUs were classified into two phylogenetically distinct sulfur-oxidizing bacteria (SOB), AprA lineages I and II (Meyer and Kuever, 2007a). However, difficulties were still associated with clearly assigning the putative sulfur-oxidizing OTUs to specific taxa, even at the family level, due to the limited number of reference *aprA* genes phylogenetically close to the OTUs and low bootstrap values (**Fig. 4-2**). A previous study proposed that the *aprBA* gene of the sulfate-reducing genus *Thermodesulfovibrio* is laterally transferred to the sulfur-oxidizing family *Chlorobiaceae* (Meyer and Kuever, 2007a). Therefore, the putative functions of three OTUs affiliated with clusters E and F (*i.e.*, OTUs 44, 100, and 135) remain unclear. In all samples analyzed, low-abundance OTUs (showing less than 5.0% of the clonal abundance in each library) comprised a total of 34.9%–56.0% of the composition in each clone library.

At Site C9010 offshore of the Boso Peninsula, the family Desulfobacteraceae-affiliated *aprA* genes comprised 60.2% of the clone library from the sediment at 3.7 mbsf (**Fig. 4-4**). The *Desulfobacteraceae*-affiliated *aprA* genes were also detected at 15.4 mbsf, which was clearly below the sulfate-depletion depth (12.6% of the total clones). In

Table 4-2. Diversity statistics based on *aprA* gene clone libraries.

Sample	Site C9010		Site C9001			Site 6K949	
	3.7 mbsf	15.4 mbsf	2.5 mbsf	5.1 mbsf	48.3 mbsf	sediment	enrichment
Total clone number	83	87	86	87	76	116	157
OTUs	28	23	26	29	20	41	43
Chao1 richness estimator[a]	85 (45–219)	31 (25–55)	39 (30–72)	89 (46–245)	21 (20–28)	62 (48–101)	64 (51–100)
ACE richness estimator[a]	105 (69–173)	33 (26–58)	83 (57–131)	49 (36–89)	24 (21–38)	67 (51–107)	85 (60–145)
Shannon diversity index[a]	2.44 (2.12–2.77)	2.49 (2.24–2.74)	2.64 (2.39–2.89)	2.91 (2.69–3.13)	2.44 (2.18–2.70)	3.19 (2.98–3.40)	2.75 (2.51–2.99)
Good's coverage value (%)	77	89	84	82	93	82	85

[a]Numbers in parentheses indicate the 95% confidence interval.

contrast, *Desulfotomaculum*-associated cluster I was identified as the major putative sulfate-reducing lineage at that depth (28.7% of all clones). In addition to cluster I, SOB AprA lineage I was frequently detected at 15.4 mbsf (49.4% of the total clones). Among the SOB AprA lineage I-associated OTUs, OTU8, which was phylogenetically closely related to the sequences of a putative autotrophic sulfur-oxidizing gammaproteobacterial lineage of Agg47 (*e.g.*, GenBank accession number ADX05650; **Fig. 4-2**), was highly dominant at 15.4 mbsf (20.7% of all clones; **Table S4-2**) (Swan *et al*., 2011). *Desulfobulbaceae*, clusters G and J, and SOB AprA lineage II were not abundant, but were detected at 15.4 mbsf (each group corresponding to 1.1%–4.6% of all clones).

The family *Desulfobacteraceae* comprised 57.0% of the clone library obtained from Site C9001 off the Shimokita Peninsula at 2.5 mbsf (**Fig. 4-4**). Two uncultured lineages, clusters G and L, were also relatively abundant at 2.5 mbsf (corresponding to 12.8% and 11.6% of the clone library, respectively). *Desulfobacteraceae* was also detected as the major component at a depth of 5.1 mbsf, which was just below the sulfate-depletion depth (26.4% of all clones). Clusters C, G, and L, and SOB AprA lineage I were identified as being abundant at 5.1 mbsf (corresponding to 19.5%, 12.6%, 10.3%, and 18.4% of all clones, respectively). At a greater depth of 48.3 mbsf, SOB AprA lineage I was the most abundant (43.4% of all clones). OTU1 was phylogenetically relatively close to cultured gammaproteobacterial sulfur oxidizers (*e.g.*, *Thiocapsa marina*; **Fig. 4-2** and **Table S4-1**) and represented the predominant SOB AprA lineage I-associated OTU at 48.3 mbsf (31.6% of all clones).

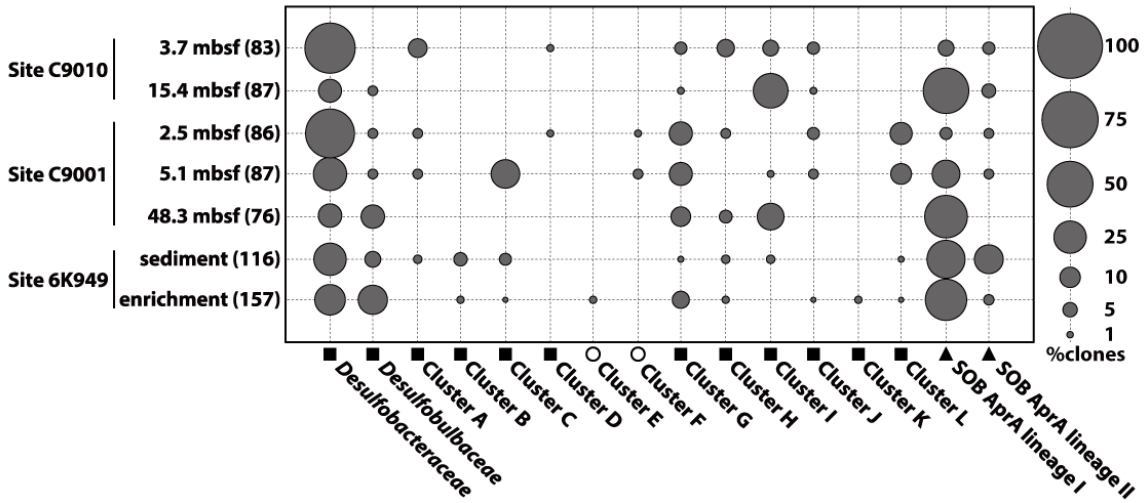

Figure 4-4. Community structures based on *aprA* gene clone libraries. The size of each dot indicates the percentage of identified *aprA* gene sequences falling within a particular taxonomic group. The symbols before the group names indicate the putative function in each taxonomic group. Closed squares, closed triangles, and open circles indicate sulfate reduction, sulfur oxidation, and uncertain function, respectively. The numbers of obtained clones in each library are shown in parentheses.

Desulfotomaculum-associated cluster I was detected as the dominant putative sulfate-reducing component at 48.3 mbsf (17.1% of all clones). In addition, other phylogenetically diverse *aprA* genes affiliated with the putative sulfate reducer lineages of *Desulfobacteraceae*, *Desulfobulbaceae*, and clusters G, H, and I were also detected at 48.3 mbsf (each group corresponding to 3.9%–13.2% of all clones).

Desulfobacteraceae and SOB AprA lineages I and II were frequently detected at Site 6K949 in the methane-seep sediment of the Nankai Trough (corresponding to 25.0%, 34.5%, and 19.8% of all clones, respectively; **Fig. 4-4**). Other putative sulfate-reducing lineages of *Desulfobulbaceae*, and clusters A, B, C, G, H, I, and L were also detected with a relatively low frequency (each group corresponded to 0.9%–6.0% of all clones). The existence of markedly diverse *aprA* genes in the 6K949 enrichment (**Fig. 4-4** and **Table 4-2**) suggested that phylogenetically diverse microorganisms possessing the *aprA* gene at Site 6K949 were culturable under certain laboratory conditions. SOB AprA lineage I-associated OTU1 was the highly dominant OTU in the enrichment (31.8% of all clones; **Table S4-1**). The frequent detection of putative sulfur oxidizer-affiliated *aprA* genes may be linked to the input of barely oxygenated artificial seawater medium and potential sulfide production via an active AOM reaction, as described in the previous study (Aoki *et al*., 2014). In contrast, it was unable to completely exclude potential anaerobic growth by putative sulfur oxidizers colonized in the enrichment (*e.g.*, disproportionation of inorganic sulfur compounds; see later).

The frequent detection of putative sulfate-reducing *aprA* genes in shallow sediment depths associated with the typical sulfate-reducing zone is not surprising. In the present study, *Desulfobacteraceae*-associated *aprA* genes were identified as the major components at Site 6K949 and shallow sediment depths of Sites C9010 and C9001

(**Fig. 4-4**). The dominance of *Desulfobacteraceae* has also been observed in geographically distinct subseafloor environments (Leloup *et al*., 2009; Blazejak and Schippers, 2011). Most cultured members of the family *Desulfobacteraceae* completely oxidize a wide range of organic compounds to carbon dioxide with sulfate or other inorganic sulfur compounds as the electron acceptor (Kuever, 2014). Growth with fermentation (Kuever, 2014), iron reduction (Kuever, 2014), the disproportionation of inorganic sulfur compounds (Milucka *et al*., 2012; Kuever, 2014), gaseous short-chain alkane degradation using sulfate (Kniemeyer *et al*., 2007), and lithoautotrophic growth with hydrogen (Kuever, 2014) have been reported in *Desulfobacteraceae* members. Therefore, *Desulfobacteraceae* sulfate reducers appear to be capable of occupying ecological niches in diverse marine environments due to their metabolic versatility. The symbiotic lifestyle of the ANME-2 group with the *Desulfosarcina*/*Desulfococcus* (DSS) group within *Desulfobacteraceae* has been reported previously (Knittel and Boetius, 2009). According to a mechanism recently proposed by Milucka *et al*. (2012), DSS disproportionates zero-valent sulfur (in the form of disulfide) formed by ANME-2 to sulfate and sulfide in a sulfate-driven AOM reaction. OTU2, which was frequently detected at Sites C9010 and 6K949, was phylogenetically close to environmental sequences retrieved from an ANME-2/DSS-dominated microbial mat (**Fig. 4-2**). Thus, the presence of some *Desulfobacteraceae aprA* genes may be solely attributed to sulfate-driven AOM activity.

Phylogenetically diverse putative sulfate-reducing *aprA* genes were also detected in sulfate-depleted (<1 mM sulfate) sediment horizons below the typical sulfate-reducing zone (**Fig. 4-4**). These results suggested that phylogenetically diverse putative sulfate reducers exhibited high sulfate affinity to adapt to low-sulfate subseafloor environments (Tarpgaard *et al*., 2011). Among the phylogenetically diverse putative sulfate-reducing groups, *Desulfotomaculum*-associated cluster I was frequently detected at greater depths. Most cultured members of the genus *Desulfotomaculum* have the ability to oxidize various organic substances with sulfate or other inorganic sulfur compounds as the terminal electron acceptor (Kuever and Rainey, 2009; Aüllo *et al*., 2013). Growth with fermentation (Kuever and Rainey, 2009; Aüllo *et al*., 2013), metal reduction (Kuever and Rainey, 2009; Aüllo *et al*., 2013), thiosulfate disproportionation (Aüllo *et al*., 2013), syntrophic association with methanogens in the absence of sulfate (Imachi *et al*., 2006), propane degradation using sulfate (Kniemeyer *et al*., 2007), and lithoautotrophic growth with hydrogen (Kuever and Rainey, 2009; Aüllo *et al*., 2013) have been reported in *Desulfotomaculum*-related lineages. Another unique physiological feature of *Desulfotomaculum* members is their sporulation capability (Kuever and Rainey, 2009; Aüllo *et al*., 2013). Sporulation is considered to be one of the microbial strategies used to resist nutrient deprivation, unfavorable temperatures, or redox conditions (Aüllo *et al*., 2013). Assuming that cluster I-affiliated members share *Desulfotomaculum*-like versatile physiological features, these members may have advantages for long-term survival in deep subseafloor environments in which nutrient availability is severely limited (Jørgensen and Boetius, 2007). In contrast, previously identified *Desulfotomaculum* members have not yet been detected and isolated from deep subseafloor environments (Aüllo *et al*., 2013). Further analyses are needed in order to obtain detailed genetic and physiological information on putative sulfate reducers

possessing the cluster I *aprA* gene.

Another interesting result of this functional gene survey was the frequent detection of SOB AprA lineage I-affiliated *aprA* genes in sulfate-depleted deep subseafloor sediment samples at Sites C9010 and C9001 (**Fig. 4-4**). Furthermore, phylogenetic analysis presented in this study suggested that some as yet uncharacterized sulfur oxidizers potentially affiliated with the class *Gammaproteobacteria* may function in the biological sulfur cycle at greater depths. Although we did not obtain quantitative data regarding general terminal electron acceptors for sulfur oxidizers (*i.e.*, oxygen, nitrate, and nitrite), these electron acceptors may be available less at sulfate-depleted depths because of higher reduction potential ranges than those of sulfate (Lam *et al*., 2011). In contrast, mRNA transcripts coding for dissimilatory nitrate reductases were expressed at the sulfate-depleted sediment depths of the Peru Margin sediment (Site 1229, Hole D) in the absence of measureable nitrate (Orsi *et al*., 2013). Thus, the presence of trace amounts of nitrate at sulfate-depleted lower-redox depths may be one of the conceivable explanations for the detection of putative sulfur oxidizer-related *aprA* genes. Another possible metabolism that may sustain the putative sulfur oxidizers possessing the *aprA* gene is the disproportionation of inorganic sulfur compounds, such as thiosulfate ($S_2O_3^{2-} + H_2O \rightarrow SO_4^{2-} + HS^- + H^+$) and elemental sulfur ($4S^0 + 4H_2O \rightarrow SO_4^{2-} + 3HS^- + 5H^+$) (Finster, 2008). Reactive metal species (*e.g.*, Mn(IV) and Fe(III)), which may be involved in the abiotic oxidation of sulfide to thiosulfate and that to elemental sulfur, have been detected at sulfate-depleted-sediment depths of diverse marine sediments (Knab *et al*., 2009; Holmkvist *et al*., 2011). Therefore, the disproportionation of inorganic sulfur compounds may occur as primary energy-yielding metabolism in the sulfate-depleted subseafloor sediment once reactive metal species are available; however, elemental sulfur disproportionation requires the removal of the produced sulfide to be thermodynamically favorable (Finster, 2008). OTU5, phylogenetically closely related to the genus *Desulfocapsa*, which contains isolates capable of the disproportionation of inorganic sulfur compounds (Finster, 2008), was one of the frequently detected OTUs at 48.3 mbsf of Site C9001 (10.5% of all clones; **Table S4-1**).

4.4 Summary of this chapter

The functional gene survey presented in this study suggested the presence of markedly diverse *aprA* sequences in subseafloor sediments on the northwestern Pacific margin off Japan, and also that the microbial ecosystems involved exhibited markedly diverse genetic potentials to mediate the sulfur cycle even below the typical sulfate-reducing zone. The family *Desulfobacteraceae* and microbes possessing the *aprA* gene associated with AprA cluster I were identified as the predominant putative sulfate-reducing components at shallow and deep sediment depths, respectively. Also, some as yet uncharacterized putative gammaproteobacterial sulfur oxidizers were suggested as key sulfur compound-metabolizing components at greater sediment depths. In contrast, the *in situ* expression of *aprA* genes, *in situ* activity rates, and the detailed physiological properties of microorganisms possessing the *aprA* gene currently remain unclear. The combination of an *in situ* metatranscriptomic analysis and

laboratory cultivation studies will provide deeper insights into the potential biogeochemical sulfur cycling in subseafloor microbial ecosystems.

4.5 References

Aoike K (2007) CK06-06 D/V Chikyu shakedown cruise offshore Shimokita laboratory operation report. CDEX-JAMSTEC, Yokohama.

Aoki M, Ehara M, Saito Y, Yoshioka H, Miyazaki M, *et al.* (2014) A long-term cultivation of an anaerobic methane-oxidizing microbial community from deep-sea methane-seep sediment using a continuous-flow bioreactor. *PLoS ONE* 9:e105356.

Aüllo T, Ranchou-Peyruse A, Ollivier B, Magot M (2013) *Desulfotomaculum* spp. and related gram-positive sulfate-reducing bacteria in deep subsurface environments. *Front Microbiol* 4:362.

Blazejak A, Schippers A (2011) Real-time PCR quantification and diversity analysis of the functional genes *aprA* and *dsrA* of sulfate-reducing prokaryotes in marine sediments of the Peru continental margin and the Black Sea. *Front Microbiol* 2:253.

Bowles MW, Mogollón JM, Kasten S, Zabel M, Hinrichs K-U (2014) Global rates of marine sulfate reduction and implications for sub-sea-floor metabolic activities. *Science* 344:889-891.

D'Hondt S, Jørgensen BB, Miller DJ, Batzke A, Blake R, *et al*. (2004) Distributions of microbial activities in deep subseafloor sediments. *Science* 306:2216–2221.

Finster K (2008) Microbiological disproportionation of inorganic sulfur compounds. *J Sulfur Chem* 29:281–292.

Holmkvist L, Ferdelman TG, Jørgensen BB (2011) A cryptic sulfur cycle driven by iron in the methane zone of marine sediment (Aarhus Bay, Denmark). *Geochim Cosmochim Acta* 75:3581–3599.

Imachi H, Sekiguchi Y, Kamagata Y, Loy A, Qiu Y-L, *et al*. (2006) Non-sulfate-reducing, syntrophic bacteria affiliated with *Desulfotomaculum* cluster I are widely distributed in methanogenic environments. *Appl Environ Microbiol* 72:2080–2091.

Jørgensen BB, Boetius A (2007) Feast and famine — microbial life in the deep-sea bed. *Nat Rev Microbiol* 5:770–781.

Knab NJ, Cragg BA, Hornibrook ERC, Holmkvist L, Pancost RD, *et al*. (2009) Regulation of anaerobic methane oxidation in sediments of the Black Sea. *Biogeosciences* 6:1505–1518.

Kniemeyer O, Musat F, Sievert SM, Knittel K, Wilkes H, *et al*. (2007) Anaerobic oxidation of short-chain hydrocarbons by marine sulphate-reducing bacteria. *Nature* 449:898–901.

Knittel K, Boetius A (2009) Anaerobic oxidation of methane: progress with an unknown process. *Annu Rev Microbiol* 63:311–334.

Kuever J, Rainey FA (2009) Genus VII. *Desulfotomaculum*. *In* De Vos P, Garrity GM, Jones D, Krieg NR, Ludwig W, Rainey FA, Schleifer K-H, Whitman WB (eds.), Bergey's Manual of Systematic Bacteriology (2nd edition), Springer, pp. 989–996.

Kuever J (2014) The Family *Desulfobacteraceae*. *In* Rosenberg E, DeLong EF, Lory S, Stackebrandt E, Thompson F (eds.), The Prokaryotes (4th edition), Springer-Verlag Berlin Heidelberg, pp. 45-73

Lam P, Kuypers MMM (2011) Microbial nitrogen cycling processes in oxygen minimum zones. Ann Rev Mar Sci 3:317–345.

Larkin MA, Blackshields G, Brown NP, Chenna R, McGettigan PA, *et al*. (2007) Clustal W and Clustal X version 2.0. *Bioinformatics* 23:2947–2948.

Leloup J, Fossing H, Kohls K, Holmkvist L, Borowski C, Jørgensen BB (2009) Sulfate-reducing bacteria in marine sediment (Aarhus Bay, Denmark): abundance and diversity related to geochemical zonation. *Environ Microbiol* 11:1278–1291.

Ludwig W, Strunk O, Westram R, Richter L, Meier H, *et al*. (2004) ARB: a software environment for sequence data. *Nucleic Acids Res* 32:1363–1371.

Meyer B, Kuever J (2007a) Molecular analysis of the diversity of sulfate-reducing and sulfur-oxidizing prokaryotes in the environment, using *aprA* as functional marker gene. *Appl Environ Microbiol* 73:7664–7679.

Meyer B, Kuever J (2007b) Molecular analysis of the distribution and phylogeny of dissimilatory adenosine-5'-phosphosulfate reductase-encoding genes (*aprBA*) among sulfur-oxidizing prokaryotes. *Microbiology* 153:3478–3498.

Milucka J, Ferdelman TG, Polerecky L, Franzke D, Wegener G, *et al*. (2012) Zero-valent sulphur is a key intermediate in marine methane oxidation. *Nature* 491:541–546.

Nunoura T, Takaki Y, Kazama H, Hirai M, Ashi J, *et al*. (2012) Microbial diversity in deep-sea methane seep sediments presented by SSU rRNA gene tag sequencing. *Microbes Environ* 27:382–390.

Orsi WD, Edgcomb VP, Christman GD, Biddle JF (2013) Gene expression in the deep biosphere. *Nature* 499:205–208.

Schloss PD, Westcott SL, Ryabin T, Hall JR, Hartmann M, *et al*. (2009) Introducing mothur: open-source, platform-independent, community-supported software for describing and comparing microbial communities. *Appl Environ Microbiol* 75:7537–7541.

Swan BK, Martinez-Garcia M, Preston CM, Sczyrba A, Woyke T, *et al*. (2011) Potential for chemolithoautotrophy among ubiquitous bacteria lineages in the dark ocean. *Science* 333:1296–1300.

Tamura K, Stecher G, Peterson D, Filipski A, Kumar S (2013) MEGA6: Molecular Evolutionary Genetics Analysis version 6.0. *Mol Biol Evol* 30:2725–2729.

Tarpgaard IH, Røy H, Jørgensen BB (2011) Concurrent low-and high-affinity sulfate reduction kinetics in marine sediment. *Geochim Cosmochim Acta* 75:2997–3010.

Toki T, Higa R, Ijiri A, Tsunogai U, Ashi J (2014) Origin and transport of pore fluids in the Nankai accretionary prism inferred from chemical and isotopic compositions of pore water at cold seep sites off Kumano. *Earth Planets Space* 66:137.

Tomaru H, Fehn U, Lu Z, Takeuchi R, Inagaki F, *et al*. (2009) Dating of dissolved iodine in pore waters from the gas hydrate occurrence offshore Shimokita Peninsula, Japan: ^{129}I Results from the D/V Chikyu Shakedown Cruise. *Resour Geol* 59:359–373.

Treude T, Krause S, Maltby J, Dale AW, Coffin R, Hamdan LJ (2014) Sulfate reduction and methane oxidation activity below the sulfate-methane transition zone in Alaskan Beaufort Sea continental margin sediments: Implications for deep sulfur cycling. *Geochim Cosmochim Acta* 144:217–237.

Tsuchiya M, Takahashi K (2009) Scientific report for cruise CK09-03 Expedition 905. JAMSTEC, Yokosuka.

4.6 Supplementary Information

Table S4-1. List of *aprA* gene OTUs detected in this study.

OTU name	Number of clones							Phylogenetic affiliation	Similar AprA sequence with validiated name (GenBank accession number)	Maximum Identity [%]
	Site C9010		Site C9001		Site 6K949		total			
	3.7 mbsf	15.4 mbsf	2.5 mbsf	5.1 mbsf	48.3 mbsf	sediment	enrichment			
OTU1	0	0	0	3	24	0	50	77	AprA lineage I	*Thiocapsa marina* (EGV16175)	95.7
OTU2	35	0	0	0	3	21	1	60	*Desulfobacteraceae*	*Desulfosarcina variabilis* (ABR92511)	95.8
OTU3	5	1	22	4	2	2	6	42	*Desulfobacteraceae*	*Desulfatibacillum alkenivorans* (ACL03267)	93.3
OTU4	3	6	12	13	0	0	0	34	*Desulfobacteraceae*	*Desulfonema magnum* (ABR92507)	96.6
OTU5	0	0	0	1	8	1	22	32	*Desulfobulbaceae*	*Desulfocapsa sulfexigens* (AAL57398)	97.5
OTU6	1	24	0	0	2	0	0	27	Cluster I	*Desulfotomaculum australicum* (ABR92565)	89.9
OTU7	0	0	0	4	2	0	17	23	*Desulfobacteraceae*	*Desulfofaba gelida* (AAL57385)	95.8
OTU8	1	18	0	0	0	0	0	19	AprA lineage I	*Thioalkalivibrio sulfidiphilus* (ACL71448)	80.3
OTU9	0	0	0	16	0	2	0	18	Cluster C	*Sedimenticola selenatireducens* (WP_029134892)	79.8
OTU10	0	0	0	0	0	13	2	15	AprA lineage II	*Thiobacillus thioparus* (ABV80027)	91.6
OTU11	0	0	0	0	1	11	1	13	AprA lineage I	*Thiobacillus denitrificans* (WP_011312794)	96.6
OTU12	0	0	8	5	0	0	0	13	Cluster L	*Desulfotomaculum gibsoniae* (ABR92567)	70.6
OTU13	0	0	0	0	11	0	0	11	Cluster I	*Desulfotomaculum australicum* (ABR92565)	92.4
OTU14	0	0	9	0	0	0	2	11	*Desulfobacteraceae*	*Desulfosarcina variabilis* (AAL57388)	96.6
OTU15	0	0	5	5	0	0	0	10	Cluster G	*Desulfotomaculum australicum* (ABR92565)	76.7
OTU16	1	0	1	0	4	3	1	10	AprA lineage I	*Thiocapsa roseopersicina* (ABV80060)	94.9
OTU17	0	0	0	0	2	0	7	9	AprA lineage I	*Halochromatium salexigens* (ABV80052)	96.6
OTU18	0	4	0	5	0	0	0	9	AprA lineage I	*Thiobacillus denitrificans* (WP_011312794)	82.1
OTU19	2	4	2	0	0	0	0	8	AprA lineage II	*Sulfuritalea hydrogenivorans* sk43H (BAJ14737)	84
OTU20	5	2	0	1	0	0	0	8	*Desulfobacteraceae*	*Desulfonema ishimotonii* (AAL57402)	93.3
OTU21	0	0	4	3	0	0	0	7	Cluster G	*Desulfotomaculum australicum* (ABR92565)	79.8
OTU22	1	5	0	0	0	0	0	6	AprA lineage I	*Thioalkalivibrio sulfidiphilus* (ACL71448)	80.3
OTU23	6	0	0	0	0	0	0	6	Cluster A	*Desulfonema magnum* (ABR92507)	88.2
OTU24	0	0	0	0	0	6	0	6	AprA lineage I	*Thioalkalivibrio thiocyanodenitrificans* (WP_018233553)	96.6
OTU25	0	0	0	4	0	2	0	6	AprA lineage I	*Chromatium okenii* (ABV80056)	83.8
OTU26	0	0	0	0	0	4	2	6	AprA lineage I	*Halochromatium salexigens* (ABV80052)	94.9
OTU27	0	0	0	0	0	5	1	6	AprA lineage I	*Thiocapsa roseopersicina* (ABV80060)	96.6
OTU28	0	0	0	0	2	0	3	5	*Desulfobulbaceae*	*Desulforhopalus singaporensis* (AAL57430)	95
OTU29	3	1	0	1	0	0	0	5	Cluster I	*Desulfotomaculum australicum* (ABR92565)	87.4
OTU30	0	0	0	0	0	5	0	5	*Desulfobacteraceae*	*Desulfofaba fastidiosa* (AAU95383)	94.1
OTU31	0	0	0	0	0	3	2	5	Cluster B	*Desulfobulbus japonicus* (WP_028580570)	82.6
OTU32	0	0	0	0	0	0	4	4	*Desulfobacteraceae*	*Desulfobacterium autotrophicum* (ABR92475)	94.1
OTU33	0	0	0	4	0	0	0	4	Cluster L	*Desulfovirgula thermocuniculi* (WP_027718700)	69.4
OTU34	0	2	2	0	0	0	0	4	*Desulfobulbaceae*	*Desulforhopalus singaporensis* (AAL57430)	96.6
OTU35	0	0	0	1	0	2	1	4	Cluster C	*Desulfurivibrio alkaliphilus* (ADH86166)	79
OTU36	0	1	1	0	1	0	1	4	Cluster G	*Desulfotomaculum australicum* (ABR92565)	75.8
OTU37	0	0	1	0	0	1	2	4	Cluster H	*Desulfatiglans anilini* (AAL57425)	86.3
OTU38	1	3	0	0	0	0	0	4	AprA lineage I	*Thioalkalivibrio sulfidiphilus* (ACL71448)	81.2
OTU39	1	0	1	0	2	0	0	4	*Desulfobacteraceae*	*Desulfobacterium indolicum* (ABR92477)	94.1
OTU40	0	0	0	0	2	1	1	4	AprA lineage I	*Halochromatium salexigens* (ABV80052)	94
OTU41	0	0	1	0	2	0	0	3	Cluster G	*Desulfotomaculum australicum* (ABR92565)	74.2
OTU42	0	0	0	0	0	3	0	3	AprA lineage I	*Halochromatium salexigens* (ABV80052)	94
OTU43	0	0	0	0	3	0	0	3	Cluster H	*Desulfatiglans anilini* (AAL57425)	87.3
OTU44	0	0	1	2	0	0	0	3	Cluster F	*Chlorobium clathratiforme* (ABV79999)	78.7

Table S4-1. —continued.

OTU45	1	0	0	1	0	1	0	3	Cluster A	*Desulfonema ishimotonii* (AAL57402)	87.4
OTU46	3	0	0	0	0	0	0	3	Cluster H	*Desulfatiglans anilini* (AAL57425)	85.5
OTU47	0	1	2	0	0	0	0	3	Cluster J	*Desulfotomaculum australicum* (ABR92565)	84
OTU48	0	0	0	3	0	0	0	3	AprA lineage I	*Thiorhodovibrio winogradskyi* (ABV80076)	80.3
OTU49	0	0	0	0	0	3	0	3	AprA lineage II	*Thiobacillus thioparus* (ABV80027)	89.1
OTU50	0	3	0	0	0	0	0	3	AprA lineage I	*Thioalkalivibrio sulfidophilus* (ACL71448)	79.5
OTU51	0	0	0	0	0	2	1	3	*Desulfobulbaceae*	*Desulfobulbus marinus* (ABR92523)	91.6
OTU52	1	2	0	0	0	0	0	3	AprA lineage I	*Halochromatium salexigens* (ABV80052)	94
OTU53	0	0	2	0	0	1	0	3	Cluster A	*Desulfonema ishimotonii* (AAL57402)	90.8
OTU54	0	0	0	0	0	0	2	2	Cluster K	*Desulfotomaculum intricatum* (BAN14411)	81
OTU55	0	1	1	0	0	0	0	2	AprA lineage I	*Thiobacillus denitrificans* (WP_011312794)	94.9
OTU56	0	0	0	0	0	2	0	2	AprA lineage II	*Thiobacillus thioparus* (ABV80027)	84.9
OTU57	2	0	0	0	0	0	0	2	Cluster H	*Desulfotomaculum thermobenzoicum* (AAL57428)	81.8
OTU58	0	2	0	0	0	0	0	2	AprA lineage I	*Thioalkalivibrio sulfidophilus* (YP_002512435)	80.3
OTU59	0	0	0	1	1	0	0	2	Cluster G	*Desulfotomaculum australicum* (ABR92565)	80
OTU60	0	0	0	0	0	1	1	2	Cluster L	*Desulfotomaculum gibsoniae* (ABR92567)	68.6
OTU61	0	0	0	0	0	2	0	2	AprA lineage II	*Thiolapillus brandeum* (BAO43367)	95
OTU62	0	0	2	0	0	0	0	2	Cluster L	*Desulfomonile tiedjei* (AAL57429)	65.3
OTU63	0	0	0	0	2	0	0	2	Cluster G	*Desulfotomaculum australicum* (ABR92565)	80
OTU64	1	0	1	0	0	0	0	2	Cluster D	*Desulfonatronovibrio hydrogenovorans* (ABR92460)	74
OTU65	0	2	0	0	0	0	0	2	*Desulfobacteraceae*	*Desulfobacterium indolicum* (ABR92477)	95
OTU66	0	0	1	1	0	0	0	2	*Desulfobacteraceae*	*Desulfococcus multivorans* (AAL57403)	92.4
OTU67	0	0	0	0	0	0	2	2	Cluster G	*Desulfotomaculum australicum* (ABR92565)	80
OTU68	0	0	0	0	0	0	2	2	Cluster G	*Desulfotomaculum australicum* (ABR92565)	81.7
OTU69	0	0	0	0	0	2	0	2	Cluster I	*Desulfotomaculum australicum* (ABR92565)	86.6
OTU70	0	0	0	0	0	0	2	2	Cluster G	*Desulfotomaculum australicum* (ABR92565)	80
OTU71	1	0	0	0	0	1	0	2	Cluster G	*Desulfotomaculum australicum* (ABR92565)	80
OTU72	0	0	2	0	0	0	0	2	*Desulfobacteraceae*	*Desulfosarcina variabilis* (AAL57388)	94.1
OTU73	0	0	0	0	0	0	2	2	*Desulfobulbaceae*	*Desulfocapsa thiozymogenes* (ABR92531)	93.3
OTU74	0	0	0	0	0	2	0	2	Cluster B	*Desulfonema ishimotonii* (AAL57402)	86.6
OTU75	0	0	0	0	0	0	2	2	*Desulfobulbaceae*	*Desulfobacterium catecholicum* (ABR92517)	99.2
OTU76	0	0	0	0	0	0	2	2	*Desulfobulbaceae*	*Desulfobacterium catecholicum* (ABR92517)	94.1
OTU77	1	0	0	0	0	0	0	1	Cluster G	*Ammonifex degensii* (ACX52207)	84.2
OTU78	0	0	0	0	0	1	0	1	*Desulfobulbaceae*	*Desulfobulbus marinus* (ABR92523)	90.8
OTU79	0	0	1	0	0	0	0	1	Cluster J	*Desulfotomaculum gibsoniae* (ABR92567)	82.9
OTU80	0	0	0	0	0	1	0	1	*Desulfobulbaceae*	*Desulfobacterium catecholicum* (ABR92517)	95.8
OTU81	0	0	0	1	0	0	0	1	Cluster G	*Desulfomonile tiedjei* (AAL57429)	79.8
OTU82	0	0	0	1	0	0	0	1	*Desulfobulbaceae*	*Desulfocapsa thiozymogenes* (ABR92531)	95
OTU83	0	0	0	0	0	1	0	1	*Desulfobulbaceae*	*Desulfurivibrio alkaliphilus* (ADH86166)	94.1
OTU84	0	0	0	0	0	1	0	1	*Desulfobulbaceae*	*Desulfocapsa thiozymogenes* (ABR92531)	94.1
OTU85	0	0	1	0	0	0	0	1	Cluster H	*Desulforhabdus amnigena* (ABR92553)	85.7
OTU86	1	0	0	0	0	0	0	1	Cluster I	*Desulfotomaculum australicum* (ABR92565)	84.9
OTU87	0	0	0	1	0	0	0	1	Cluster G	*Desulfomonile tiedjei* (AAL57429)	82.2
OTU88	1	0	0	0	0	0	0	1	*Desulfobacteraceae*	*Desulfobacterium indolicum* (ABR92477)	91.6
OTU89	0	0	1	0	0	0	0	1	*Desulfobacteraceae*	*Desulfobacterium indolicum* (ABR92477)	92.4
OTU90	1	0	0	0	0	0	0	1	Cluster G	*Desulfomonile tiedjei* (AAL57429)	76.3
OTU91	0	0	0	0	0	0	1	1	*Desulfobacteraceae*	*Desulfofaba fastidiosa* (AAU95383)	92.4

Table S4-1. —continued.

OTU92	0	0	0	0	0	0	1	1	*Desulfobacteraceae*	*Desulfofaba gelida* (AAL57385)	91.6
OTU93	0	0	0	1	0	0	0	1	Cluster A	*Desulfonema ishimotonii* (AAL57402)	89.1
OTU94	0	0	0	0	0	1	0	1	*Desulfobacteraceae*	*Desulfobacterium vacuolatum* (AAL57391)	96.6
OTU95	0	0	0	0	0	0	1	1	*Desulfobacteraceae*	*Desulfobacula toluolica* (ABR92493)	93.3
OTU96	0	0	0	0	0	0	1	1	*Desulfobacteraceae*	*Desulfobacula toluolica* (ABR92493)	92.4
OTU97	0	0	0	0	0	0	1	1	*Desulfobacteraceae*	*Desulfobacula toluolica* (ABR92493)	92.4
OTU98	0	0	0	1	0	0	0	1	AprA lineage II	*Thiothrix nivea* (EIJ35356)	88.2
OTU99	0	0	0	0	0	0	1	1	Cluster G	*Desulfotomaculum australicum* (ABR92565)	81.7
OTU100	0	0	0	0	0	0	1	1	Cluster E	*Chlorobaculum thiosulfatiphilum* (ABV79991)	70.9
OTU101	0	0	0	0	0	0	1	1	Cluster G	*Desulfotomaculum thermoacetoxidans* (ABR92588)	80.8
OTU102	1	0	0	0	0	0	0	1	Cluster H	*Desulfatiglans anilini* (AAL57425)	82.2
OTU103	0	0	0	0	0	0	1	1	Cluster G	*Desulfotomaculum australicum* (ABR92565)	78.3
OTU104	0	0	1	0	0	0	0	1	*Desulfobacteraceae*	*Desulfatibacillum alkenivorans* (ACL03267)	92.4
OTU105	0	0	0	0	0	0	1	1	Cluster G	*Desulfotomaculum australicum* (ABR92565)	80.8
OTU106	0	0	0	0	1	0	0	1	*Desulfobacteraceae*	*Desulfonema ishimotonii* (AAL57402)	92.4
OTU107	0	0	0	0	0	1	0	1	Cluster H	*Desulfatiglans anilini* (AAL57425)	88.1
OTU108	0	0	0	0	1	0	0	1	Cluster G	*Desulfotomaculum australicum* (ABR92565)	79.2
OTU109	0	0	0	0	0	1	0	1	AprA lineage II	*Thiolapillus brandeum* (BAO43367)	90.8
OTU110	0	0	0	0	0	1	0	1	AprA lineage II	*Thiobacillus denitrificans* (ABV80031)	92.4
OTU111	0	0	0	0	0	1	0	1	AprA lineage I	*Halochromatium salexigens* (ABV80052)	95.7
OTU112	0	0	0	0	0	0	1	1	AprA lineage II	*Sedimenticola selenatireducens* (WP_029134892)	94.1
OTU113	0	0	0	1	0	0	0	1	AprA lineage I	*Thioalkalivibrio sulfidiphilus* (ACL71448)	83.8
OTU114	0	0	0	1	0	0	0	1	AprA lineage II	*Thiolapillus brandeum* (BAO43367)	95
OTU115	0	0	0	0	0	0	1	1	AprA lineage I	*Rhabdochromatium marinum* (ABV80078)	82.9
OTU116	0	0	0	1	0	0	0	1	Cluster J	*Desulfotomaculum australicum* (ABR92565)	85.7
OTU117	0	1	0	0	0	0	0	1	AprA lineage I	*Thioalkalivibrio sulfidiphilus* (ACL71448)	78.6
OTU118	0	1	0	0	0	0	0	1	AprA lineage I	*Thiohalocapsa halophila* (ABV80050)	78.6
OTU119	0	1	0	0	0	0	0	1	AprA lineage I	*Thioalkalivibrio nitratireducens* (AGA35241)	79.5
OTU120	0	1	0	0	0	0	0	1	AprA lineage I	*Thioalkalivibrio sulfidophilus* (WP_012636937)	80.3
OTU121	0	1	0	0	0	0	0	1	AprA lineage I	*Thioalkalivibrio sulfidophilus* (WP_012636937)	80.3
OTU122	0	0	0	0	0	0	1	1	AprA lineage II	*Thioploca ingrica* (BAP57403)	85.7
OTU123	0	0	0	0	0	0	1	1	Cluster J	*Desulfotomaculum australicum* (ABR92565)	84
OTU124	1	0	0	0	0	0	0	1	Cluster J	*Desulfotomaculum gibsoniae* (ABR92567)	84.5
OTU125	0	0	0	0	0	1	0	1	AprA lineage I	*Thioalkalivibrio sulfidophilus* (WP_012636937)	82.9
OTU126	0	0	0	0	0	1	0	1	AprA lineage I	*Rhabdochromatium marinum* (ABV80078)	79.5
OTU127	0	0	0	0	0	1	0	1	AprA lineage II	*Thiolapillus brandeum* (BAO43367)	95
OTU128	0	0	0	0	0	1	0	1	AprA lineage I	*Thiococcus pfennigii* (ABV80074)	76.9
OTU129	1	0	0	0	0	0	0	1	Cluster J	*Desulfotomaculum australicum* (ABR92565)	82.2
OTU130	0	0	0	1	0	0	0	1	Cluster J	*Desulfotomaculum solfataricum* (ABR92576)	81.5
OTU131	0	0	0	0	0	1	0	1	AprA lineage I	*Thioalkalivibrio sulfidiphilus* (ACL71448)	95.7
OTU132	1	0	0	0	0	0	0	1	Cluster J	*Desulfotomaculum australicum* (ABR92565)	83.2
OTU133	0	0	1	0	0	0	0	1	AprA lineage I	*Thiobacillus denitrificans* (WP_011312794)	92.3
OTU134	1	0	0	0	0	0	0	1	AprA lineage II	*Sulfurisoma sediminicola* (BAO37334)	83.2
OTU135	0	0	0	0	0	0	1	1	Cluster E	*Chlorobium clathratiforme* (ABV79999)	73.2

Chapter V: Summary of this thesis

Marine sedimentary microbes significantly contribute the carbon and sulfur cycling on the Earth. However, despite the significance of the microbes, still little is known about the ecology of the microbes relevant to carbon and sulfur cycling. Therefore, in this thesis, culture-dependent and -independent experiments were performed using marine sediment samples collected from the northwestern Pacific margin off Japan to better understand the ecology of marine sedimentary carbon and sulfur cycling-associated microbes. Follow-up studies using this data and enrichment cultures obtained in this thesis should provide deeper insights into the biogeochemical processes in marine sediments. The experimental outcomes and conclusions in each chapter are as follows:

In Chapter II, a continuous-flow bioreactor with polyurethane sponges, called the down-flow hanging sponge (DHS) bioreactor, was utilized for cultivating an anaerobic oxidation of methane (AOM) microbial community from the deep-sea methane-seep sediment of the Nankai Trough. The main objective of Chapter II was to investigate the applicability of the DHS bioreactor for cultivating an AOM microbial community and identification of active AOM-associated entities in the methane-seep sediment of the Nankai Trough. As a result of the enrichment achieved using the DHS bioreactor, anaerobic methanotroph (ANME)-related lineages (*i.e.*, ANME-1, -2a, -2c, and -3) were detected in the enrichment. Also, an active potential AOM activity was confirmed in the enrichment by a tracer experiment using ^{13}C-labeled methane. These results suggest that these putative AOM entities thriving in the methane-seep sediment of the Nankai Trough would be metabolically active and might involve *in situ* AOM activity (potentially coupled with sulfate reduction; arrow (1) in **Fig. 5-1**). The selective enrichment result of ANME-2a in the coexistence of phylogenetically distinct ANME lineages supported the hypothesis that the existence of certain physical-chemical condition(s) controls the ANME community structure. Fluorescence *in situ* hybridization analysis showed that active ANME-1, -2a, and most ANME-2c cells occurred without close physical interaction with potential bacterial partners, implying that the AOM entities thrive in the methane-seep sediment have the potential to mediate bacteria-independent AOM. In addition to ANMEs, phylogenetically diverse microbes, including uncultured archaeal lineages of Deep-Sea Archaeal Group and Marine Benthic Group-D, and an uncultured gammaproteobacterial lineage, were detected in the enrichment. The data provided in this chapter demonstrates that the DHS bioreactor is a useful system for cultivating fastidious AOM-associated microbes and would offer an initiative step to obtain a pure culture of ANMEs and other phylogenetically diverse and elusive microbial life.

In Chapter III, the methane-seep sedimentary microbial community obtained in Chapter II was subsequently

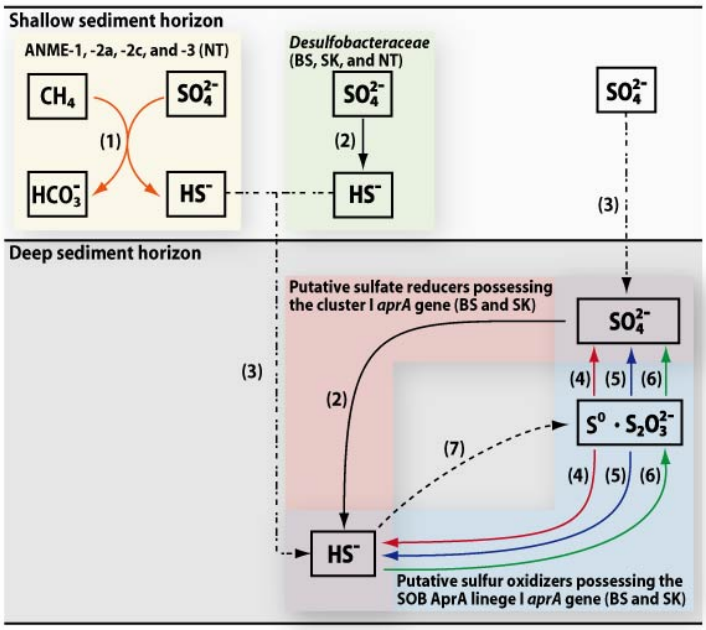

Figure 5-1. Conceptional network of potential carbon and sulfur cycling-related reactions in marine sediment on the northwestern Pacific margin off Japan. BS, marine sediment off Boso Peninsula; SK, marine sediment off Shimokita Peninsula; NT, methane-seep sediment of the Nankai Trough. Arrows indicate as follows: arrow (1), anaerobic oxidation of methane coupled to sulfate reduction; arrow (2), sulfate reduction with an unidentified electron donor; arrow (3), physical diffusion; arrow (4), elemental sulfur disproportionation; arrow (5), thiosulfate disproportionation; arrow (6), sulfur (compound) oxidation with an unidentified electron acceptor; arrow (7), abiotic sulfide oxidation with an unidentified sulfide scavenger. Important microbes as suggested by this thesis are also noted in the figure.

cultivated using a continuous-flow bio-electrochemical reactor (BER). The objective of this chapter was to clarify possible effect of quinone compound-mediated anaerobic redox potential difference on AOM-associated microbial community structure development in the methane-seep sediment of the Nankai Trough. In the present study, a model quinone compound of anthraquinone-2, 6-disulfonate was added to the cultivation medium as an electrochemically active redox mediator to control the redox potential of cultivation medium using BER. The working electrode potential of the BER was set at −0.4 V or −0.6 V (vs. Ag/AgCl reference electrode). 16S rRNA gene-targeted clone analysis suggested that distinct archaeal and bacterial phylotypes were dominated in the BER in response to the poised electrode potential. The ANME-2a-affiliated archaeal and *Sulfurimonas*-affiliated bacterial phylotypes were predominant components in the cultivation vessel poised at −0.4 V, while the *Methanococcoides*-affiliated archaeal and *Helicobacteraceae*-affiliated bacterial phylotypes were highly enriched in the cultivation vessel poised at −0.6 V. The data obtained in this study implies that the quinone compound-mediated anaerobic redox potential difference is a factor that controls the microbial community structure development in the methane-seep sediment. In addition, this study also hints at laboratory cultivation

methods for uncultivated microbes, including a member of a widely distributed yet uncultivated *Helicobacteraceae* lineage, predominantly detected in the cultivation vessel poised at −0.6 V.

Chapter IV described the phylogenetic diversity of the *aprA* gene, which encodes a key enzyme in dissimilatory sulfate reduction and sulfur oxidation, in the subseafloor sediment. The objective of Chapter IV was to identify putative sulfur-metabolizing microbial components and obtain new insights into the microbial sulfur cycling in the sedimentary environment. The *aprA* gene sequences obtained using PCR and subsequent clone library construction were grouped into 135 operational taxonomic units at 90% sequence identity. On the basis of the relative abundance of *aprA* gene clones, the family *Desulfobacteraceae* and microbes possessing the AprA cluster I (tentatively defined group in this study)-associated *aprA* gene might have an important role in sulfate-rich shallow and sulfate-poor deep sediment-associated sulfate reductions, respectively (arrow (2) in **Fig. 5-1**). The concomitant detection of putative sulfate-reducing and sulfur-oxidizing bacteria-associated *aprA* genes in deep subseafloor sediment samples implies that the occurrence of coupled oxidative and reductive microbial sulfur cycling in the deep sediment. On the basis of previously published reports on deep subseafloor sulfur cycling, sulfur compound disproportionation (arrows (4) and (5) in **Fig. 5-1**) and/or sulfur oxidation (arrow (6) in **Fig. 5-1**) might occur in the deep subseafloor environment. The high relative abundance of sulfur-oxidizing bacteria (SOB) AprA lineage I-associated *aprA* gene suggested that the microbes possessing the *aprA* gene might have a crucial role in the deep subseafloor cryptic sulfur cycling, especially for oxidative sulfur cycling. Although the *in situ* expression of *aprA* genes, *in situ* activity rates, and the detailed physiological properties of sulfur-metabolizing microbes possessing the *aprA* gene remain unknown, the results presented in this chapter suggested that the microbial ecosystems involved exhibited markedly diverse genetic potentials to mediate the sulfur cycling.

Acknowledgement

I would like to thank my supervisors, Professor Takashi Yamaguchi and Dr. Masashi Hatamoto at Nagaoka University of Technology (NUT), for accepting me as a doctoral student and for providing me the opportunity to do the course of works relevant to this thesis; Dr. Hiroyuki Imachi at Japan Agency for Marine-Earth Science and Technology (JAMSTEC) for all the support and valuable discussions during my time as a doctoral student; Dr. Wataru Ogasawara at NUT and Dr. Tomoyuki Hori at National Institute of Advanced Industrial Science and Technology (AIST) for providing constructive comments, which helped to improve this thesis; and, past and present lab members at NUT and JAMSTEC for their assistance and providing an excellent working atmosphere.

Finally, I would like to express my deep gratitude to my family for their moral support and warm encouragements throughout my doctoral student period.

Masataka Aoki

Nagaoka University of Technology

March 2016